Beyond-mean-field effects in ultracold gases

Alexandre Pricoupenko

université
PARIS-SACLAY

Beyond-mean-field effects in ultracold gases

Effets au-delà du champ moyen dans les gaz ultra-froids

Thèse de doctorat de l'université Paris-Saclay

École doctorale n° 564, physique en Ile-de-France (PIF)
Spécialité de doctorat : Physique
Unité de recherche : université Paris-Saclay, CNRS, LPTMS, 91405, Orsay, France.
Référent : Faculté des sciences d'Orsay

Thèse présentée et soutenue à Paris-Saclay le 6 Septembre 2021, par

Alexandre PRICOUPENKO

Composition du jury:

Frédéric CHEVY Professeur, Laboratoire Kastler Brossel	Président
Mario GATTOBIGIO Maître de conférences, HDR, Institut de Physique de Nice	Rapporteur & Examinateur
Luis SANTOS Professeur, Institut für Theoretische Physik	Rapporteur & Examinateur
Denis LACROIX Directeur de recherche, IJCLab (Paris-Saclay)	Examinateur
Leticia TARRUELL Professeure, ICFO - The Institute of Photonic Sciences	Examinatrice

Direction de la thèse :

Dmitry PETROV Directeur de recherche, LPTMS (Paris-Saclay)	Directeur de thèse

Thèse de doctorat

NNT: 2021UPASP070

Remerciements

Je tiens tout d'abord à remercier infiniment mon directeur de thèse Dima pour sa bienveillance au cours de toutes ces années, et à qui je dois énormément dans cette thèse. Son talent de physicien et plus particulièrement son sens physique ne cesseront de m'impressioner. Je retiendrai l'image de quelqu'un de passioné et profondément gentil, qui en font un chercheur d'exception.

Bien évidemment, je remercie toute ma famille qui a toujours été présente et m'a toujours encouragé durant ce doctorat (et même avant !). J'ai une pensée particulière pour ma grande soeur qui présentera sa thèse l'année prochaine et à laquelle j'envois mon plus grand soutien.

Il va sans dire que je remercie chaleureusement tous mes amis, avec qui j'ai partagé de merveilleux moments durant ces années de thèse. Outre la période faste du Ter-Ter et les nombreuses péripéties dont je garderai des souvenirs impérissables, je retiendrai aussi toutes ces choses du quotidien, ces rues du 5e que l'on a traversées en long et en large, ce cher labo dont je connais bien le piano, et tous ces lieux où nous avons vécu ensemble, du Pantalon au Supersonic, en passant par la petite cour du 115 (et bien sûr, le regret de ne jamais être allé à l'indémodable Soleil Club).

Enfin, je remercie bien sûr Claudine et Karolina, qui ont toujours été là pour moi, et dont je garderai le souvenir d'une sympathie sans égale. J'ai également une pensée émue pour toute l'équipe du feu 1er étage que nous étions avec Giampaolo, Antonio et Sebastián, et envois une dédicace toute particulière à mon cher camarade Hugo. Bien évidemment, je remercie également tous les étudiants et autres membres du laboratoire, anciens comme nouveaux, qui ont contribué à l'excellente atmosphère régnant au sein du LTPMS durant ma thèse.

List of publications

Dimer-dimer zero crossing and dilute dimerized liquid in a one-dimensional mixture
A. Pricoupenko and D. S. Petrov
Phys. Rev. A 97, 063616 (2018)

One-dimensional three-boson problem with two- and three-body interactions
G. Guijarro, A. Pricoupenko, G. E. Astrakharchik, J. Boronat, and D. S. Petrov
Phys. Rev. A 97, 061605(R) (2018)

Three-body interaction near a narrow two-body zero crossing
A. Pricoupenko and D. S. Petrov
Phys. Rev. A 100, 042707 (2019)

Higher-order effective interactions for bosons near a two-body zero crossing
A. Pricoupenko and D. S. Petrov
Phys. Rev. A 103, 033326 (2021)

Contents

Introduction **1**

1 Few-body basics **9**
1.1 Interactions . . . 10
1.2 Two-body scattering . . . 11
1.3 Model potentials . . . 17
1.4 The method of Skorniakov and Ter-Martirosian . . . 20

2 LHY and Quantum Stabilization **23**
2.1 Bose-Bose mixture . . . 24
2.2 Dipolar gases . . . 29

3 One dimensional Bose-Bose mixture **33**
3.1 Dimer-dimer zero crossing and dilute dimerized liquid . . . 34
3.1.1 Trimer energy . . . 34
3.1.2 Dimer-dimer scattering problem . . . 36
3.1.3 Dilute liquid of dimers . . . 38
3.1.4 Discussion and outlook . . . 41
3.2 Three-boson problem with two- and three-body interactions . . . 43
3.2.1 Derivation of the formula . . . 44
3.2.2 Back to the 1D mixture problem . . . 48

4 A perturbative approach for bosons near a two-body zero crossing **53**
4.1 Few-body perturbative approach . . . 55
4.2 Applications . . . 59
4.2.1 Double-Gaussian potential . . . 59
4.2.2 Yukawa-plus-delta potential . . . 60
4.2.3 Quasi-two-dimensional dipoles . . . 61
4.2.4 Quasi-one-dimensional dipoles . . . 66
4.3 Bogoliubov theory . . . 69
4.4 Conclusions . . . 71

5 Three-body interaction near a narrow two-body zero crossing **73**
5.1 Mean-field analysis 74
5.1.1 Application to two-dimensional dipoles 76
5.1.2 Inelastic losses 77
5.2 Regularized model and two-body problem 77
5.3 Three-body problem 80
5.3.1 One dimension 85
5.3.2 Two dimensions 87
5.3.3 Three dimensions 88
5.4 Discussion and conclusions 89

Conclusion and perspectives **91**

A Detailed derivation of Eq.(3.18) **95**

B Synthèse en français **101**

Bibliography **107**

Introduction

Dealing with few-body or many-body interacting systems is at the heart of a large variety of domains in physics. Unfortunately, it appears that already in the case of $N = 3$ particles, the general solution is too complicated. From there, one has to rely actively on a set of approximations (all associated with various theoretical approaches), guided by the parameters scale of the system at hand. Here, one might ask:

Is there a particular branch of physics that offers a good platform, both theoretically and experimentally, to study few-body and many-body interacting systems?

The ***ultracold gases***, a domain where one works with gases of atoms at very low temperature, appears to be a really good candidate as it benefits from a remarkable separation of scales. Hence, a very small number of parameters is needed to describe the interacting system, and just as important, most of these parameters can be fine-tuned in experiments. In itself, this domain provides us a wonderful playground to better understand quantum matter at an atomic level [1]. It also appears to start answering other many-body problems, ranging from condensed matter to astrophysics, by playing the role of a quantum simulator, thanks to its ability to reproduce artificially some phenomena which are hard to compute numerically [2–4].

As the reader might expect from the title of this thesis, we embark on this domain for the rest of the manuscript and recall here basic properties of these gases before moving on.

Ultracold gases are very dilute systems, as they are approximately 10^5 times less dense than the ambient air (the density $n \simeq 10^{14}$ atoms/cm^3). The atomic de Broglie wavelength $\lambda_T = (2\pi\hbar^2/mk_BT)^{1/2}$ is made very large since the temperature T is typically ranging from 100 nK to 1 μK. At these typical scales, the gas can no longer be considered classical and obeys quantum statistics, with its nature changing radically according to the bosonic or fermionic character of its components. For the bosonic case, one eventually obtains a remarkable state of matter, the so-called Bose-Einstein-Condensate (BEC), where atoms occupy the ground state of the gas macroscopically. It has been first observed experimentally in 1995 [5–7], and the field has developed a lot since this breakthrough. The incredible methods to achieve such systems, which mainly use the physics of laser and the use of evaporative cooling are given in Ref. [8].

Actually, the formation of a BEC emerges purely from quantum statistics and does

not need interactions, but those ones have a dramatic effect on the gas (not to mention their necessity in the evaporative cooling [8], or in the appearance of the superfluid state [9]). Introducing R_e, the *range* of the interatomic potential (typically few nm), we recall that in the regime where $\lambda_T \gg R_e$, often referred to the ultracold limit, one parameter is generally sufficient to describe the two-body interaction between particles: the so-called *scattering length* a. This leads to the equivalence of all two-body short-range potentials with the same scattering length: we talk here of *universality*. From this parameter, we usually define the *strength* g_2 of an effective two-body potential modeling the interaction.

Let us now have an insight on the homogeneous many-body interacting system of N atoms in a volume V at $T = 0$. As the mean interparticle distance $l = n^{-1/3}$ between atoms satisfies the dilute limit condition $l \gg R_e$, we usually only consider pair interactions. That leads us to perform a mean-field (MF) analysis of the system: to obtain the interacting energy E_{MF}, we multiply the energy of one interacting pair $\propto g_2$ by the number of pairs in the system, leading for large N to $E_{\mathrm{MF}} = g_2 N^2/2V$. For $g_2 > 0$, corresponding to an overall repulsion, the system is in the gaseous phase and expands to minimize its energy. It then requires to be trapped with an external potential to be localized for experiments. For $g_2 < 0$, associated with an overall attraction, the system collapses on itself. At this stage, one might ask:

Are these two scenarios (gaseous phase and collapse) exhaustive? Or is it possible to obtain a liquid state, i.e., a (very dilute) self-bound state in equilibrium with vacuum without external potential?

Such a state would require that the total interacting energy per particle $E_{\mathrm{int}}/N(n)$ exhibits a nontrivial minimum at a certain density n_0. A way to obtain such a property is to take into account the existence of ***beyond-mean-field*** (BMF) energy terms $E_{\mathrm{BMF}} = E_{\mathrm{int}} - E_{\mathrm{MF}}$ to counterbalance the mean-field one. Usually, these BMF terms correspond to higher-order corrections to the total energy and do not really change the properties of the system. Here, let us assume that the leading order of these terms $\propto g_\alpha n^\alpha$ where $\alpha > 2$ [1]. One can then write the total energy per particle as

$$E_{\mathrm{int}}/N \propto g_2 n + g_\alpha n^{\alpha-1}, \quad \text{with } \alpha > 2. \tag{1}$$

To have a minimum at n_0, one needs to have the particular scaling $g_2 \sim g_\alpha n_0^{\alpha-2}$, where both terms need to have different signs: a mean-field attraction being stabilized by a beyond mean-field repulsion and inversely. Moreover, the gas should remain dilute to not suffer from a short lifetime due to inelastic collisions. In three dimensions, where $g_2 \propto a$, one can show that a simultaneous small a and large g_α with a small α is preferable. Note

[1] In the general case, and especially for low-dimensions, the leading order of the BMF terms can have a different and more complicated dependence on the density n. However, the possible mechanism of stabilization stays the same.

also that one might expect the BMF term to be strongly dependent on the MF term, arising the fact that it is a priori not evident to control these terms independently.

There, one might wonder the different options which are offered to obtain such a self-stable system. Let us approach the problem from a historical point of view. In 1957, Lee, Huang, and Yang (LHY) derived in the case of a homogeneous weakly repulsive Bose gas (where $na^3 \ll 1$) the first two leading terms of the energy density [10, 11] with a pseudopotential method (in agreement with the Bogoliubov approach [12, 13]), which read

$$E/V = \frac{4\pi\hbar^2 a}{m}\frac{n^2}{2}\left(1 + \frac{128}{15\sqrt{\pi}}\sqrt{na^3} + ...\right). \tag{2}$$

In our notations, this LHY correction corresponds to a term $\alpha = 5/2$. It is universal, as it depends only on the scattering length ($\propto a^{5/2}$), and a striking property lies in its pure quantum nature (as it corresponds to *quantum fluctuations*, or in a more theoretical picture, to the zero-point energy of Bogoliubov phonons). However, although this term has indeed been observed [14] and can be manipulated, one can see that this effect is perturbative and the LHY term is then always much smaller than the MF term. Hence, we *a priori* need to look elsewhere to obtain this self-stable state we pursue.

Almost five decades after LHY, Bulgac asked himself the question of engineering quantum liquid droplets [15]. His proposal lies in the ability to fine-tune the scattering length in experiments thanks to an external magnetic field through the so-called Feshbach mechanism. Following the resonant case where $|a| \to +\infty$ which involves the Efimov physics [16, 17], he shows that a three-body repulsion (i.e., $\alpha = 3$ and $g_3 > 0$) can contribute to stabilize an attractive ($g_2 < 0$) interacting system of bosons, hence leading to a self-bound state of density $n_0 = -2g_2/g_3$ he called a *boselet* (a boson droplet). Although it was a great theoretical step, these droplets appear difficult to observe because in the resonant case, inelastic collisions [2] are really important and lead to a short lifetime of the sample [18, 19].

However, Petrov presented in 2014 a way to control two-body and effective three-body interactions in the non-resonant case [20], opening the way to observe self-bound quantum droplets. Indeed, this proposal lies on a system of dipoles in a bilayer geometry with interlayer tunneling, where one can drastically reduce inelastic collisions.

One year later, Petrov realized that the tunneling was not needed for liquefaction. He looked in Ref. [21] at a Bose-Bose mixture ($\uparrow$, $\downarrow$) with two-body attractive interspecies ($g_{\uparrow\downarrow} < 0$) and two-body repulsive intraspecies ($g_{\uparrow\uparrow}, g_{\downarrow\downarrow} > 0$) close to the region where mean-field predicts collapse and defined by the condition $g_{\uparrow\downarrow}^2 > g_{\uparrow\uparrow}g_{\downarrow\downarrow}$ (i.e., the *attractive part* of the system overcomes the *repulsive part*). Analyzing the energy density of the mixture up to the LHY correction for this system, he showed that this term can actually

[2] Typically, in a three-body inelastic collision, two atoms can form a molecule such that the third particle carries then a kinetic energy surplus sufficient to leave the trap.

stabilize the collapsing mixture with a fine-tuning of the interactions, and that the system gets instead into a dilute liquid droplet. In other words, the unstable classical system (i.e., from a MF viewpoint) is stabilized by " switching on " quantum mechanics. Here, the fundamental difference with the single component Bose gas is that the MF term and the LHY correction can be controlled independently and hence tuned to the same order. Various properties of this exotic phase (excitations spectrum, surface tension, etc ...) were described in this paper, as the experimental road to obtain such a state: a few years later, it was successfully observed in a potassium mixture (^{39}K, ^{41}K) at ICFO in Barcelona [22], then later at LENS in Florence [23].

This new liquid-like state differs quite strongly from the classical picture of liquids we know, which is explained through the Van der Waals theory [24]. Indeed, they are much more dilute (the droplet is 10^8 times less dense than water !) and the frame is here rather universal as the liquid depends on a set of few parameters, in contrast to classic liquids where the description depends on the details of the interatomic potentials [25].

Meanwhile, dipolar quantum droplets have been observed in groups of Stuttgart and Innsbruck using dipolar gases (respectively with Dy and Er dipoles) [26–29]. They are explained by the same mechanism of stabilization as the Bose-Bose mixture case, i.e., thanks to quantum fluctuations (LHY term). Here, the MF term is weakened via a balance between an attractive dipolar tail and a repulsive short-range contact interaction.

Although the observation of this liquid-like droplet state was a major breakthrough as it goes beyond the Van der Waals paradigm, it also appeared to open the road to the realization of an even more intriguing state: the *supersolid*. This state of matter, which exhibits both a crystalline structure and a frictionless motion, has a long story as it was predicted theoretically for many decades [30] but was never observed. Nevertheless, three groups have recently observed the first evidence of supersolid properties through the formation of coherent arrays of quantum dipolar droplets, which rely genuinely on interactions between particles [31–33].

These seminal ideas and experimental observations have considerably raised the attention for systems with an intentionally weakened MF term (thus enhancing the importance of the BMF ones) over the past few years. The Ref. [34] is a very useful review on this new domain .

Theoretically wise, these systems where an attractive part and a repulsive part compete with each other are a way to appreciate better the BMF physics in all its richness of possibilities. From non-local collective excitations (quantum fluctuations) to effective local higher-body interactions, we now see that these terms can no longer be reduced to an academical problem as they can dramatically change the nature of the system. It raises the following question:

What do these BMF terms depend on?

Of course, they are mainly linked to the shape and strength of the interactions in the system at hand, as well as the trap potential, but one of their major features is that they generally strongly depend on dimensionality. For example, the LHY term involves a sum in the momentum space, and its dependence on the particle density greatly varies ($n^{5/2}$ for $D = 3$, $n^2 \ln n$ for $D = 2$ and $n^{3/2}$ for $D = 1$). It allows wide possibilities as experimentalists are capable of strongly confining the system in desired directions, hence freezing degrees of freedom for the atoms, entering *quasi-low-dimensional* regimes. Usually, one uses harmonic potentials trap to do so, often leading the system to exhibit a cigar (quasi-1D) or a pancake (quasi-2D) shape. Note also that reducing the problem to a pure low-dimensional model often contributes to add effective higher-body interactions in the system, which find their origin in the virtual excitations of the trapped atoms. In a more general way, following an Effective Field Theory (EFT) approach, one can show that effective higher-body forces arise *naturally* when one integrates out frozen degrees of freedom in a system [35].

Overview of the Manuscript and Principal Results

In this thesis, we intend to study beyond-mean-field effects close to a *two-body zero-crossing* (i.e., with weakened mean-field interaction associated with $g_2 \to 0$) in various systems, geometries, and interactions. Although it will lead us to navigate between few- and many-body problems, an emphasis will be put on the few-body approach. This manuscript is divided into five chapters, the first two which serve as a pedagogical introduction.

In the **first chapter**, we recall useful few-body concepts which will act as building blocks to understand all the next chapters. We look at the typical interaction between two neutral atoms and present some two-body scattering properties at low-energy, as well as the Feshbach mechanism. We then introduce effective potentials much easier to manipulate than the true interactions, which encapsulate the low-energy scattering properties of the system, using the so-called zero-range approximation. In particular, we present the Skorniakov-Ter-Martirosian method, being particularly handy for three and four-body problems we will face later.

In the **second chapter**, we enter the many-body world and present more in detail the principal motivations of this thesis, namely systems where the MF interaction can be fined tuned to an arbitrary small value, emphasizing the importance of BMF effects, and leading ultimately to new exotic states of matter. Following first the example of a mass-balanced Bose-Bose mixture with attractive interspecies and repulsive intraspecies contact interactions, we explain how the LHY term can stabilize the system close to the regime where the MF approach predicts collapse, leading to a liquid-like droplet formation. The question is addressed in every dimension. We also give some brief insights on dipolar gases, which can exhibit the same phenomenon of quantum stabilization.

In the **third chapter**, we enrich the phase diagram of the 1D Bose-Bose mixture defined in the previous chapter. Starting from the regime where the system maps to a repulsive gas of dimers, we solve the dimer-dimer scattering problem. In the plane parametrized by the ratios of the coupling constants $g_{\uparrow\uparrow}/|g_{\uparrow\downarrow}|$ and $g_{\downarrow\downarrow}/|g_{\uparrow\downarrow}|$ we trace out the curve where the dimer-dimer interaction switches from attractive to repulsive. We find this curve to be significantly (by more than a factor of 2) shifted towards larger $g_{\sigma\sigma}$(or smaller $|g_{\uparrow\downarrow}|$) compared to the mean-field stability boundary $g_{\uparrow\uparrow}g_{\downarrow\downarrow} = g_{\uparrow\downarrow}^2$. For a weak dimer-dimer attraction, we predict a dilute dimerized liquid phase stabilized against collapse by a repulsive three-dimer force. Motivated by the verification of this prediction, we turn on solving the three-boson problem with contact two-body and three-body interactions in one dimension and analytically calculate the ground and excited trimer-state energies. This theoretical result is in itself an important step to understand one-dimensional bosonic systems. By using the diffusion Monte Carlo technique, our collaborators calculated the binding energy of three dimers formed in the previously studied one-dimensional Bose-Bose or Fermi-Bose mixture. Combining these results with our three-body analytics, we extract the three-dimer scattering length close to the dimer-dimer zero-crossing. In both considered cases, the three-dimer interaction turns out to be repulsive. By using an appropriate wave-function mapping, our results also apply to one-dimensional Bose-Fermi mixtures. They also constitute a concrete proposal for obtaining a one-dimensional gas with a pure three-body repulsion.

In the **fourth chapter**, we develop the perturbation theory for bosons interacting via a weak two-body potential V, attractive and repulsive parts of which cancel each other. We find that the leading nonpairwise contribution to the energy emerges in the third order in V and represents an effective three-body interaction, the sign of which in most cases (although not in general) is anticorrelated with the sign of the long-range tail of V. We apply our theory to a few particular two-body interaction potentials and calculate the leading two-body and three-body interaction corrections for tilted dipoles in quasi-low-dimensional geometries. We show that our approach is consistent with the many-body Bogoliubov treatment.

In the **fifth chapter**, motivated by some cases where the LHY term appears not to be able to counterbalance the unstable MF term (single component Bose gas, low dimension geometry, etc ...), we propose a way to engineer an effective three-body force to ensure this property: for bosons interacting with each other by a two-body potential tuned to a narrow zero-crossing, we show the emergence of an effective three-body force which we calculate in any dimension. We use the standard two-channel model parameterized by the background atom-atom interaction strength, the amplitude of the open-channel to closed-channel coupling, and the atom-dimer interaction strength. The three-body force originates from the atom-dimer interaction, but it can be dramatically enhanced for narrow crossings, i.e., for small atom-dimer conversion amplitudes. This effect can be used to stabilize quasi-two-dimensional dipolar atoms and molecules.

Finally, we conclude by mentioning exciting perspectives and new challenges related to BMF effects, both theoretical and experimental.

Chapter 1

Few-body basics

Contents

1.1 Interactions 10
1.2 Two-body scattering 11
1.3 Model potentials 17
1.4 The method of Skorniakov and Ter-Martirosian 20

The goal of this chapter is to introduce relevant few-body parameters used in the manuscript. We previously mentioned the importance of interactions for ultracold gases. Experiments are done with neutral atomic gas at very low densities ($nR_e^3 \ll 1$) such that we can limit ourselves to the model of binary collisions to describe the system since higher-order ones are much less probable. After presenting some features of the interatomic potential, we study the two-body scattering problem and define the main parameter to describe interactions at low-energy: the s-wave scattering length a. Finally, we look for model potentials to describe interactions easily, introducing especially the zero-range approximation. In this chapter, an emphasis is put on the three-dimensional case to introduce the basic notions. Still, we also briefly discuss some low-dimensional scattering properties, helpful for the next chapters.

1.1 Interactions

Let us take two neutral atoms of the same species, prepared in their electronic ground state [1]: how do they interact?

We will assume in this section they interact via an isotropic interatomic potential $V(r)$ where r is the interatomic distance. [2]

Let us begin with the long-range behavior, which is the easiest to describe. For the two atoms far away from each other, where the exchange of electrons is negligible (typical value is $\sim 10^{-10}$ m), the dominant interaction is the electric dipole-dipole interaction. It leads, thanks to a perturbative development to the second-order, to an attractive potential, the so-called van der Waals (vdW) potential, which can be written as

$$V_{\mathrm{vdW}}(r) = -C_6/r^6, \tag{1.1}$$

where C_6 is a positive coefficient that defines the strength of this interaction. As its value directly depends on the matrix elements of the dipole-dipole operator between the fundamental and excited atomic wavefunctions, it generally involves complicated calculations, which are then performed numerically. However, for alkali and alkali earth atoms, this value can surprisingly be well approached with a simple two-level energy model [36].

One can define the characteristic length R_{vdW} associated with the range of the vdW potential, that is to say, the distance beyond which the action of the potential becomes negligible (i.e., where the potential term becomes negligible compared to the kinetic energy) which reads

[1] For the case of two excited neutral atoms, we provide here a good introduction reference [36].

[2] We hence neglect anisotropic interaction like the magnetic dipole-dipole interaction. This is a good approximation for most of the usual atoms used in experiments. However, we present in Chapter 2 some systems (like Dy or Er atoms) where these interactions play a significant role.

$$R_{\mathrm{vdW}} = \frac{1}{2}\Big(\frac{2\mu C_6}{\hbar^2}\Big)^{1/4}. \tag{1.2}$$

This value is generally on the order of 10^{-9} m (for potassium atoms $R_{\mathrm{vdW}} \simeq 65$ Å).

Note that this vdW approach neglects delay effects [37] which lead to a change in the long-range asymptote from r^{-6} to r^{-7}.

We now turn to the short-range behavior of the interatomic potential: this region provides a strong repulsive interaction as electronic clouds repel each other thanks to the Pauli principle. For alkali, which are widely used in experiments, the interatomic potential depends then typically on the electronic spin configuration of the atoms (singlet or triplet state).

Finally, we note that the interatomic potential generally contains many deep bound states: for the considered densities and temperature we work with, it arises the fact that at the complete thermal equilibrium, the system is in a solid state (that is why the BEC is often called a *metastable* state).

1.2 Two-body scattering

Let us now turn to the two-body scattering problem. We take two particles with a relative position $\mathbf{r}$ and a reduced mass μ, interacting through a potential $V(\mathbf{r})$ of range R_e such that it vanishes when $r > R_e$. We can decouple their center of mass motion and their relative motion: the center of mass moves as a free particle, while the relative motion is governed by the following Schrödinger equation

$$-\frac{\hbar^2}{2\mu}\boldsymbol{\Delta}_{\boldsymbol{r}}\psi(\boldsymbol{r}) + V(\boldsymbol{r})\psi(\boldsymbol{r}) = E\psi(\boldsymbol{r}), \tag{1.3}$$

where ψ is the relative motion wavefunction.

We look first at scattering states ($E = \hbar k^2/2\mu > 0$) and write $\psi_{\boldsymbol{k}}$ the relative motion wavefunction associated with the incoming momentum $\boldsymbol{k}$. We treat here the case of elastic collisions where there is no change in internal states for the two particles before and after the collision: the norm of the incoming momentum for the relative motion is then conserved. A good approach to solve this scattering problem is to treat Eq. (1.3) with a Green function formalism. This is done using small rearrangements to make a source term appear at the right of Eq. (1.3) and depending on $\psi_{\boldsymbol{k}}$ itself,

$$(\boldsymbol{\Delta}_{\boldsymbol{r}} + k^2)\psi_{\boldsymbol{k}}(\boldsymbol{r}) = \frac{2\mu}{\hbar^2}V(\boldsymbol{r})\psi_{\boldsymbol{k}}(\boldsymbol{r}). \tag{1.4}$$

A particular solution without the source term is the plane wave $e^{i\boldsymbol{k}\boldsymbol{r}}$ with $\boldsymbol{k} = k\boldsymbol{n}$ which will be seen as the incoming free wave of the collision. We look now for a Green's function G^D, where D is the dimension, which satisfies

$$(\boldsymbol{\Delta}_{\boldsymbol{r}} + k^2)G^D(\boldsymbol{r}) = \delta(\boldsymbol{r}). \tag{1.5}$$

We choose the Green's functions corresponding physically to an outgoing wave for $r \to +\infty$ which read

$$\begin{cases} G^{D=3}(\boldsymbol{r}) = -\dfrac{1}{4\pi}\dfrac{e^{ikr}}{r}, & \text{(1.6a)} \\ G^{D=2}(\boldsymbol{r}) = -\dfrac{i}{4}H_0^{(1)}(kr), & \text{(1.6b)} \\ G^{D=1}(\boldsymbol{r}) = -\dfrac{i}{2k}e^{ikr}, & \text{(1.6c)} \end{cases}$$

where $H_0^{(1)}$ is the Hankel function of the first kind.

It leads to the following integral equation known as the Lippman Schwinger equation,

$$\psi_{\boldsymbol{k}}(\boldsymbol{r}) = e^{i\boldsymbol{k}.\boldsymbol{r}} + \frac{2\mu}{\hbar^2}\int G^D(\boldsymbol{r}-\boldsymbol{r'})V(\boldsymbol{r'})\psi_{\boldsymbol{k}}(\boldsymbol{r'})d^3r'. \tag{1.7}$$

An important remark is that we did not solve Eq. (1.4) as $\psi_{\boldsymbol{k}}$ appears both on the left and on the right sides of Eq. (1.7). Nevertheless, it is handy when the potential V has a finite range R_e. Indeed, Eq. (1.7) links the value of $\psi_{\boldsymbol{k}}$ at an arbitrary point $\boldsymbol{r}$ to the values of $\psi_{\boldsymbol{k}}$ in a sphere of radius R_e.

From now on until the next section, we will focus on the scattering problem in three dimensions as it is the most physical one, but leave to the reader a useful reference to treat the scattering in pure and quasi-low dimensions [38]. Thus, let us develop Eq. (1.7) when $r \gg R_e$, and $r \gg kR_e^2$, using the fact that [3]

$$\frac{e^{ik|\boldsymbol{r}-\boldsymbol{r'}|}}{|\boldsymbol{r}-\boldsymbol{r'}|} \sim \frac{e^{ikr}}{r}e^{-ik\hat{\boldsymbol{r}}.\boldsymbol{r'}}, \tag{1.8}$$

where we call $\hat{\boldsymbol{r}} = \boldsymbol{r}/r$.

In this condition, we can then write the asymptotic form of $\psi_{\boldsymbol{k}}$ as

$$\psi_{\boldsymbol{k}}(\boldsymbol{r}) \sim e^{i\boldsymbol{k}.\boldsymbol{r}} + f(\boldsymbol{k},\hat{\boldsymbol{r}})\frac{e^{ikr}}{r}, \tag{1.9}$$

where $f(\boldsymbol{k},\hat{\boldsymbol{r}})$ is the so-called *scattering amplitude*. It does not depend on the distance r and reads

$$f(\boldsymbol{k},\hat{\boldsymbol{r}}) = -\frac{\mu}{2\pi\hbar^2}\int e^{-ik\hat{\boldsymbol{r}}.\boldsymbol{r'}}V(\boldsymbol{r'})\psi_{\boldsymbol{k}}(\boldsymbol{r'})d^3r'. \tag{1.10}$$

[3] The first condition is to expand $|\boldsymbol{r}-\boldsymbol{r'}|$, the second one is to neglect a contribution to the phase of $e^{ik|\boldsymbol{r}-\boldsymbol{r'}|}$.

The Born Approximation

If the potential V is weak enough [4], the idea is to replace the term $\psi_{\boldsymbol{k}}(r')$ in the integral Eq. (1.10) by its value at the zeroth order of V, which corresponds to the incoming wave function $e^{i\boldsymbol{k}.\boldsymbol{r}}$, leading to write

$$f(\boldsymbol{k}, \hat{\boldsymbol{r}}) = -\frac{\mu}{2\pi\hbar^2} \int e^{ik(\boldsymbol{n}-\hat{\boldsymbol{r}}).\boldsymbol{r'}} V(\boldsymbol{r'}) d^3r'. \tag{1.11}$$

This approximation at first order in V can be helpful to evaluate some scattering properties quickly. But we can even push the idea further and pursue what we did by doing successive iterations: we can approximate ψ at order $n+1$ in V by using its approximation at the order n. It corresponds to the Born expansion where we expand ψ in powers of V. Nevertheless, whether this sum is convergent or not is actually a delicate point. One can show that one condition is that the potential carries no bound state, which directly eliminates this development for the real interatomic potential. However, we will see that it can be used for model potentials which will carry the scattering properties of the actual real potential.

Cross-section

Before going any further, let us relate the scattering amplitude to physical observables. Thanks to detectors, we can measure flux of particles far from the scattering region, where the asymptotic form of our wavefunction we derived is valid. So if we define the ingoing flux of particles per surface J_{inc} and the flux of particles J_{diff} scattered into a solid angle $d\Omega$ (defined by $\hat{\boldsymbol{r}}$), we can define the so-called differential cross section $\frac{d\sigma}{d\Omega}$ and the scattering cross section σ as

$$\frac{d\sigma}{d\Omega}(k, \Omega) = \frac{J_{\text{diff}}}{J_{\text{inc}}}, \qquad \text{and} \qquad \sigma(k) = \int \frac{d\sigma}{d\Omega} d\Omega. \tag{1.12}$$

Physically, $d\sigma$ corresponds to the area that *captures* the amount of incident flux which is going into the solid angle $d\Omega$.

The tool to calculate flux in quantum mechanics is the probability current. Hence, after some calculations, one can find the relation between the diffusion amplitude and the differential cross section which reads

$$\frac{d\sigma}{d\Omega} = |f(\boldsymbol{k}, \hat{\boldsymbol{r}})|^2. \tag{1.13}$$

Identical particles

So far we neglected the fact that our particles can be identical, so our approach has to be slightly modified in this case since particles are then indiscernible. We have to

[4] This condition is fulfilled if $|V| \ll \hbar^2/mR_e^2$ where $|V|$ is the order of magnitude of the potential in its principal region of existence [13].

symmetrize (or antisymmetrize) the relative wavefunction of our two particles according to the parity of their total spin. Calling $\epsilon = +1$ (-1) for polarized bosons (fermions), we find

$$\frac{d\sigma}{d\Omega} = |f(\boldsymbol{k}, \hat{\boldsymbol{r}}) + \epsilon f(\boldsymbol{k}, -\hat{\boldsymbol{r}})|^2. \tag{1.14}$$

Low-energy limit

The next thing is obviously to search for a more explicit expression for the scattering amplitude. In the case where we deal with a central potential $V(\boldsymbol{r}) = V(r)$, one can use the development in partial waves, which leads to express the so-called *phase shifts* to solve the scattering problem. We leave this to reference [13] and use a shortcut by considering low energy collisions (or equivalently, collisions at sufficiently low temperature). Indeed, if $kR_e \ll 1$ (called the *ultracold limit*) we can see that in Eq. (1.10) we can omit the exponential in the integral, leading to the independence of the scattering angle described by $\hat{\boldsymbol{r}}$ in the diffusion amplitude. The asymptotic form of the scattered wavefunction is thus spherically symmetric (even if we consider non-symmetric potential !) and we deal with the so-called s-wave, corresponding to the azimuthal quantum number $l = 0$ in the partial wave expansion. Hence, in the ultracold limit, we will consider that the scattering problem occurs only in the s-wave.

A fundamental point is that in this limit, fermions do not *see* each other since by using Eq. (1.14) we find $\sigma_{\text{fermions}} = 0$, whereas σ_{bosons} is a priori non zero . This result is linked to the more general result that scattering of fermions (bosons) takes place only through partials waves of odd (even) parity. Actually, this peculiar feature for fermions leads to difficulties in the evaporative cooling of a polarized fermionic gas. To circumvent this problem, one way is to use a two-component Fermi gas [39].

Scattering length

Going back to the expression of the scattering amplitude at low energy, one finds

$$\lim_{k \to 0} f(\boldsymbol{k}, \hat{\boldsymbol{r}}) = -a, \tag{1.15}$$

where a is the so-called s-wave scattering length describing the scattering process at low energy. The cross section for both nonidentical atoms (n.i.) and polarized bosons then read

$$\sigma_{\text{n.i.}} = 4\pi a^2, \quad \text{and} \quad \sigma_{\text{bosons}} = 8\pi a^2. \tag{1.16}$$

When $a > 0$, the scattering length corresponds to the node of the extrapolated wavefunction at zero energy [5] since

[5] That remark permits actually to define the notion of scattering length in two dimensions.

$$\lim_{k\to 0} \psi_{\boldsymbol{k}}(\boldsymbol{r}) = 1 - a/r + O(\frac{1}{r^2}). \tag{1.17}$$

Physically it means that at low energy, any potential with a positive scattering length can be seen as a hard-core potential of radius a. Note, however, that a can be either positive or negative, hence defining respectively the effectively attractive (or repulsive) interaction. It also naturally scales as the range R_e of the potential but can be fine-tuned using the mechanism of Feshbach resonance, to which we will come later.

As we can see, the scattering length fully characterizes interactions at low energy. This feature is often referred to as the *universality* of potentials at low energy in the sense that one can forget about the complicated short-range details of the potential. That is to say, if two potentials, really different (one being repulsive at distance where the other is attractive for example) have the same scattering length, then, at sufficiently low energies, the collective behavior of atoms will be basically the same.

Effective range

Let us briefly continue our study of the scattering amplitude at low energy. Since the number of particles has to be conserved during the scattering process [6], one can show that in the case of a central sufficiently short-ranged potential, the s-wave scattering amplitude f_s reads [13]

$$f_s(k) = \frac{1}{g_s(k) - ik}, \quad \text{with} \quad \lim_{k\to 0} g_s(k) = -1/a + \frac{r_e k^2}{2} + O(k^4), \tag{1.18}$$

where we introduce r_e, the so-called *effective range* which determines the next order term in k (after the scattering length) in the scattering amplitude at low energy. This term is generally negligible in the ultracold limit since a and r_e are typically of the order of the range R_e of the potential and $kR_e \ll 1$.

Real life

We used a finite range R_e for the potential such that when $r > R_e$, the potential vanishes. It is obviously not the case in real life (see Sec.1.1), and one may be scared that our results do not hold. However, our conclusions stay true as long as the potential decreases faster than $1/r^3$ at large distances (if not, the s-wave effective-range expansion is different, and we have to consider all partial waves at low energy).

Dimers

Let us briefly consider the case where $E = -\hbar\kappa^2/2m < 0$ with $\kappa > 0$ in Eq. 1.3. In contrast to the scattering states associated with a continuous positive energy spectrum, one can show that the system has a discrete spectrum of negative energies possible.

[6] Which corresponds equivalently to the unitarity of the S-matrix, resulting in the optical theorem.

These two-body bound states (b.s.) are called dimers, and their number depends on the nature of the potential. For $r \gg R_e$, their wavefunction satisfy

$$\psi_{\text{b.s.}} \propto \frac{e^{-\kappa r}}{r}. \tag{1.19}$$

Feshbach resonances

We now shortly illustrate how one can tune the s-wave scattering length a using a magnetic field $\boldsymbol{B}$, permitting us to free ourselves from its *natural* scaling. The standard theoretical approach is to use a *two-channel* model. We decide here to present the main concepts behind it and leave the details aside as we will give some of them in a future chapter.

Due to their electronic spin configuration and internal states (hyperfine states), a pair of two colliding atoms can scatter through many different channels. Let us consider two channels: an open channel called V_O, where we consider the scattering of two free atoms at a low energy E and another channel above, where scattering states at energy E cannot exist, which is then referred to as the closed-channel V_C. Let us assume that the closed channel carries a bound state at energy E_{res}. When applying an external magnetic field B, the difference of energy $\Delta E = E_{res} - E$ varies proportionally to it as there is a difference of magnetic moments $\delta\tilde{\mu}$ between the atomic pair in the open channel and the bound state in the closed channel. When both energies are sufficiently close to each other, a resonance between the two states occurs [7], hence changing the value of the scattering length a as

$$a(B) = a_{bg}\Big(1 - \frac{\Delta B}{B - B_0}\Big), \tag{1.20}$$

where a_{bg} is the *background* scattering length far away from the resonance, ΔB is the width of the resonance, and B_0 the value of the magnetic field corresponding to the resonance. We hence see that we can tune the value of a from $-\infty$ to $+\infty$, associated with an attractive or repulsive character of the two-body interaction.

This mechanism gives rise to scattering states no matter the sign of a, and bound states when a is positive. These last ones are called Feshbach molecules. When $a \gg R_e$, one can write their energy E_b as

$$E_b = -\frac{\hbar^2}{2\mu a}. \tag{1.21}$$

In the case where R_e is large, corrections to Eq. 1.21 have to be made [40, 41].

One can see that Feshbach resonances lead to a vast range of possibilities: one can transform a *natural* repulsive gas into an attractive gas (or vice-versa), it can offer the opportunity to engineer a perfect gas (i.e., with no interactions), to study the strongly

[7] Providing they have the same total angular momentum.

interacting regime and its correlations, or to transform a pair of free atoms into molecules (and vice versa). This mechanism is extensively used in ultracold atoms experiments and was the fundamental tool to study the BEC-BCS crossover [42, 43].

Inelastic scattering

Of course, neutral atoms can also undergo inelastic collisions. These events are important since they contribute to a decrease of the atom density in the trap with a typical relaxation time τ, hence giving an upper bound for the lifetime of ultracold experiments. They depend a lot on the atoms which are considered. There are three types of these events:

The first one is the collision of trapped atoms with the background gas and depends then on the vacuum quality (typically, $\tau_{\text{back}} \sim$ min).

The second arises from the use of a magnetic field to trap the atoms. Indeed the resulting magnetic dipolar interaction between two atoms can induce a change of the hyperfine state in one (or two) of the considered atom(s), resulting in an energy release sufficient for the two atoms to leave the trap ($\tau_{\text{m.dip.}} \sim$ min).

The third and most important event for a loss of atoms in a BEC relates to a three-body process (often called the three-body recombination): two atoms can form a molecule thanks to the existence of deep bound states in the interatomic potential, such that the third particle carries the kinetic energy surplus sufficient to leave the trap. At BEC typical densities, $\tau_{\text{rec}} \sim$ s, but this value can be greatly reduced when particles are strongly interacting (i.e. for resonances where $a \to +\infty$) !

In the rest of the manuscript, we will neglect these effects in the theoretical approach, keeping in mind that going into the strongly interacting regime in three dimensions is associated with a short lifetime of the sample, which is not convenient for experiments.

1.3 Model potentials

The true interatomic potential V is difficult to calculate with precision, and a small error in its expression can result in a large error of its scattering properties. Moreover, since it carries deep bound states, we cannot use some thermal equilibrium theory tools as the BEC is a metastable state. In addition, the strong repulsion at small distances prevents us from using V in the Born approximation.

Nevertheless, we recall that at sufficiently low energy and for sufficiently fast decaying potential, the system can be described via a single parameter: the scattering length a. The idea is then to construct a potential with the same a easier to manipulate, hence forgetting about the details of the true potential.

The δ-potential

The first naive approach to modelize the true potential, that one can use in every dimensions, would be to consider a simple δ contact interaction, namely a zero-range potential $V_\delta(\boldsymbol{r}) = g_0\delta(\boldsymbol{r})$, where g_0 would then take the role of the *strength* of the potential (also referred as the *bare coupling constant*). Let us see what happens if we substitute this potential in Eq. (1.7). Calculating ψ_k to the first Born approximation we get

$$\psi_{\boldsymbol{k}}(\boldsymbol{r}) = e^{i\boldsymbol{k}.\boldsymbol{r}} + \frac{2\mu}{\hbar^2} g_0 G^D(\boldsymbol{r}) + O(g_0^2), \tag{1.22}$$

where G^D is the Green's function in D dimensions which satisfies Eq. (1.6).

As we can see, everything is here well defined but we need to relate g_0 to physical parameters such as the scattering length. For $D = 3$, comparing Eq. (1.22) with Eq. (1.17) gives us instantly the extensively used result which links at low-energy the parameter g_0 to the s-wave scattering length a in the first Born approximation, namely

$$g_0 = \frac{2\pi\hbar^2}{\mu} a. \tag{1.23}$$

In pure and especially quasi-low-dimensions, the link between g_0 and the physical quantities of the system necessitates a more careful work [38, 44].

Moving on now to the second order in g_0, we find

$$\psi_{\boldsymbol{k}}(\boldsymbol{r}) = e^{i\boldsymbol{k}.\boldsymbol{r}} + \frac{2\mu}{\hbar^2} g_0 G^D(\boldsymbol{r}) + \frac{2\mu}{\hbar^2} g_0 \int G^D(\boldsymbol{r} - \boldsymbol{r'}) V_\delta(\boldsymbol{r'}) G^D(\boldsymbol{r'}) d\boldsymbol{r'} + O(g_0^3). \tag{1.24}$$

The third term in the right hand side of 1.24 is divergent for $D > 1$. Hence, choosing the V_δ as a model potential fails to describe terms beyond the first Born approximation [8].

We emphasize here that the divergences appear here just because we went *too far* in the simplification of the true interaction. Nevertheless, one can remark that this approach is actually well defined for $D = 1$. Indeed, defining a_{1D} as the zero of the extrapolated one-dimensional wavefunction at $E = 0$, one can recover that using $V_\delta(x) = g_{1D}\delta(x)$ with

$$g_{1D} = \frac{-\hbar^2}{\mu a_{1D}}, \tag{1.25}$$

permits to model the real potential in a much simpler way, keeping its physical implications at low energy as this effective potential leads to the same scattering length.

[8] In fact, one can think that the divergence is due to the singular behavior of the δ- function. However, in three-dimensions, if one changes the δ potential into a soft sphere potential $\delta_\epsilon(r) = 3/4\pi\epsilon^2$ for $r < \epsilon$ and which vanishes for $r > \epsilon$, one can show that when $\epsilon \to 0$, the particles do not see each other, which reveals that the model potential V_δ is not sufficient to describe the interactions of the true potential.

For $D > 1$ we can use the notion of *cut-off* to circumvent the divergences: the idea is basically to introduce a parameter Λ, value at which we cut-off the divergent integrals and which is related to physical limitations of the system or a regime where the theory breaks down. This way, one can define the δ-potential in a more rigorous way for $D = 2$ and $D = 3$ [45]. This cut-off approach is used extensively in physics to remove both infrared and ultraviolet divergences. We point out that one has to make a bridge to real observables such that the final result does not depend on the cut-off parameter. All these processes refer to the approach of regularization and renormalization, which is itself a very wide and interesting topic [46].

The pseudopotential

Going further in the idea of a model potential with a zero range, we now present an efficient method to not deal with divergences for $D > 1$. We will focus on the general idea for the case $D = 3$ and leave the more technical two-dimensional case to Ref. [47].

For $D = 3$, the main goal is to properly account for the $1/r$ divergence when $r \to 0$. This is done by defining the action of an operator, the so-called *pseudo-potential* V_{pp} as

$$V_{\text{pp}}[\psi(\boldsymbol{r})] = g\delta(\boldsymbol{r})\partial_r[r\psi(\boldsymbol{r})]. \tag{1.26}$$

Defining $g \equiv 2\pi\hbar^2 a/\mu$, the exact scattering amplitude of this model potential f_{pp} reads

$$f_{\text{pp}}(k) = \frac{-a}{1+ika}. \tag{1.27}$$

We see that it matches the s-wave scattering amplitude of the true potential at low-energy Eq.(1.18). So in the low-energy limit, V_{pp} describes very well the scattering [9]. This approach is also often called the zero-range approximation, as it involves considering the potential only in the singularity region where $r \to 0$.

In the continuity of this last remark, we mention the Bethe-Peierls approach [48] which encapsulates the same idea as the pseudo-potential, but in the form of a limit condition for the wavefunction ψ, or more specifically, a *contact condition*. It is defined by the following requirements,

$$\begin{cases} \text{For } r \neq 0, \quad -\dfrac{\hbar^2}{2\mu}\boldsymbol{\Delta}_{\boldsymbol{r}}\psi(\boldsymbol{r}) = E\psi(\boldsymbol{r}). & \text{(1.28a)} \\ \text{When } r \to 0, \exists\, C \text{ such that } \quad \psi(\boldsymbol{r}) = C(\dfrac{1}{r} - \dfrac{1}{a}) + O(r). & \text{(1.28b)} \end{cases}$$

Finally, before embarking on the many-body world, let us present a helpful extension of the zero-range approximation for the N-body case.

[9] Note however it leads to a vanishing effective range r_e ($\sim R_e$ for the true potential).

1.4 The method of Skorniakov and Ter-Martirosian

Direct solution of the Schrödinger equation may not be the most efficient way of solving the problem of particles interacting via zero-range potentials. Skorniakov and Ter-Martirosian (STM), by using the zero-range approximation for internucleon forces, reduced the three-body problem of neutron-deuteron scattering to a one-dimensional integral equation [49]. The STM approach [10] has proven its power for many problems with ultracold atoms where the interactions can indeed with a very good accuracy be considered zero range. A great advantage of the method is that it works directly in the zero-range limit using two-body scattering parameters (scattering length, effective range) as the starting point. This allows one to concentrate on few- and many-body processes, bypassing the task of solving the two-body scattering problem on the way. Let us illustrate the general idea behind this method by presenting a self-contained derivation in the one-dimensional case keeping arbitrary N, masses, and number of species for future reference.

The Schrödinger equation for N particles of masses m_i moving in free space and interacting via zero-range potentials with coupling constants g_{ij} reads

$$\left[-\sum_{i=1}^{N}\frac{1}{2m_i}\frac{\partial^2}{\partial x_i^2}-E\right]\psi(x_1,...,x_N)=-\sum_{i<j}g_{ij}\delta(x_i-x_j)\psi(x_1,...,x_N), \tag{1.29}$$

where E is the energy and we set $\hbar=1$. Introducing the Fourier transform $\psi(p_1,...,p_N)=\int e^{-ip_1x_1...-ip_Nx_N}\psi(x_1,...,x_N)dx_1...dx_N$, switching to momentum space, and restricting our analysis to negative energies $E<0$ we rewrite Eq. (1.29) in the form

$$\psi(p_1,...,p_N)=-\frac{\sum_{i<j}g_{ij}\mathcal{F}_{ij}(p_1,...,p_{i-1},p_{i+1},...,p_{j-1},p_{j+1},...,p_N;Q)}{\sum_{i=1}^{N}p_i^2/2m_i-E}, \tag{1.30}$$

where $Q=\sum_{i=1}^{N}p_i$ and $\mathcal{F}_{ij}$ is the Fourier transform of $\delta(x_i-x_j)\psi(x_1,...,x_N)$ or, alternatively, by introducing $\mathbf{P}_{ij}=(p_1,...,p_{i-1},p_{i+1},...,p_{j-1},p_{j+1},...,p_N)$

$$\mathcal{F}_{ij}(\mathbf{P}_{ij};Q)=\int\psi(p_1,...,p_i{}',...,p_j{}',...,p_N)2\pi\delta(p_i{}'+p_j{}'-p_i-p_j)\frac{dp_i{}'dp_j{}'}{(2\pi)^2}. \tag{1.31}$$

The center of mass momentum Q is a conserved parameter and without loss of generality we take $\mathcal{F}_{ij}(\mathbf{P}_{ij};Q)=2\pi\delta(Q)F_{ij}(\mathbf{P}_{ij})$. We can now substitute Eq. (1.30) into Eq. (1.31). This eliminates ψ and straightforwardly leads to the STM equations

[10] We mention that the well known Faddeev equations, used extensively in nuclear physics, can be seen as a generalization of the STM method in the particular case of finite and long-range potentials.

$$F_{ij}(\mathbf{P}_{ij}) = -\int \frac{\sum_{k<l} g_{kl} F_{kl}(\mathbf{P}_{kl})}{\sum_{k=1}^{N} p_k^2/2m_k - E} \delta\left(\sum_{k=1}^{N} p_k\right) \frac{dp_i dp_j}{2\pi}. \tag{1.32}$$

One can think of the function F_{ij} as a wave function for $N-2$ atoms plus a pair with momentum opposite to the total momentum of the atoms. Therefore, there are only $N-2$ arguments in F. The function F_{ij} has the same symmetry with respect to permutation of its arguments as the total wave function ψ. When these symmetries are taken into account, the number of different functions F_{ij} needed to describe the system reduces to the number of coupling constants characterizing the different interactions.

From Eq. 1.32, one usually turns into a numerical approach and puts the equations on a grid to transform it into a matrix problem, thus accessing the desired scattering properties of the system. Note, however, that pretty quickly (for example, the study of a $N = 6$-body problem formed by three pairs of $\uparrow, \downarrow$ particles, hence with three different g_{ij}), these numerics based on deterministic grid methods becomes too hard. One has then to turn into other methods like the Diffusion Monte Carlo technique (DMC) [50].

Chapter 2

LHY and Quantum Stabilization

Contents

2.1 Bose-Bose mixture 24

2.2 Dipolar gases 29

In this chapter, we adopt a many-body viewpoint at $T = 0$, and we present more in detail how one can obtain a dilute self-bound state from bosonic systems with competing attractive and repulsive interactions, where the MF interaction term can be made weak and of the order of the BMF term. We first study the case of the Bose-Bose (BB) mixture in every dimension by calculating the leading BMF term (corresponding to the LHY term) and show how it can stabilize the MF unstable system. This section is based on Ref. [21, 51]. We then briefly mention some insights on bosonic dipolar gases, which share the same interesting feature of quantum stabilization, and which are at the center stage in the recent observation of supersolidity [31–33].

The weakly interacting regime

A usual way to appreciate the many-body interacting problem is to first study the perturbative regime where the interaction between particles is weak. Assuming a short-range potential in D dimensions between particles, we saw earlier one can define a coupling constant g characterizing the strength of a pair interaction, such that we can write the leading interacting energy term as $E_{\mathrm{MF}} = gN^2/2V$. This is true in the so-called weakly interacting regime, where the wavefunction of particles is not influenced by the interaction between them at the mean interparticle distance $l \sim n^{-1/D}$. In other words, if we consider a box of size l containing on average one particle, the interaction energy per particle $I = ng$ has to be much weaker than the kinetic energy $K = \hbar^2/2ml^2$. The weakly interacting regime in D dimensions is then defined by the condition

$$\frac{mgn^{1-2/D}}{\hbar^2} \ll 1. \tag{2.1}$$

In the natural scale (away from resonances), this inequality leads to recover the dilute limit $nR_e^D \ll 1$ we introduced before. Notably, one can see how the dimensions dramatically affect this equation, leading to interesting effects. For example, a decrease in density makes the system more and more interacting in one dimension.

2.1 Bose-Bose mixture

Hamiltonian in the homogeneous case

Let us first consider the problem of the homogeneous bosonic mixture in D dimensions of two components $\sigma = \uparrow, \downarrow$, of densities $n_\uparrow, n_\downarrow$ with same mass m. Following a second quantization formalism, we introduce $\hat{a}^\dagger_{\sigma,\mathbf{k}}$ and $\hat{a}_{\sigma,\mathbf{k}}$, the creation and annihilator operators associated respectively to the creation and destruction of a boson σ with momentum $\mathbf{k}$. The system is governed by the following Hamiltonian

$$H = \sum_{\sigma,\mathbf{k}} \frac{k^2}{2} \hat{a}^\dagger_{\sigma,\mathbf{k}} \hat{a}_{\sigma,\mathbf{k}} + \frac{1}{2} \sum_{\sigma,\sigma',\mathbf{k_1},\mathbf{k_2},\mathbf{q}} \hat{a}^\dagger_{\sigma,\mathbf{k_1}+\mathbf{q}} \hat{a}^\dagger_{\sigma',\mathbf{k_2}-\mathbf{q}} \tilde{U}_{\sigma\sigma'}(\mathbf{q}) \hat{a}_{\sigma,\mathbf{k_1}} \hat{a}_{\sigma',\mathbf{k_2}}, \tag{2.2}$$

where we set $m = \hbar = 1$, and $\tilde{U}_{\sigma\sigma'}$ represent the Fourier transform of the short-range interaction potentials $U_{\sigma\sigma'}$ between the components. As introduced in Sec 1.3, we use effective potentials with the same scattering properties at low-energy but easier to manipulate: we then substitute $U_{\sigma\sigma'}$ by a simple contact interaction characterized by a bare coupling constant $g_{\sigma\sigma}$ which satisfies the weakly interacting criterion Eq.(2.1). [1]

Below, we use the standard Bogoliubov theory to derive the ground state energy density. The idea is to treat the mixture as an almost ideal gas as we consider that the different components are weakly interacting. Hence we assume a macroscopic occupation of the ground state $N_{\sigma,p=0} = N_{\sigma,0} \simeq N_\sigma \gg 1$, and $N_{\sigma,p\neq 0}/N_\sigma$ is assumed very small. Under these conditions, the operators $\hat{a}_{\sigma,0} = \hat{a}^\dagger_{\sigma,0}$ become numbers ($= \sqrt{n_{0,\sigma}}$).

MF approach and Stability

The zeroth order of the expansion in terms of operators $\hat{a}_{\sigma,p\neq 0}$ (and in the first order of g) give us the MF energy density of the system, namely

$$\frac{E_{\rm MF}}{\Omega_D} = \frac{g_{\uparrow\uparrow} n_\uparrow^2 + g_{\downarrow\downarrow} n_\downarrow^2 + 2 g_{\uparrow\downarrow} n_\uparrow n_\downarrow}{2}, \tag{2.3}$$

where we introduce Ω_D as the volume in D dimensions. This quadratic form Eq.(2.3) is stable with respect to small changes in densities if it is positive definite, namely if

$$g_{\uparrow\uparrow} > 0 \quad , \quad g_{\downarrow\downarrow} > 0 \quad \text{and} \quad g_{\uparrow\downarrow}^2 < g_{\uparrow\uparrow} g_{\downarrow\downarrow}. \tag{2.4}$$

In the regime where $|g_{\uparrow\downarrow}| < \sqrt{g_{\uparrow\uparrow} g_{\downarrow\downarrow}}$ the two condensates overlap: the system is miscible. For $g_{\uparrow\downarrow} > \sqrt{g_{\uparrow\uparrow} g_{\downarrow\downarrow}}$, the system is not miscible since the repulsive interspecies interaction is so large than the system separate spatially the two species to minimize its energy. For $g_{\uparrow\downarrow} < -\sqrt{g_{\uparrow\uparrow} g_{\downarrow\downarrow}}$, the system collapses as the intraspecies interactions cannot overcome the interspecies attraction. The transition between the miscible and immiscible phase, as well as the transition to the collapse region has already been extensively studied.

Taking into account the external potential and finite temperature effects, Eq. (2.4) has to be slightly modified [52], but we will neglect these modifications in what follows.

The LHY term

Let us now calculate the next order correction to the ground state energy to the second order in $g \sim g_{\sigma\sigma'}$. The first order terms of the Bogoliubov expansion vanish by conservation of momentum. Hence, we expand Eq. (2.2) up to bilinear terms in the operators $\hat{a}^\dagger_{\sigma,\mathbf{k}}$ and $\hat{a}_{\sigma,\mathbf{k}}$ for $k \neq 0$ and we diagonalize the resulting form using an adequate linear transformation, arriving at the following energy density [53]

[1] For the sake of simplicity, we present this common method. If one wants to be formally more rigorous, a pseudopotential or a cutoff approach would remove unwanted divergences which will appear from this simple choice, see Sec 1.3.

$$\frac{E}{\Omega_D} = \underbrace{\frac{g_{\uparrow\uparrow}n_\uparrow^2 + g_{\downarrow\downarrow}n_\downarrow^2 + 2g_{\uparrow\downarrow}n_\uparrow n_\downarrow}{2}}_{\text{MF term}} + \underbrace{\frac{1}{2}\sum_{\pm}\sum_{\mathbf{k}}\left[E_\pm(k) - k^2/2 - c_\pm^2\right]}_{\text{LHY term}}, \tag{2.5}$$

$$E_\pm(k) = \sqrt{c_\pm^2 k^2 + k^4/4} \quad , \quad c_\pm^2 = \frac{g_{\uparrow\uparrow}n_\uparrow + g_{\downarrow\downarrow}n_\downarrow \pm \sqrt{\left(g_{\uparrow\uparrow}n_\uparrow - g_{\downarrow\downarrow}n_\downarrow\right)^2 + 4g_{\uparrow\downarrow}^2 n_\uparrow n_\downarrow}}{2}. \tag{2.6}$$

The first term of Eq. (2.5) corresponds to the MF energy density, whereas the second term refers to the leading order correction term known as the LHY correction and arising from quantum fluctuations. As we can see, in contrast to the single-component gas, the Bogoliubov treatment of our mixture gives two excitation branches $E_\pm$ with different sound velocities $c_\pm$. Notably, the integral over the momentum in the present Eq. (2.5) leads to ultraviolet divergences for $D > 1$, due to the oversimplification of the bare effective potential we chose.

Let us first discuss the case $D = 3$, and write $\Omega_3 = V$. We saw in the previous chapter that the relation $g_{\sigma\sigma} = 4\pi a_{\sigma\sigma'}$ holds for the first Born approximation but not beyond. The common method to take care of this artefact is then to formally renormalize the bare coupling constants in the first term of Eq. (2.5) to take care of the second Born approximation $g_{\sigma\sigma'} \to g_{\sigma\sigma'}(1 + g_{\sigma\sigma'}/V\sum_k 1/k^2)$ [13].

We can then perform analytically the integral associated with the LHY term to obtain

$$\frac{E_{\text{LHY}}}{V} = \frac{8}{15\pi^2}(c_+^5 + c_-^5). \tag{2.7}$$

Crucially, in contrast to the single-component gas, we see that the MF and LHY terms depend on a different combination of $g_{\sigma\sigma'}n_\sigma$ and can be then controlled independently. Note that the main contribution to this integral comes from momenta of order $1/\xi = \sqrt{gn}$, the inverse of the so-called *healing length*.

Quantum stabilization

Introducing $\delta g = g_{\uparrow\downarrow} + \sqrt{g_{\uparrow\uparrow}g_{\downarrow\downarrow}}$, we look at the regime where δg is negative, hence collapsing from the MF viewpoint [see Eq.(2.4)] and very small compared to $g = \sqrt{g_{\uparrow\uparrow}g_{\downarrow\downarrow}}$ i.e. close to the MF collapse line. In this region, the MF term fixes the densities ratio to $n_2/n_1 = \sqrt{g_{\uparrow\uparrow}/g_{\downarrow\downarrow}}$ as it is energetically favorable. Looking at the LHY term, we remark that since in the region $k \sim 1/\xi$ mostly contributing to the integral, $E_\pm$ are not sensitive to small variations of δg and its sign, we can still use the LHY form calculated in Eq.(2.7) [2]. Close to the MF collapse line, there is a softening of the lower Bogoliubov mode such

[2] A careful derivation actually shows that for small momenta $k \sim \sqrt{m|\delta g|n}$, E_- becomes complex, reflecting instability. However, this effect can be carefully neglected as it is related to a higher order correction in $\delta g/g$ [54].

that $c_- \ll c_+$. Therefore we can consider that only the *hard* branch c_+ will contribute to the LHY term. Assuming $g \sim g_{\uparrow\uparrow} \sim g_{\downarrow\downarrow}$ to enhance the energy dependence on the different parameters easily, we find by omitting prefactors

$$\frac{E}{V} \sim \delta g n^2 + (gn)^{5/2}. \tag{2.8}$$

For $\delta g < 0$, that is to say, a MF attraction, the repulsive LHY term prevents the system from collapsing, and the energy per particle exhibits a minimum at $n_0 \sim a^{-3}(\delta g/g)^2$ corresponding to the apparition of a self-bound state: a liquidlike droplet (see Fig.2.1). Indeed, in addition to its self-bound property, it exhibits a saturation of the peak density characteristic of a liquid with low compressibility. Moreover, as it remains in the weakly interacting regime, it strikingly differs from droplets like atomic nuclei or helium, which are strongly correlated self-bound systems [34, 55, 56].

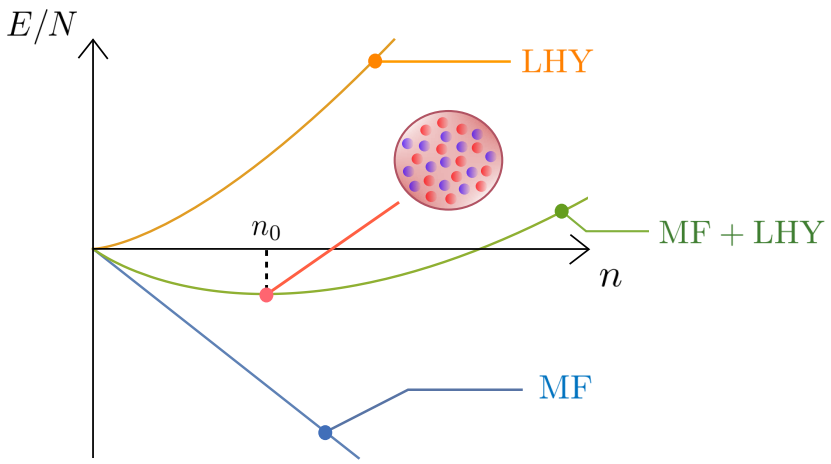

Figure 2.1: Energy per particle E/n as a function of the density n close to the MF collapse line for the three-dimensional BB mixture. The quantum stabilization of the MF attractive term (in blue) by the repulsive LHY term (in orange) leads to the existence of a liquidlike droplet at the density n_0 (small red and purple disks play the role of the two species $\uparrow$ and $\downarrow$).

To have an insight into the equilibrium and dynamic aspect of this system in actual experiments, note that the LHY correction can be cast in the form of an effective local term added to the mean-field Gross-Pitaevskii energy-density functional for two components of a homonuclear mixture, if we assume they have the same spatial mode. Note then that the three-body recombination also has to be included in the model since the larger density of the droplet compared to the gas leads to rapid losses.

Finally, a careful study of the droplet properties, as the necessity of a critical atom

number to exist, its surface modes, and its capacity to self evaporate, are described in detail in Ref. [21].

Low dimensional cases

As we can see from the previous paragraphs, apart from the appropriate definition of the coupling constant $g_{\sigma\sigma}$, the dimension of space enters our problem in the calculation of the LHY term, which carries a sum in the momentum space.

Two-dimensional case

In 2D, we take care of the ultraviolet divergence thanks to a more careful definition of the coupling constant by introducing a cutoff κ such that

$$g_{\sigma\sigma'}(q) = \begin{cases} 2\pi/\ln\left(2e^{-\gamma}/a^{2D}_{\sigma\sigma'}\kappa\right) \text{ for } q \leq \kappa \\ 0 \text{ for } q > \kappa \end{cases} \tag{2.9}$$

where γ is the Euler's constant and $a^{2D}_{\sigma\sigma'}$ is the s-wave two-dimensional scattering length [38]. Performing the LHY integral, and rewriting $\Omega_2 = S$ we find

$$\frac{E_{2D}}{S} = \frac{E_{\rm MF}}{S} + \frac{1}{8\pi}\sum_{\pm} c_{\pm}^4 \ln\left(\frac{c_{\pm}^2}{\kappa^2}\right). \tag{2.10}$$

One can actually verify that to the second-order in g, this result does not depend on the value κ. A striking difference with the three-dimensional case is that the liquid phase exists whenever the interspecies interaction is weakly attractive and the intraspecies are weakly repulsive close to the MF collapse line (i.e., not just when $\delta g < 0$). The energy density reads

$$\frac{E}{S} \sim g^2 n^2 (\ln\frac{n}{n_0} - 1). \tag{2.11}$$

Interestingly, a quasi-low dimensional analysis of the symmetric mixture ($a^{3D}_{\uparrow\uparrow} = a^{3D}_{\downarrow\downarrow} = a^{3D}$) permits to study the crossover between three and two dimensions: in the regime where $0 < -a^{3D}_{\uparrow\downarrow} < a^{3D}$, the mixture is in gas phase for $D = 3$. If one then confines the mixture in one direction providing $a^{3D} \ll l_0$ with l_0 the oscillator length in the confined direction, the system goes into a liquid phase !

One-dimensional case

In 1D, there is no condensate, but it is known that the Bogoliubov theory describes well the properties of the weakly interacting Bose gas [57]. For the LHY term, there is here no problem of divergence, and we use simply $g_{\sigma\sigma'} = -2/a^{1D}_{\sigma\sigma'}$, where $a^{1D}_{\sigma\sigma'}$ is the one-dimension s-wave scattering length. The LHY integral is then calculated analytically, where we set $\Omega_1 = L$

$$\frac{E_{1D}}{L} = \frac{E_{\mathrm{MF}}}{L} + \frac{2}{3\pi}\sum_{\pm} c_{\pm}^3. \tag{2.12}$$

In the regime where $|\delta g|/g \ll 1$, i.e. close to the MF collapse line, the energy density reads

$$\frac{E}{L} \sim \delta g n^2 - (gn)^{3/2}. \tag{2.13}$$

Here, we observe a surprising behavior: the LHY correction is effectively attractive, meaning the mixture goes in the liquid phase close to the MF collapse line for a weak MF repulsion ($\delta g > 0$).

As we just saw, each low dimensional case has peculiar features compared to the three-dimensional one. In the next chapter, we focus on the one-dimensional system and explore more about its phase diagram: what happens if we go in the strong interaction regime, where the ratio $\delta g/g$ is large?

2.2 Dipolar gases

As mentioned in the introduction, dipolar BEC was the first system where one observed the formation of a dilute self-bound state arising from BMF effects. This was done using Dy or Er atoms, which feature naturally strong magnetic dipolar-dipolar interaction. The formation of this exotic state is explained by the same mechanism as for a BB mixture in three dimensions, thanks to a repulsive LHY term that counterbalances a MF attraction predicting collapse. We discuss here some similarities and differences with BB mixtures and take advantage of this comparison by introducing some peculiar features of BEC dipolar gases for future chapters. The topic of dipolar gases is so wide that we leave here a useful review to enter its very rich physics [58].

Let us consider first a BEC of magnetic dipoles in three-dimensions in the homogeneous case, of density n with dipole moments $\boldsymbol{m}$ oriented along the direction $\boldsymbol{z}$ of a magnetic field $\boldsymbol{B}$. The interaction V_{int} between two dipoles of relative position $\boldsymbol{r}$ reads

$$V_{\mathrm{int}}(\boldsymbol{r}) = g\delta(\boldsymbol{r}) + \underbrace{\frac{C_{dd}}{4\pi r^3}(1 - 3\cos^2\theta)}_{V_{dd}}, \tag{2.14}$$

where $g = 4\pi a$ is the coupling constant characterizing the short-range interaction with a the s-wave scattering length, and where V_{dd} represents the dipole-dipole interaction (DDI) with $C_{dd} = \mu_0|\boldsymbol{m}|^2$ being the dipolar interaction strength (μ_0 is the vacuum permittivity). Finally, θ is the angle between $\boldsymbol{r}$ and the polarization direction $\boldsymbol{z}$. Importantly, from now on, we will limit ourselves to the case of repulsive contact interaction $a > 0$ in order to avoid local collapse of the system [59].

From the definition of the total interaction, one can see that there is a short- and long-range interaction that can compete with each other (such as the inter- and intra-species for BB mixture), leading to a regime where the overall MF term can be made weak and of the order of the BMF correction. One of the significant differences from the mixture case will lie in the anisotropy of the long-range interaction.

If we Fourier transform Eq.(2.14), we obtain

$$\tilde{V}_{\text{int}}(\boldsymbol{k}) = g[1 + \epsilon_{dd}(3\cos^2\theta_{\boldsymbol{k}} - 1)], \tag{2.15}$$

where $\theta_{\boldsymbol{k}}$ is the angle between the vector $\boldsymbol{k}$ and the polarization direction $\boldsymbol{z}$ and where we introduced $\epsilon_{dd} = a_{dd}/a_s$ with $a_{dd} = C_{dd}/12\pi$ the length associated to the DDI. As the reader might see, ϵ_{dd} then characterizes the competition between the DDI and the contact interactions. When $\epsilon_{dd} \sim 1$ we then expect to observe interesting BMF effects.

Importantly, the anisotropy leads us to a problem to define the MF energy density in the homogeneous three-dimensional case. This can be understood by the non uniqueness of the MF value of the chemical potential since

$$\mu_{\text{MF}} = n \lim_{\boldsymbol{k}\to\boldsymbol{0}} \tilde{V}_{\text{int}}(\boldsymbol{k}). \tag{2.16}$$

Indeed, since physically μ_{MF} represents the value of energy necessary to bring one dipole at infinity into the condensate, we understand that for a particle coming from an infinitely parallel or a perpendicular direction to the magnetic field, the result will be different. This problem is not present in the inhomogeneous systems [60, 61] (which is associated with the real case of experiments !) where the MF term depends dramatically on the trap anisotropy and is usually derived through a Gross Pitaevskii formalism. In the usual case of harmonic confinement, we just mention that the ratio of the trapping frequencies $\lambda = \omega_\perp/\omega_\parallel$, where $\omega_\perp$ (resp. $\omega_\parallel$) is the trapping frequency perpendicular (resp. parallel) to the polarization direction, plays a key role in the phase diagram of the system [58, 62, 63].

However, let us continue our discussion in the homogeneous case for the sake of simplicity. It is motivated by the fact that the results we derive here from homogeneous cases can be included in the more realistic models using a local-density approximation (LDA) [64,65] [3]. In this approximation, the homogeneous leading BMF term we calculate is then typically cast into a so-called extended Gross-Pitaevskii equation (eGPE) [34].

Hence, let us perform a Bogoliubov approach of the homogeneous BEC dipolar gas. From its common formalism, we obtain one excitation branch E_d with a sound velocity c which read

[3] LDA assumes that the system is locally homogeneous such that we introduce a space-dependent chemical potential $\mu(r) = \mu_h - V_{\text{trap}}(r)$, where μ_h is the homogeneous chemical potential and V_{trap} the trapping potential

$$E_d(\boldsymbol{k}) = \sqrt{c^2(\theta_{\boldsymbol{k}})k^2 + k^4/4}, \qquad \text{and} \qquad c^2(\theta_{\boldsymbol{k}}) = gn[1 + \epsilon_{dd}(3\cos^2\theta_{\boldsymbol{k}} - 1)], \quad (2.17)$$

First, let us point out the anisotropy of the sound velocity, which is a peculiar feature of DDIs and which has been observed in a group of Paris [66]. Secondly, we observe that for small momenta such that $\cos^2\theta_{\boldsymbol{k}} < 1/3$ and in the regime where $\epsilon_{dd} > 1$, E_d becomes imaginary, consistent with the fact that the system becomes unstable. Indeed, the system collapses due to the partial attraction of the dominant DDI, similar to one-component Bose gas characterized by a short-range attraction.

In the stable regime where $0 < \epsilon_{dd} < 1$ we can calculate the LHY integral (renormalizing the contact interaction as we did for BB mixture) leading to write [64]

$$\frac{E_{\text{LHY}}}{V} = \frac{8}{15\pi^2}\langle c^5(\hat{k})\rangle_{\hat{\boldsymbol{k}}}, \quad (2.18)$$

where $\langle f\rangle_{\hat{\boldsymbol{k}}} = \frac{1}{4\pi}\int d\phi_{\boldsymbol{k}} d\theta_{\boldsymbol{k}} \sin\theta_{\boldsymbol{k}} f(\boldsymbol{k})$ is the average of the function f over its angular part in three dimensions. In this form, one can appreciate the similarities and differences with the BB mixture Eq.(2.7), since we find again $E_{\text{LHY}} \propto n^{5/2}$. Here, the main contribution to the LHY integral comes from the *hard* modes $\cos^2\theta_{\boldsymbol{k}} > 1/3$.

Note that as opposed to the MF term, the LHY correction suffers no problem of definition when $\boldsymbol{k} \to 0$, stemming from the fact the LHY term is defined by an integral over all the possible momentum.

Close to $\epsilon_{dd} \sim 1$, we saw that the system becomes unstable. However in the same spirit as for BB mixtures, we can still use the expression Eq.(2.18) since in this regime, the *soft* modes $\cos^2\theta_{\boldsymbol{k}} < 1/3$ can be neglected compared to the stable hard modes $\cos^2\theta_{\boldsymbol{k}} > 1/3$ which mostly contribute to the LHY term. Therefore, close to the limit when the system becomes partially attractive $\epsilon_{dd} \sim 1$, the system is stabilized by a repulsive LHY term [61, 65, 67].

As mentioned before, a more careful study is needed to appreciate the rich physics in dipolar gases, where one takes into account the interaction parameters a_{dd}, a, but also the trap geometry parameter such as λ as or the atom number N. It leads then to a wide variety of exotic phases: dilute BEC, single droplet, multidroplet, array of droplets, with indeed, ultimately, the supersolid state [26–29, 34, 68].

We just presented two systems (BB mixture, dipolar gases) where the leading BMF term corresponds to the LHY term in a particular regime. Nevertheless, as mentioned in the introduction, it is not always the case. There are various reasons to consider other configurations where the LHY term is not the dominant BMF term (single-component contact-interacting atoms, low-dimensional geometries, etc.). In these cases, an effective three-body interaction, associated with a three-body term $\propto n^3$ in the energy density can become dominant if the leading-order two-body forces are suppressed. In particular,

we have already mentioned systems where three-body forces have been considered in the context of droplet formation in three dimensions [15, 20].

In the next chapters, following mainly a few-body approach of systems close to a two-body zero crossing, we will discuss BMF effects associated with effective three-body forces.

Chapter 3

One dimensional Bose-Bose mixture

Contents

3.1 Dimer-dimer zero crossing and dilute dimerized liquid . . . 34

3.1.1 Trimer energy . . . 34

3.1.2 Dimer-dimer scattering problem . . . 36

3.1.3 Dilute liquid of dimers . . . 38

3.1.4 Discussion and outlook . . . 41

3.2 Three-boson problem with two- and three-body interactions 43

3.2.1 Derivation of the formula . . . 44

3.2.2 Back to the 1D mixture problem . . . 48

In this chapter, we present the first results of this thesis: we explore the rich physics of the one-dimensional BB mixture, and we provide an analytical solution of the three-boson problem with two-body and three-body interactions. This chapter is divided into two parts.

3.1 Dimer-dimer zero crossing and dilute dimerized liquid

Background and Goal

In Chapter 2, we saw that the one-dimensional BB mixture collapses for $g_{\uparrow\downarrow} < -\sqrt{g_{\uparrow\uparrow}g_{\downarrow\downarrow}}$ and liquefies otherwise (due to the existence of an effectively attractive LHY correction) close to the MF collapse line $g_{\uparrow\downarrow} = -\sqrt{g_{\uparrow\uparrow}g_{\downarrow\downarrow}}$, where the weakly-interacting regime is valid and where the saturation density of the liquid is high [51].

Departing from this line (by increasing $g_{\sigma\sigma}$ or decreasing $|g_{\uparrow\downarrow}|$) makes the system more dilute, which, in one dimension, leads to stronger correlations. For $g_{\sigma\sigma} \gg |g_{\uparrow\downarrow}|$ the one-dimensional mixture with equal $\uparrow$ and $\downarrow$ populations eventually becomes a gas of $\uparrow\downarrow$ dimers with interdimer repulsion. Indeed, in the limit $g_{\uparrow\uparrow} = g_{\downarrow\downarrow} = \infty$ the two bosonic components can individually be mapped to noninteracting fermions [69, 70], and their mixture becomes equivalent to the exactly solvable fermionic Gaudin-Yang model [71–73] which has no bound states other than $\uparrow\downarrow$ dimers.

Our goal is then to make a step towards understanding the nonperturbative intermediate region by starting from the repulsive gas of dimers and decreasing the ratio $g_{\uparrow\uparrow}g_{\downarrow\downarrow}/g_{\uparrow\downarrow}^2$ for finite generally different intraspecies coupling constants (see Fig. 3.1).

This chapter is organized as follows. In Sec. 3.1.1 we calculate the $\uparrow\uparrow\downarrow$ trimer binding energy and thus determine the trimer-formation threshold in dimer-dimer collisions. In Sec. 3.1.2 we find the dimer-dimer scattering parameters in the regime of a nearly vanishing effective dimer-dimer interaction. In Sec. 3.1.3 we apply the mean-field theory of Bulgac to the dilute system of dimers taking care of the one-dimensional three-dimer interaction. In Sec. 3.1.4 we discuss other possible scenarios for the mixture and present an outlook for further studies.

3.1.1 Trimer energy

Before we embark on the dimer-dimer scattering let us make a brief detour into the three-body problem. We need to know the trimer binding energies in order to determine the trimer-formation threshold in dimer-dimer collisions. In the considered case of repulsive intraspecies couplings three identical bosons do not bind. Below, we analyze the $\uparrow\uparrow\downarrow$ combination, the results being obviously valid for the $\uparrow\downarrow\downarrow$ system upon interchanging $g_{\uparrow\uparrow}$

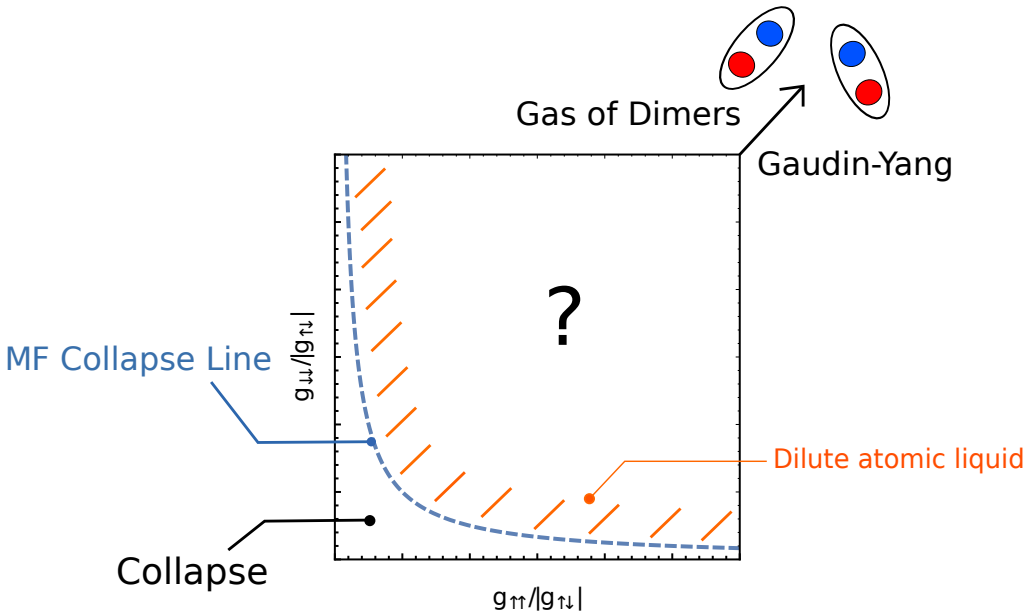

Figure 3.1: Initial knowledge of the phase diagram in the plane $\{g_{\uparrow\uparrow}/|g_{\uparrow\downarrow}|, g_{\downarrow\downarrow}/|g_{\uparrow\downarrow}|\}$ at the stage of the introduction. In blue is shown the MF collapse line which separates the collapse region below, and the stability region above. We know that close to this mean-field collapse line there is the existence of a dilute atomic liquid (region in orange). Finally, in the limit $g_{\uparrow\uparrow} = g_{\downarrow\downarrow} = \infty$ we have a gas $\uparrow\downarrow$ dimers. The idea is to start from this point and decrease the ratio $g_{\uparrow\uparrow}g_{\downarrow\downarrow}/g_{\uparrow\downarrow}^2$ to access to the unknown region (cf. question mark).

and $g_{\downarrow\downarrow}$ (we consider $m_\uparrow = m_\downarrow$). The $\uparrow\uparrow\downarrow$ trimer can be formed if $\epsilon_{\uparrow\uparrow\downarrow}$ is smaller than E, which, for zero dimer-dimer collision energy, equals twice the $\uparrow\downarrow$ dimer energy.

Consider the $\uparrow\uparrow\downarrow$ equal-mass bosonic problem characterized by the coupling constants $g_{\uparrow\uparrow} = -2/a_{\uparrow\uparrow}$ and $g_{\uparrow\downarrow} = -2/a_{\uparrow\downarrow} < 0$, where $a_{\sigma\sigma'}$ are the one-dimensional scattering lengths and we set $m_\uparrow = m_\downarrow = 1$. We apply the STM method presented in Chapter 1 where 1 and 2 refer to $\uparrow$ particles and 3 to the $\downarrow$ particle. We can write $F_{\uparrow\uparrow}(p) = F_{12}(p)$ and $F_{\uparrow\downarrow}(p) = F_{13}(p) = F_{23}(p)$, the latter equality follows from Eq. (1.31) and the symmetry $\psi(p_1, p_2, p_3) = \psi(p_2, p_1, p_3)$. The STM equations read

$$\begin{aligned}\left(1 + \frac{g_{\uparrow\uparrow}}{\sqrt{3p^2 - 4E}}\right) F_{\uparrow\uparrow}(p) &= \int \frac{2g_{\uparrow\downarrow}F_{\uparrow\downarrow}(q)}{E - p^2 - pq - q^2}\frac{dq}{2\pi}, \\ \left(1 + \frac{g_{\uparrow\downarrow}}{\sqrt{3p^2 - 4E}}\right) F_{\uparrow\downarrow}(p) &= \int \frac{g_{\uparrow\downarrow}F_{\uparrow\downarrow}(q) + g_{\uparrow\uparrow}F_{\uparrow\uparrow}(q)}{E - p^2 - pq - q^2}\frac{dq}{2\pi}.\end{aligned} \tag{3.1}$$

In Fig. 3.2 we plot the trimer energy $\epsilon_{\uparrow\uparrow\downarrow} < 0$ in units of the dimer binding energy $|\epsilon_{\uparrow\downarrow}| = 1/a_{\uparrow\downarrow}^2$ as a function of the ratio $g_{\uparrow\uparrow}/|g_{\uparrow\downarrow}|$. The curve is obtained by discretizing the momentum, transforming the integrals in Eqs. (3.1) into sums, and solving the resulting matrix-eigenvalue problem. Also shown are the atom-dimer (dotted) and dimer-dimer (dashed) scattering thresholds, as well as the ground state energy of three identical

attractive bosons (see red circle).

For the considered case of negative $g_{\uparrow\downarrow}$ the $\uparrow\uparrow\downarrow$ trimer is always bound. However, in the limit $g_{\uparrow\uparrow} = \infty$ the trimer binding energy $\epsilon_{\uparrow\uparrow\downarrow} - \epsilon_{\uparrow\downarrow}$ vanishes and the atom-dimer even-channel scattering length diverges. This limit is a particular case of the exactly solvable $N + 1$ McGuire [74, 75] or more general Gaudin-Yang model [71, 72] of attractive spin-1/2 fermions. The connection with our bosonic system is obtained by the wave-function mapping $\psi_{\text{Bose}}(x_{\uparrow 1}, x_{\uparrow 2}, x_{\downarrow}) = \psi_{\text{Fermi}}(x_{\uparrow 1}, x_{\uparrow 2}, x_{\downarrow})\text{sign}(x_{\uparrow 1} - x_{\uparrow 2})$ [69, 70]. In the fermionic case it is thus the odd-channel atom-dimer scattering length that diverges. The explicit expression for the atom-dimer transmission amplitude (there is no reflection) in this case is given in Ref. [76].

The trimer state deepens with decreasing $g_{\uparrow\uparrow}/|g_{\uparrow\downarrow}|$. We find numerically that it crosses the dimer-dimer threshold, i.e., its energy equals $\epsilon_{\uparrow\uparrow\downarrow} = 2\epsilon_{\uparrow\downarrow}$, for $g_{\uparrow\uparrow} = 0.0738|g_{\uparrow\downarrow}|$. It is worth mentioning that for $g_{\uparrow\uparrow} = -|g_{\uparrow\downarrow}|$ the ground state of our $\uparrow\uparrow\downarrow$-system is the same as the ground state of three identical attractive bosons. The trimer energy here equals four times the dimer energy [77].

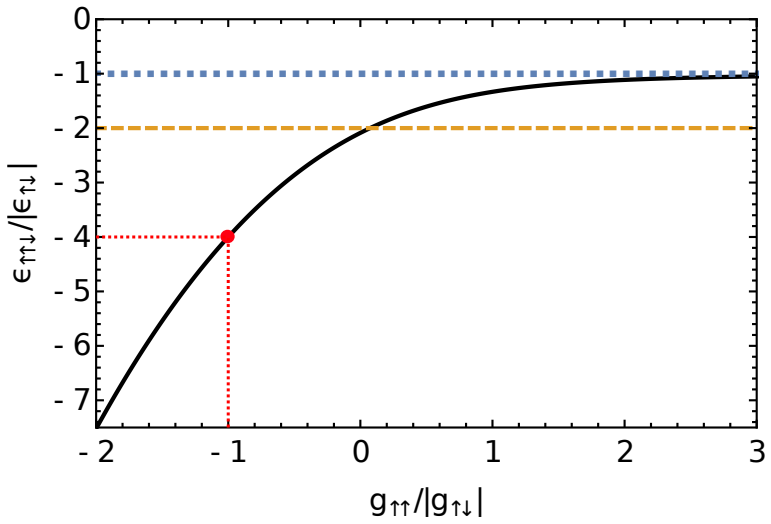

Figure 3.2: The $\uparrow\uparrow\downarrow$-trimer energy in units of the $\uparrow\downarrow$-dimer energy as a function of $g_{\uparrow\uparrow}/|g_{\uparrow\downarrow}|$ (solid). The dotted and dashed lines indicate, respectively, the atom-dimer and dimer-dimer scattering thresholds. The red circle indicates the ground state energy of three identical attractive bosons.

3.1.2 Dimer-dimer scattering problem

Consider now the scattering problem of two $\uparrow\downarrow$ dimers and let 1 and 2 refer to $\uparrow$ particles and 3 and 4 – to $\downarrow$ particles. Then, from Eq. (1.31) and from the symmetry relations $\psi(p_1, p_2, p_3, p_4) = \psi(p_2, p_1, p_3, p_4) = \psi(p_1, p_2, p_4, p_3) = \psi(p_2, p_1, p_4, p_3)$, one can show that $F_{13} = F_{14} = F_{23} = F_{24}$. We thus denote this function by $F_{\uparrow\downarrow}$ and also define $F_{\uparrow\uparrow} = F_{12}$ and $F_{\downarrow\downarrow} = F_{34}$. Equations (1.32) then transform into a set of three coupled two-dimensional homogeneous equations for $F_{\sigma\sigma'}$. We do not write these rather bulky equations to avoid

cluttering. However, they are well suitable for numerical calculations on a grid. Let us just explain how we deduce the dimer-dimer scattering amplitude from the numerics.

We look for the dimer-dimer scattering solution at the collision energy $p_0^2/2$, which corresponds to $E = -2|\epsilon_{\uparrow\downarrow}| + p_0^2/2$. In real space, when the two dimers are separated from each other by more than their size, $|x_1 + x_3 - x_2 - x_4|/2 \gg a_{\uparrow\downarrow}$, the four-body wave function factorizes into

$$\psi(x_1, x_2, x_3, x_4) \approx \phi_0(x_{13})\phi_0(x_{24})\chi[(x_1 + x_3 - x_2 - x_4)/2], \tag{3.2}$$

where $x_{ij} = x_i - x_j$, $\phi_0(r) = \sqrt{1/a_{\uparrow\downarrow}}\exp(-|r|/a_{\uparrow\downarrow})$ is the normalized dimer wave function, $\chi(R) = \cos(p_0 R) + f(p_0)\exp(ip_0|R|)$ describes the relative dimer-dimer motion, and $f(p_0)$ is the dimer-dimer scattering amplitude.

In order to understand the behavior of $F_{\uparrow\downarrow}(p_2, p_4)$ corresponding to the asymptote (3.2) we multiply Eq. (3.2) by $\delta(x_{13})$ and Fourier transform it arriving at $\mathcal{F}_{13}(p_2, p_4; Q) = 2\pi\delta(Q)F_{\uparrow\downarrow}(p_2, p_4)$ with $F_{\uparrow\downarrow}(p_2, p_4) \propto \tilde{\phi}_0[(p_2 - p_4)/2]\tilde{\chi}(-p_2 - p_4)$, where $\tilde{\phi}_0$ and $\tilde{\chi}$ are Fourier transforms of ϕ_0 and χ, respectively. Accordingly, $F_{\uparrow\downarrow}(p_2, p_4)$ has a singularity at $|p_2 + p_4| = p_0$, close to which it behaves as

$$F_{\uparrow\downarrow}(p_2, p_4) \propto \frac{2\pi\delta(|P| - p_0) - 4ip_0 f(p_0)/(P^2 - p_0^2 - i0)}{p^2 + 1/a_{\uparrow\downarrow}^2}, \tag{3.3}$$

where we have introduced the pair center-of-mass and relative-coordinate representation, $P = p_2 + p_4$ and $p = (p_2 - p_4)/2$. Motivated by Eq. (3.3) we make the substitution

$$F_{\uparrow\downarrow}(p_2, p_4) = \frac{2\pi\delta(|P| - p_0) - 4G(P, p)/(P^2 - p_0^2)}{p^2 + 1/a_{\uparrow\downarrow}^2} \tag{3.4}$$

in the STM equations and obtain an inhomogeneous set of equations for G, $F_{\uparrow\uparrow}$, and $F_{\downarrow\downarrow}$. For numerical convenience we restrict ourselves to real-valued functions and understand integration of terms proportional to $1/(P^2 - p_0^2)$ in the principal-value sense. Once G is calculated, f can be deduced by comparing Eqs. (3.3) and (3.4) and by using the convention $1/(P - p_0 - i0) = 1/(P - p_0) + \pi i\delta(P - p_0)$. We arrive at the identification

$$f(p_0) = -\frac{1}{1 - ip_0/G(p_0)}, \tag{3.5}$$

where $G(p_0) = G(p_0, p)$ does not depend on p. The value $G(p_0)$ thus determines the dimer-dimer scattering amplitude and, in particular, the dimer-dimer effective-range expansion through $G(p_0) = -1/a_{\rm dd} + r_e p_0^2/2 + ...$, where $a_{\rm dd}$ and r_e are, respectively, the dimer-dimer scattering length and effective range. The dimer-dimer coupling constant is defined as $g_{\rm dd} = -1/a_{\rm dd} = G(0)$. More generally, one can think of $G(p_0)$ as the energy-dependent coupling constant.

The solid black curve in Fig. 3.3 corresponds to the values of $g_{\uparrow\uparrow}/|g_{\uparrow\downarrow}|$ and $g_{\downarrow\downarrow}/|g_{\uparrow\downarrow}|$

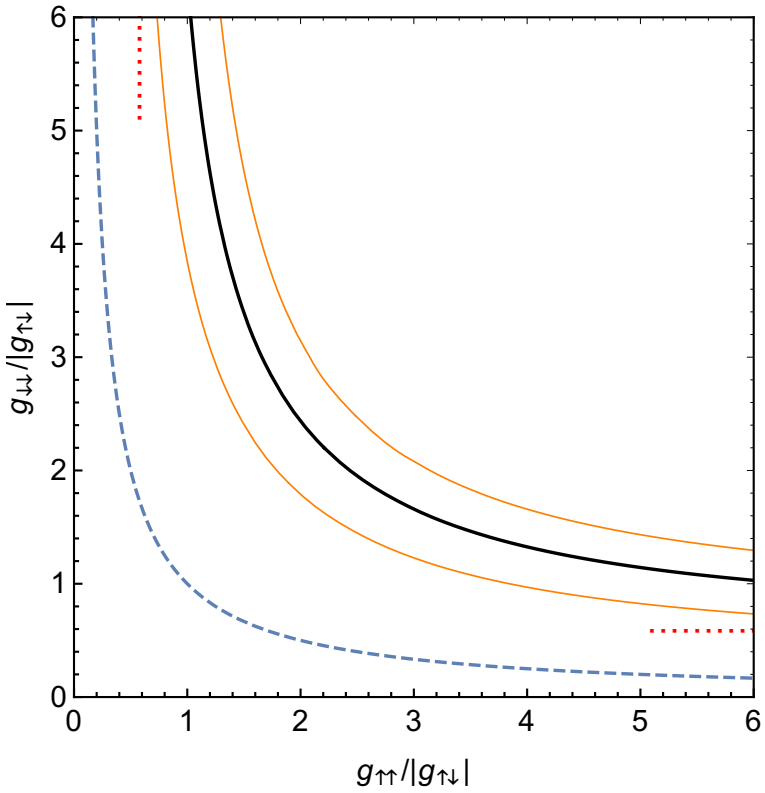

Figure 3.3: Zero crossing for the interaction between two $\uparrow\downarrow$ dimers (thick black). The dotted red horizontal and vertical lines are the corresponding asymptotes for $g_{\uparrow\uparrow} = \infty$ and $g_{\downarrow\downarrow} = \infty$, respectively. The thin orange curves indicate parameters where $g_{\rm dd}/|g_{\uparrow\downarrow}| = 0.1$ (upper curve) and -0.1 (lower curve). The dashed blue curve is the mean-field collapse boundary $g_{\uparrow\downarrow} = -\sqrt{g_{\uparrow\uparrow} g_{\downarrow\downarrow}}$.

where $g_{\rm dd}$ vanishes and $a_{\rm dd}$ diverges. This curve is obviously symmetric with respect to the interchange of $g_{\uparrow\uparrow}$ and $g_{\downarrow\downarrow}$. For infinite $g_{\uparrow\uparrow}$ the dimer-dimer zero crossing is located at $g_{\downarrow\downarrow}/|g_{\uparrow\downarrow}| = 0.575(3)$. This asymptote is indicated by the horizontal dotted red line. The vertical one is its symmetric analog. The upper and lower thin orange curves correspond, respectively, to $g_{\rm dd}/|g_{\uparrow\downarrow}| = 0.1$ (repulsion) and -0.1 (attraction). The dashed blue curve represents the collapse boundary $g_{\uparrow\uparrow} g_{\downarrow\downarrow} = g_{\uparrow\downarrow}^2$.

We have also calculated the dimer-dimer effective range r_e along the zero-crossing line. We find that $r_e/|a_{\uparrow\downarrow}|$ does not change much on the scale of Fig. 3.3. This ratio approximately equals 1.25 for $g_{\uparrow\uparrow} = g_{\downarrow\downarrow}$ and increases to 1.3 as one reaches the point where $g_{\sigma\sigma}/|g_{\uparrow\downarrow}| = 6$. We see that r_e is on the order of the dimer size. One can thus think of the dimer-dimer interaction in terms of an effective potential with the range $\sim r_e \sim a_{\uparrow\downarrow}$ and competing attractive and repulsive parts.

3.1.3 Dilute liquid of dimers

In this section we argue that sufficiently close to the dimer-dimer zero-crossing line, on its attractive side, many dimers form a dilute dimerized liquid. The liquid state is a

result of a competition between two- and three-dimer forces as predicted by Bulgac [15]. In the one-dimensional case that we consider the three-body scattering is kinematically equivalent to the two-dimensional two-body scattering and the corresponding mean-field energy shift depends logarithmically on the energy itself (see, for example, [20, 78]). This logarithmic running makes the mean-field description of the system slightly more complicated than in the three-dimensional case discussed in [15]. On the other hand, it also allows us to make quantitative predictions of liquid properties without actually solving the three-dimer problem. In our analysis we will use analogies with the well-studied problem of two-dimensional two-body-interacting bosons.

Consider $N_\mathrm{d} > 2$ dimers close to the dimer-dimer zero crossing in the attractive regime where $a_\mathrm{dd} \gg a_{\uparrow\downarrow} \sim r_e$. To the zeroth order in the dimer size one can think of the dimers as point-like particles neglecting their composite nature (see Fig. 3.4).

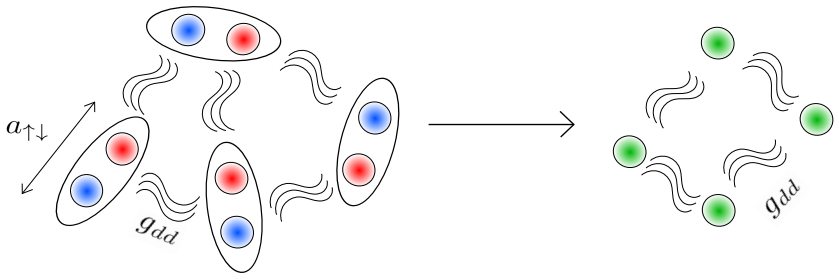

Figure 3.4: Mapping of our gas of dimers of size $a_{\uparrow\downarrow}$ close to the dimer-dimer zero crossing lines to point like bosons weakly interacting through the two-body coupling constant g_{dd}.

As follows from Sec. 3.1.1, trimers can be excluded from this picture since they are not sufficiently deeply bound and we consider the population-balanced case. Thus, to the leading order, we deal with a gas of N_d attractive point-like bosons, the ground state of which is a soliton with the energy [77]

$$E_{N_d} = -g_\mathrm{dd}^2 N_\mathrm{d}(N_\mathrm{d}^2 - 1)/12 \tag{3.6}$$

and size $L \sim 1/\sqrt{\epsilon} \sim a_\mathrm{dd}/N_\mathrm{d}$, where $\epsilon \sim E_{N_d}/N_d$ is the energy per dimer and we do not count the dimer binding energies. The central density of dimers diverges with increasing N_d (keeping a_dd fixed). This is obviously an artefact of the point-like approximation. That the system does not collapse can be shown by contradiction. Indeed, if the average distance between dimers becomes smaller than their size, the mixture enters into the mean-field "atomic" regime where it should be mechanically stable since we are above the mean-field collapse line $g_{\uparrow\uparrow}g_{\downarrow\downarrow} = g_{\uparrow\downarrow}^2$ [79].

We will now show that a repulsive three-dimer interaction stops the grows of the dimer density at a much lower value $n_\mathrm{d} \ll 1/a_{\uparrow\downarrow}$. Before we discuss the three-dimer interaction energy shift let us give general considerations on the three-body scattering in one dimension [20, 78]. After separating the center-of-mass motion the configurational space of three dimers is a two-dimensional plane parameterized by the hyperra-

dius $\rho = \sqrt{2/3}\sqrt{x_{12}^2 + x_{13}^2 + x_{23}^2}$ and hyperangle $\phi = \arcsin(x_{12}/\rho)$, where x_{ij} is the distance between dimers i and j. The three-dimer interaction is an effective potential originating from virtual excitations of internal and external degrees of freedom of three colliding dimers (pair-wise dimer-dimer processes are excluded to avoid double counting). This potential is thus physically localized at $\rho \sim a_{\uparrow\downarrow}$ and is characterized by the scattering length $a_3 > 0$ defined as the position of the (extrapolated) node of the zero-energy three-body wave function $\propto \ln(\rho/a_3)$. An important consequence of this hyper-two-dimensional kinematics is that at low energies the three-body interaction becomes repulsive, equivalent to a hard-wall constraint at $\rho = a_3$. Even without solving the three-dimer problem one can assume that for small $a_{\uparrow\downarrow}/a_{\rm dd}$ the scattering length a_3 can be approximated by its value at $a_{\rm dd} = \infty$ and that it is of the same order of magnitude as the dimer size $a_{\uparrow\downarrow}$ (we will return to this point in the next section).

In order to proceed to the many-body problem we assume that the state of the system is homogeneous in the thermodynamic limit and that it is susceptible to the mean-field treatment. The corresponding applicability condition requires that the interaction-induced chemical potential μ be much smaller than the quantity $n_{\rm d}^2$, comparable to the chemical potential in the strongly interacting Tonks-Girardeau regime. The inequality $|\mu| \ll n_{\rm d}^2$ also means that there is a macroscopic number of dimers per healing length (allowing for the classical description), where the healing length is $\sim 1/\sqrt{|\mu|}$. Here we require that the mean-field condition be satisfied separately for the two- and three-dimer interaction parts. In particular, for the two-dimer part we need $a_{\rm dd} n_{\rm d} \gg 1$.

The treatment of the three-dimer interaction proceeds in the same manner as for the short-range two-body interaction in the two-dimensional case (see, for example, [57, 80, 81]). In one way or another, these approaches consist of replacing the short-range (in our case three-dimer) potential by an effective potential with the same scattering length but with the range larger than the mean interparticle distance and smaller than the healing length. This effective potential then looks short ranged at relevant momenta $\sim \sqrt{|\mu|}$ and, on the other hand, it is sufficiently weak for the applicability of the Born-series expansion. In our case, the three-dimer effective potential can be taken as a constant in momentum space [78],

$$g_3 = \frac{\sqrt{3}\pi}{2\ln(2e^{-\gamma}/a_3\kappa)}, \tag{3.7}$$

where $\gamma \approx 0.5772$ is the Euler constant and the overall numerical coefficient (different from the two-dimensional two-body scattering case) is related to the Jacobian of the transformation from the coordinates x_{12} and x_{23} to the two-dimensional hyperradius-hyperangle pair [20]. The potential is assumed to vanish above the (hyper)momentum cut-off κ, which satisfies $n_{\rm d} \ll \kappa \ll \sqrt{|\mu|}$. The three-body energy shift per dimer then equals $g_3 n_{\rm d}^2/6$ and the mean-field applicability condition is $g_3 \ll 1$, which is satisfied, in particular, if a_3 is exponentially smaller than the mean inter-dimer separation. Note that in this case $g_3 > 0$.

For negative $g_{\rm dd}$ and positive g_3 the energy per dimer

$$\epsilon = g_{\rm dd} n_{\rm d}/2 + g_3 n_{\rm d}^2/6 \tag{3.8}$$

has a minimum at a finite saturation density [15] given by

$$n_{\rm d} = -3g_{\rm dd}/2g_3. \tag{3.9}$$

For this density $\epsilon = \mu = -(3/8)g_{\rm dd}^2/g_3$ and it is easy to see that the two- and three-body mean-field applicability conditions reduce to $g_3 \ll 1$.

The exact value of the cut-off momentum κ is, in fact, not important if one sticks to the leading order in g_3. At this level of approximation the three cut-off values $\kappa = n_{\rm d} \sim 1/a_{\rm dd} g_3$, $\kappa = \sqrt{\mu} \sim 1/a_{\rm dd}\sqrt{g_3}$, and $\kappa = 1/a_{\rm dd}$ lead to the same result since they differ only by a power of g_3 rather than exponentially. Indeed, by substituting these cut-off momenta into Eq. (3.7) one obtains three values of g_3 different from each other by $\sim g_3^2 \ln g_3 \ll g_3$. We thus take $\kappa = 1/a_{\rm dd}$. Similarly, we neglect other numerical factors under the logarithm and set $a_3 = a_{\uparrow\downarrow}$ in Eq. (3.7). This leads to the explicit expressions $g_3 = \sqrt{3}\pi/2\ln(a_{\rm dd}/a_{\uparrow\downarrow}) \ll 1$,

$$n_{\rm d} = (\sqrt{3}/\pi a_{\rm dd}) \ln(a_{\rm dd}/a_{\uparrow\downarrow}), \tag{3.10}$$

and

$$\mu = \epsilon = -(\sqrt{3}/4\pi a_{\rm dd}^2) \ln(a_{\rm dd}/a_{\uparrow\downarrow}). \tag{3.11}$$

With increasing $N_{\rm d}$ the peaked soliton solution corresponding to Eq. (3.6) transforms into a liquid-like droplet characterized by an approximately constant bulk density $n_{\rm d}$ given by Eq. (3.10). By comparing densities or energies per dimer in these two limits one can see that the soliton-droplet crossover happens at $N_{\rm d} \sim \sqrt{\ln(a_{\rm dd}/a_{\uparrow\downarrow})}$ (see Fig. 3.5).

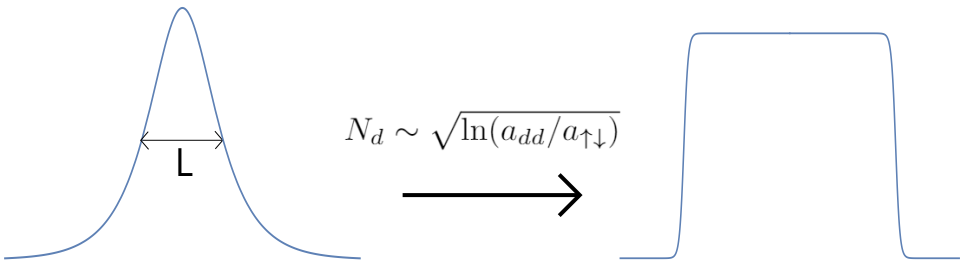

Figure 3.5: Density probability function of the system of dimers before and after the soliton- droplet crossover by increasing the number of dimers N_d.

3.1.4 Discussion and outlook

The perturbative expansion in powers of $g_3 \ll 1$ can be continued beyond the mean-field term. The next order requires the application of the Popov theory [57] and a more

precise knowledge of a_3. Note that dimer-dimer effective-range effects are beyond this power-law expansion. The effective-range energy correction per dimer scales as $r_e \epsilon n_\mathrm{d}$ and is thus smaller than ϵ by $r_e n_\mathrm{d} \sim g_3^{-1} e^{-\sqrt{3}\pi/2g_3}$ which is smaller than any power of g_3. The MF and BMF treatment of effective-range effects for one-dimensional bosons has been discussed in Refs. [82, 83].

In Sec. 3.1.3 we have substituted $a_{\uparrow\downarrow}$ for a_3 since distinguishing these two quantities is exceeding the accuracy of the leading-order calculation in the low-energy dilute regime defined by $a_{\uparrow\downarrow} \sim a_3 \ll 1/n_\mathrm{d}$ or, more precisely, by $1/\ln(1/a_{\uparrow\downarrow} n_\mathrm{d}) \sim 1/\ln(1/a_3 n_\mathrm{d}) \ll 1$. An interesting alternative appears in the regime

$$a_{\uparrow\downarrow} \ll 1/n_\mathrm{d} \ll a_3 \tag{3.12}$$

corresponding to a weak three-body attraction studied by Sekino and Nishida [78]. More precisely, they find that one-dimensional bosons with a pure three-body zero-range attraction form solitons with binding energies exponentially increasing and sizes exponentially decreasing with N_d, similar to solitons of two-body-interacting two-dimensional bosons discovered by Hammer and Son [84]. The relevance of the Sekino-Nishida states for our mixture depends on the exact solution of the three-dimer problem. We distinguish two possibilities: (1) There is no three-dimer bound state. This typically corresponds to a_3 being comparable to or smaller than the dimer size. In this case, our dilute liquid is a stable state. (2) a_3 is larger than the dimer size and the three-dimer bound state exists on or even above the dimer-dimer zero crossing. In this case our dilute solution still exists but becomes metastable with respect to the formation of clusters of the higher-density Sekino-Nishida phase. The fate of this phase in this case is an interesting problem by itself since the unlimited grows of density with N_d would eventually contradict the first inequality of (3.12). In any case, this discussion motivates solving the three-dimer ($\uparrow\uparrow\uparrow\downarrow\downarrow\downarrow$) problem, calculating a_3, and looking for eventual three-dimer bound states. An interesting possibility to check is whether there is a three-dimer zero-crossing point on the dimer-dimer zero-crossing curve.

It is tempting to speculate on the behavior of our dilute dimerized liquid as one moves from the dimer-dimer zero crossing towards the mean-field collapse curve in Fig. 3.3. The liquid phase just above this curve has been studied in Ref. [51]. Pairing correlations have not been discussed for this "atomic" liquid, but they seem to be irrelevant for its self-trapping character. Moreover, Ref. [51] suggests that for $g_{\uparrow\uparrow} \neq g_{\downarrow\downarrow}$ the liquid is density imbalanced, $n_\uparrow/n_\downarrow = \sqrt{g_{\downarrow\downarrow}/g_{\uparrow\uparrow}}$. Hence, for example, for $g_{\uparrow\uparrow} > g_{\downarrow\downarrow}$, a dimerized liquid droplet does not adiabatically connect to the atomic one as it should somehow get rid of the $\uparrow$ component. We thus expect more details to appear in the many-body analog of the diagram in Fig. 3.3, at least, outside of the diagonal $g_{\uparrow\uparrow} = g_{\downarrow\downarrow}$. Note that this region can be investigated experimentally in the two-component mixture of ^{39}K studied in Refs. [22, 23, 85]. These speculations bring up a potentially interesting few-body problem in the $\uparrow\uparrow\uparrow\downarrow\downarrow$ configuration, which can be thought of as two dimers and an atom. As

we have shown (see Fig. 3.2), the atom always binds to a dimer. In addition, it can hop from one dimer to the other thus mediating an exchange attraction between them. Therefore, even above the dimer-dimer zero crossing this attraction can overcome the dimer-dimer repulsion and bind the system into a pentamer state. More generally, this scenario suggests that the liquid phase in the population-imbalanced configuration may extend above the zero-crossing curve in Fig. 3.3.

Finally, there appears a fascinating possibility of observing self trapping in a one-dimensional Fermi-Bose mixture with interspecies attraction and Bose-Bose repulsion. We predict that fermionic Fermi-Bose dimers in this case bind for $g_{\mathrm{BB}} < 0.575|g_{\mathrm{FB}}|$ (assuming equal masses) and can thus form a dilute dimerized liquid. This effect can be studied, in particular, in the ^{40}K-^{41}K mixture by utilizing the wide interspecies Feshbach resonance at 540 G [86]. Very recently, Pan and coworkers [87] have discussed a one-dimensional (atomic) Fermi gas near a p-wave resonance and argued that in the collapse regime (equivalent to our $g_{\mathrm{dd}} < 0$) the system can be stabilized by effective-range effects. No three-atom interaction is included in their model.

3.2 Three-boson problem with two- and three-body interactions

Directly motivated by our prediction in Sec. 3.1.3, we now look at the one dimensional three-boson problem with two- and three-body interactions.

Background and Goal

The one-dimensional N-boson problem with the two-body contact interaction $g_2\delta(x)$ is exactly solvable. Lieb and Liniger [88] have shown that for $g_2 > 0$ the system is in the gas phase with positive compressibility. McGuire [77] has demonstrated that for $g_2 < 0$ the ground state is a soliton with the chemical potential diverging with N. In the case $N = \infty$ the limits $g_2 \to +0$ and $g_2 \to -0$ are manifestly different: The former corresponds to an ideal gas whereas the latter corresponds to collapse. Accordingly, the behavior of a realistic one- or quasi-one-dimensional system close to the two-body zero crossing strongly depends on higher-order terms not included in the Lieb-Liniger or McGuire zero-range models. Sekino and Nishida [78] have considered one-dimensional bosons with a pure zero-range three-body attraction and found that the ground state of the system is a droplet with the binding energy exponentially increasing with N, which also means collapse in the thermodynamic limit. In the last section, we have argued that in a sufficiently dilute regime the three-body interaction is effectively repulsive, providing a mechanical stabilization against collapse for $g_2 < 0$. The competition between the two-body attraction and three-body repulsion leads to a dilute liquid state similar to the one discussed by Bulgac [15] in three dimensions.

The three-body scattering in one dimension is kinematically equivalent to a two-dimensional two-body scattering [20, 78]. Therefore, the corresponding interaction shift depends logarithmically on the product of the scattering momentum and three-body scattering length a_3. An important consequence of this fact is that, in contrast to higher dimensions, the one-dimensional three-body interaction can become noticeable even if a_3 is exponentially small compared to the mean interparticle distance. Therefore, three-body effects can be studied in the universal dilute regime essentially in any one-dimensional system that preserves a finite residual three-body interaction close to a two-body zero crossing. Universality means that the effective-range effects are exponentially small and the relevant interaction parameters are the two- and three-body scattering lengths a_2 and a_3.

This rest of this Chapter is organized as follows. In Sec. 3.2.1 we solve the problem of three point-like bosons with contact two- and three-body interactions and analytically relate the ground and excited trimer energies with the scattering lengths. In particular, we follow the evolution of these states as the ratio a_3/a_2 is changed. In Sec. 3.2.2 we consider the previously defined 1D BB mixture where the dimer-dimer interaction is tunable by changing the intraspecies repulsion. Our analytical predictions are complemented by diffusion Monte Carlo calculation of the hexamer energy permitting to determine the three-dimer scattering length close to the dimer-dimer zero crossing. We perform this procedure for equal intraspecies coupling constants and in the case where their ratio is infinite. In the latter limit one of the components is in the Tonks-Girardeau regime and the system is equivalent to a Fermi-Bose mixture. We find that the three-dimer interaction is repulsive in both cases, which confirm our previous prediction.

3.2.1 Derivation of the formula

Consider three bosons of mass m interacting via contact two- and three-body forces characterized by the scattering lengths a_2 and a_3, respectively. The correct boundary condition for the wave function at the two-body coincidences is ensured by the two-body pseudopotential $g_2\delta(x_{ij})$ with $g_2 = -2/ma_2$, where $x_{ij} = x_i - x_j$ is the distance between particles i and j and we set $\hbar = 1$. The three-body boundary condition implies that in the limit of vanishing hyperradius $\rho = \sqrt{2/3}\sqrt{x_{12}^2 + x_{13}^2 + x_{23}^2}$ the three-body wave function should be proportional to $\ln(\rho/a_3)$. This small-hyperradius asymptote holds for all finite g_2 since at $\rho \ll |a_2|$ the two-body interaction can be neglected and the three-body kinematics corresponds to the two-dimensional scattering on a zero-range potential. The logarithmic scaling does not hold only in the case of impenetrable particles ($g_2 = \infty$), where a_3 is ill defined. However, this case is trivial since the contact three-body interaction is completely screened by the two-body one and plays no role. The applicability conditions for the zero-range model that we use here requires, as usual, that the de Broglie wavelengths of particles be much larger than the ranges of the potentials.

In order to construct the wave function $\psi(x_1, x_2, x_3)$, let us for a moment think of it

as Green's function which solves the equation

$$(\hat{H}_1 + \hat{V}_2 - mE)\psi(x_1, x_2, x_3) = \delta(x_{12})\delta(x_{13}), \tag{3.13}$$

where $\hat{H}_1 = -(\partial^2_{x_1} + \partial^2_{x_2} + \partial^2_{x_3})/2$ and $\hat{V}_2 = -2[\delta(x_{12}) + \delta(x_{13}) + \delta(x_{23})]/a_2$. In the limit $\rho \to 0$ one can neglect $\hat{V}_2$ and mE in Eq. (3.13) which then acquires the Poisson form $-\nabla^2_{\boldsymbol{\rho}}\psi = 2\delta(\boldsymbol{\rho})/\sqrt{3}$, where $\boldsymbol{\rho} = \{x_{12}, (x_{13} + x_{23})/\sqrt{3}\}$. For small ρ, we thus have $\psi = -\ln(\rho/\xi)/\sqrt{3}\pi$, where ξ depends on details of the full Eq. (3.13) and is, therefore, a function of mE and a_2. Note that if $\xi(mE, a_2)$ were equal to a_3, ψ would satisfy the correct two- and three-body boundary conditions, thus solving our original problem. Therefore, the logic of our approach is to solve Eq. (3.13), extract $\xi(mE, a_2)$, and find E from the implicit equation $\xi(mE, a_2) = a_3$.

The solution of Eq. (3.13) exists for any energy E and is unique, if mE does not belong to the spectrum of the operator $\hat{H}_1 + \hat{V}_2$. Here, we will be interested in three-body bound states and will assume E below the three-atom (for $a_2 < 0$) or atom-dimer (for $a_2 > 0$) scattering thresholds. Since $\hat{H}_1 + \hat{V}_2$ can be diagonalized by the Bethe ansatz, one could, in principle, expand ψ in terms of Bethe-ansatz states. This, however, involves the summation over a two-dimensional parameter space of free-atom states. Here we will use a different approach which allows us to work only with the trimer and atom-dimer scattering states.

Assuming zero center-of-mass momentum, we define $F(x) = 2\psi(2x/3, -x/3, -x/3)/a_2$ and move $\hat{V}_2$ to the right-hand side of Eq. (3.13) arriving at

$$(\hat{H}_1 - mE)\psi = \sum_{i=1}^{3} F(x_i - x_j)\delta(x_{jk}) + \delta(x_{12})\delta(x_{13}), \tag{3.14}$$

where j and k are different from each other and from i. We now solve Eq. (3.14) with respect to ψ by switching to momentum representation where the operator $(\hat{H}_1 - mE)^{-1}$ is a number. Expressing ψ in terms of F and using the definition of F, we obtain the closed equation for $\tilde{F}(p) = \int F(x)e^{-ipx}dx$,

$$(\hat{L} - a_2/2)\tilde{F}(p) = -1/\sqrt{3p^2 - 4mE}, \tag{3.15}$$

where

$$\hat{L}\tilde{F}(p) = \frac{\tilde{F}(p)}{\sqrt{3p^2 - 4mE}} + \int \frac{2\tilde{F}(q)}{p^2 + pq + q^2 - mE}\frac{dq}{2\pi}. \tag{3.16}$$

The three-body contact boundary condition is taken into account by noting that ψ is the sum of two functions corresponding, respectively, to the first and second terms on the right-hand side of Eq. (3.14).

The former is nonsingular and equals $3\int \tilde{F}(p)(3p^2 - 4mE)^{-1/2}dp/2\pi$ at $\rho = 0$. The latter equals $K_0(\sqrt{-mE}\rho)/\sqrt{3}\pi \approx -\ln\big(\sqrt{-mE}\rho e^{\gamma}/2\big)/\sqrt{3}\pi$, where K_0 is the decaying

Bessel function and $\gamma = 0.577$ is Euler's constant. The condition $\psi \propto \ln(\rho/a_3)$ then gives

$$\ln \frac{\sqrt{-mE}a_3 e^{\gamma}}{2} = 3\sqrt{3}\pi \int \frac{\tilde{F}(q)}{\sqrt{3q^2 - 4mE}} \frac{dq}{2\pi}. \tag{3.17}$$

The spectrum and eigenfunctions of $\hat{L}$ can be derived analytically from the Bethe ansatz. One can thus solve Eq. (3.15) for $\tilde{F}$ and substitute the result into Eq. (3.17) directly relating the trimer energy $E = E_3$ with a_2 and a_3. Although solving Eqs. (3.13) and Eq. (3.15) are conceptually similar tasks, the latter involves a much smaller eigenfunction basis. Note that when passing from Eq. (3.13) to Eq. (3.15) the roles of E and a_2 get interchanged; E is now a parameter and $a_2/2$ plays the role of an eigenvalue. Since we are dealing with $E < 0$, the spectrum of $\hat{L}$ now contains only the trimer and atom-dimer scattering states. The former is characterized by the eigenfunction $\tilde{F}_{\mathrm{McG}}(p) = 2(-mE)^{-1/4}/(1 - p^2/mE)$ and eigenvalue $\lambda_{\mathrm{McG}} = 1/\sqrt{-mE}$ consistent with the relation $E = -4/ma_2^2$ for the trimer state in the absence of three-body interaction [77]. The continuum spectrum of $\hat{L}$ consists of atom-dimer scattering states parameterized by the atom-dimer relative momentum k and characterized by eigenvalues $\lambda_k = (3k^2 - 4mE)^{-1/2}$. The explicit form of $\tilde{F}_k$ is obtained by Fourier transforming $F_k(x)$ extracted from the Bethe-ansatz eigenstate of $\hat{H}_1 + \hat{V}_2$ with $a_2 = 2\lambda_k$. These manipulations result in

$$\ln \frac{a_3 \kappa e^{\gamma}}{a_2} = \frac{2}{\kappa^2 - 1} \left[\frac{\pi}{3\sqrt{3}} + \frac{3\kappa^2 - 1}{\sqrt{4\kappa^2 - 1}} \arctan \sqrt{\frac{2\kappa + 1}{2\kappa - 1}} \right], \tag{3.18}$$

where $\kappa = \sqrt{-mE}a_2/2$.

A more detailed calculation of Eq.(3.18) is given in Appendix A.

Discussions

In Fig. 3.6, we plot $E = E_3 < 0$ in units of the dimer binding energy $|E_2| = 1/ma_2^2$ as a function of $\ln(a_3/a_2)$ for positive a_2 where $E_3/E_2 = 4\kappa^2$. We find that there are always two trimer states in this case. For $a_3 \ll a_2$ the ground trimer is bound by the dominant three-body force and its energy tends to $-4e^{-2\gamma}/ma_3^2$ (red dotted curve). In the opposite limit $a_3 \gg a_2$, the three-body interaction is subleading and the ground-trimer energy asymptotes to the McGuire result $E_3 = 4E_2$ [77] (blue dot-dashed lines). The limits of large and small a_3 correspond to the weak three-body attraction and repulsion, respectively. The trimer follows this transition adiabatically and, in the zero-range approximation, becomes an excited state, which remains bound for any a_3/a_2. In the limit $a_3 \to \infty$, the energy of this excited trimer asymptotically approaches the atom-dimer scattering continuum (red filled area in Fig. 3.6) following the threshold law $E_3/E_2 - 1 \approx (\pi/3)^2/\ln^2(a_3/a_2)$.

For the case $a_2 < 0$ (two-body repulsion), there is no dimer and κ is negative.

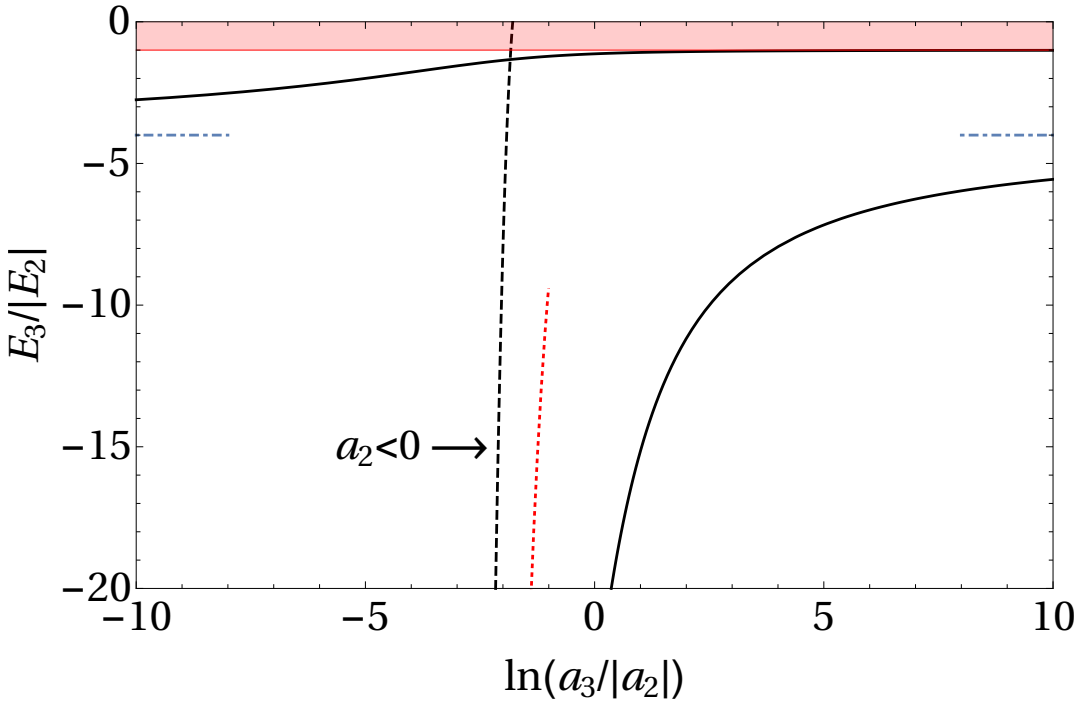

Figure 3.6: The trimer energy in units of $|E_2| = 1/ma_2^2$ versus $\ln(a_3/|a_2|)$ for positive a_2 (solid black). The red filling indicates the atom-dimer scattering continuum, the blue dash-dotted lines correspond to $E_3 = 4E_2$ valid in the absence of the three-body force, and the red dotted line shows the asymptote $E_3 = -4e^{-2\gamma}/ma_3^2$ valid in the absence of the two-body force. The black dashed curve is the trimer energy for $a_2 < 0$. The repulsive two-body interaction in this case pushes the trimer into the three-atom continuum at a finite value of $\ln(a_3/|a_2|)$ (see text).

Equation (3.18) remains valid provided that its right-hand side is analytically continued from $\kappa > 0$ to $\kappa < 0$ just above the real axis. This gives a single trimer state, the energy of which (black dashed curve in Fig. 3.6) tends to $-4e^{-2\gamma}/ma_3^2$ (red dotted curve) for $a_3 \ll |a_2|$. With increasing the two-body repulsion this trimer gets pushed above the three-atom threshold at $\ln(a_3/|a_2|) = -\gamma - 2\pi/3\sqrt{3}$. That we know the energy analytically makes it one of rare examples of a three-body resonance where one can study the threshold behavior to any desired order. In particular, one can show that the branch-cut singularity in this case corresponds to a two-dimensional resonance in the angular-momentum channel with $l = 3$, consistent with the observation that we are dealing with a localized trimer coupled to the continuum of highly fermionized three-atom states (see the Supplemental Material of Ref. [20]).

Returning to the two-body attraction ($a_2 > 0$), we note that the relative deviation of the trimer energy from the McGuire asymptote amounts to about 30% for $a_3/a_2 = e^{\pm 10}$, illustrating that even an extremely weak three-body interaction is important in one dimension. Our results can be applied to three-dimensional bosonic atoms in the quasi-one-dimensional geometry. By integrating out the radial degrees of freedom this system reduces to a pure one-dimensional model characterized by effective two- and

three-body coupling constants. In the regime where the three-dimensional scattering length a is much smaller than the oscillator length l_0 of the radial confinement, the two-body coupling constant equals $g_2 = 2a/ml_0^2$ [44] and the three-body one is $g_3 = -12\ln(4/3)a^2/ml_0^2$ [89–91]. On the other hand, with the logarithmic accuracy the latter can be written in terms of a_3 as $g_3 = \sqrt{3}\pi/[m\ln(l_0/a_3)]$ as depicted in Sec 3.1. We thus identify $\ln(a_3/a_2) \approx \pi/[4\sqrt{3}\ln(4/3)]l_0^2/a^2$, which allows us to relate the trimer energies with the three-dimensional parameters a and l_0 by using Eq. (3.18). Note that in this model of quasi-one-dimensional point-like bosons the two- and three-body coupling constants vanish simultaneously with the three-dimensional scattering length a. Yet, three-body effects are visible and even lead to a qualitative change of the system behavior, particularly to the excited trimer state not present in the McGuire model (its existence has been first pointed out in the quasi-dimensional geometry [92]).

3.2.2 Back to the 1D mixture problem

Systems where two- and three-body effective interactions can be controlled more independently are difficult to produce or engineer (see [20] and references therein). We now discuss a model tunable to the regime of pure three-body repulsion. Namely, we consider the mixture of one-dimensional pointlike bosons $\uparrow$ and $\downarrow$ of unit mass characterized by the coupling constants $g_{\uparrow\downarrow} = -2/a_{\uparrow\downarrow} < 0$ (interspecies attraction) and $g_{\sigma\sigma} = -2/a_{\sigma\sigma} > 0$ (intraspecies repulsions). The interspecies attraction leads to the formation of $\uparrow\downarrow$ dimers of size $a_{\uparrow\downarrow}$ and energy $E_{\uparrow\downarrow} = -1/a_{\uparrow\downarrow}^2$. We showed in Sec 3.1 that the two-dimer interaction changes from attractive to repulsive with increasing $g_{\sigma\sigma}$. In particular, the two-dimer zero crossing is predicted to take place for $g_{\uparrow\uparrow} = g_{\downarrow\downarrow} = 2.2|g_{\uparrow\downarrow}|$ [Bose-Bose (BB) case] and for $g_{\downarrow\downarrow} = 0.575|g_{\uparrow\downarrow}|$ if $g_{\uparrow\uparrow} = \infty$ [Fermi-Bose (FB) case]. Here we consider three such dimers and characterize their three-dimer interaction by calculating the hexamer energy $E_{\uparrow\uparrow\uparrow\downarrow\downarrow\downarrow}$ and by comparing it with the tetramer energy $E_{\uparrow\uparrow\downarrow\downarrow}$ on the attractive side of the two-dimer zero crossing where the tetramer exists. The idea is that sufficiently close to this crossing the dimers behave as pointlike particles weakly bound to each other. One can then extract the three-dimer scattering length a_3 from our zero-range three-boson formalism [Eq. (3.18)] with $m = 2$, $E_2 = E_{\uparrow\uparrow\downarrow\downarrow} - 2E_{\uparrow\downarrow}$, $E_3 = E_{\uparrow\uparrow\uparrow\downarrow\downarrow\downarrow} - 3E_{\uparrow\downarrow}$, and using the asymptotic expression for the dimer-dimer scattering length $a_2 = 1/\sqrt{2|E_2|}$.

Diffusion Monte Carlo [1]

In order to calculate E_2 and E_3, we resort to the diffusion Monte Carlo (DMC) technique, which is a projection method based on solving the Schrödinger equation in imaginary time [50]. The importance sampling is used to reduce the statistical noise and also to impose the Bethe-Peierls boundary conditions stemming from the δ-function interactions.

[1] This calculation is done by Grecia Guijaro.

We construct the guiding wave function ψ_T in the pair-product form

$$\psi_T = \prod_{i<j} f^{\uparrow\uparrow}(x_{ij}^{\uparrow\uparrow}) \prod_{i<j} f^{\downarrow\downarrow}(x_{ij}^{\downarrow\downarrow}) \prod_{i,j} f^{\uparrow\downarrow}(x_{ij}^{\uparrow\downarrow}) \,, \tag{3.19}$$

where $x_{ij}^{\sigma\sigma'} = x_i^{\sigma} - x_j^{\sigma'}$ is the distance between particles i and j of components σ and σ', respectively.

The intercomponent correlations are governed by the dimer wave function $f^{\uparrow\downarrow}(x) = \exp(-|x|/a_{\uparrow\downarrow})$ and the intracomponent terms are $f^{\sigma\sigma}(x) = \sinh(|x|/a_{\uparrow\downarrow} - |x|/2a_{\rm dd}) - (a_{\sigma\sigma}/a_{\uparrow\downarrow} - a_{\sigma\sigma}/2a_{\rm dd})$. These functions satisfy the Bethe-Peierls boundary conditions, $\partial f^{\sigma\sigma'}(x)/\partial x|_{x=+0} = -f^{\sigma\sigma'}(0)/a_{\sigma\sigma'}$, which, because of the product form, also ensures the correct behavior of the total guiding function ψ_T at any two-body coincidence. At the same time, the long-distance behavior of $f^{\sigma\sigma}(x)$ is chosen such that ψ_T allows dimers to be at distances larger than their size. When the distance x between pairs $\{x_1^{\uparrow}, x_1^{\downarrow}\}$ and $\{x_2^{\uparrow}, x_2^{\downarrow}\}$ is much larger than the dimer size $a_{\uparrow\downarrow}$, Eq. (3.19) reduces to $\psi_T \propto f^{\uparrow\downarrow}(x_{11}^{\uparrow\downarrow}) f^{\uparrow\downarrow}(x_{22}^{\uparrow\downarrow}) \exp(-|x|/a_{\rm dd})$. For $a_{\rm dd} \gg a_{\uparrow\downarrow}$, this wave function describes two dimers weakly-bound to each other. While $a_{\sigma\sigma'}$ are fixed by the Hamiltonian, we treat $a_{\rm dd}$ as a free parameter in Eq. (3.19). Close to the dimer-dimer zero crossing $a_{\rm dd} \approx a_2$ and this parameter is related self-consistently to the tetramer energy while far from the crossing its value is optimized according to the variational principle. It is useful to mention that in case FB, where $a_{\uparrow\uparrow} = 0$, the $\uparrow$ component is in the Tonks-Girardeau limit and can be mapped to ideal fermions by Girardeau's mapping [69]. Replacing $|x|$ by x in the definition of $f^{\uparrow\uparrow}(x)$ makes ψ_T antisymmetric with respect to permutations of $\uparrow$ coordinates.

Results

In Fig. 3.7, we show $E_3/|E_2|$ for cases BB (red squares) FB (blue circles) as a function of $\delta = 1/\ln\left(\sqrt{2|E_2|}a_3\right)$ along with the prediction of Eq. (3.18) (solid black). The quantity a_3 is a fitting parameter to the DMC results; changing it essentially shifts the data horizontally. We clearly see that in both cases the three-dimer interaction is repulsive since $E_3/|E_2|$ is above the McGuire trimer limit [77] (dash-dotted line). For rightmost data points the hexamer is about ten times larger than the dimer and the data align with the universal zero-range analytics. For the other points we observe significant effective range effects related to the finite size of the dimer. In the universal limit $a_{\uparrow\downarrow} \ll a_2$, we previously showed the leading effective-range correction to the ratio $E_3/|E_2|$ is expected to be proportional to $a_{\uparrow\downarrow}/a_2 \propto e^{1/\delta}$. Indeed, adding the term $Ce^{1/\delta}$ to the zero-range prediction well explains deviations of our results from the universal curve and we have checked that other exponents do not work that well. We thus treat a_3 and C as fitting parameters; in case BB we obtain $a_3 = 0.01a_{\uparrow\downarrow}$ and in case FB $a_3 = 0.03a_{\uparrow\downarrow}$. Both cases are fit with $C = -100$ (dashed curve in Fig. 3.7). We emphasize that we are dealing with

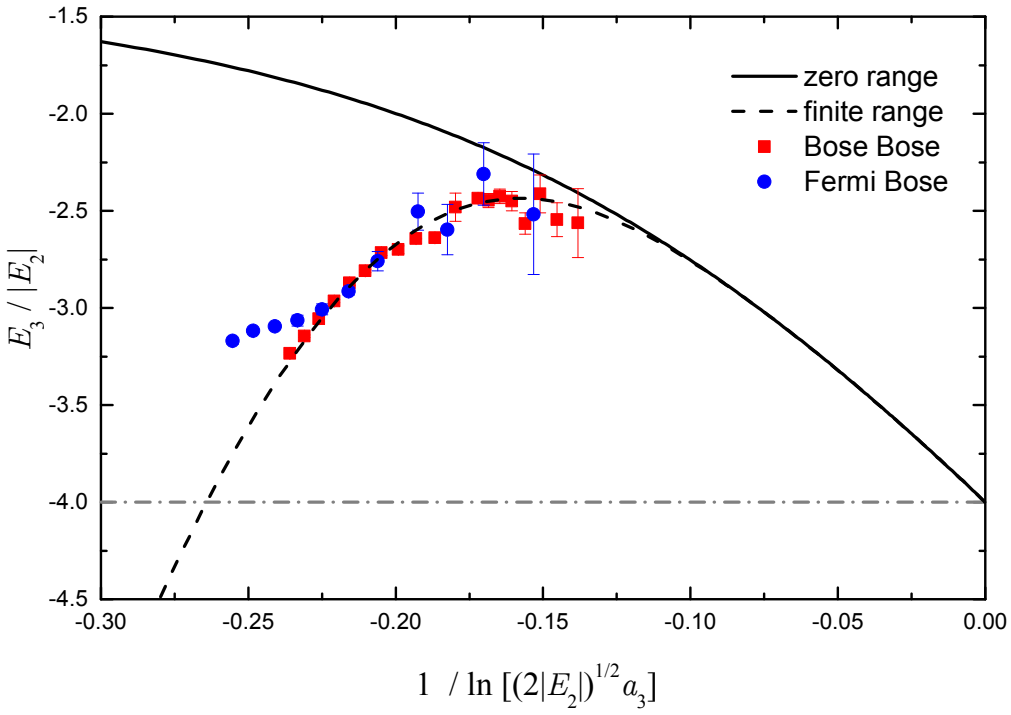

Figure 3.7: $E_3/|E_2|$ vs $1/\ln\left(\sqrt{2|E_2|}a_3\right)$ (same as Fig. 3.6 except for the inverse of the horizontal axis) for one-dimensional dimers. Here E_2 and E_3 are the tetramer and hexamer energies measured relative to the two- and three-dimer thresholds, respectively. The solid curve is the prediction of Eq. (3.18) and the dashed curve is a fit, which includes finite-dimer-size effects into account (see text). The dash-dotted line is the McGuire result $E_3 = 4E_2$ for three pointlike bosons with no three-body interaction. The red squares are the DMC data for case BB plotted using $a_3 = 0.01a_{\uparrow\downarrow}$ and the blue circles stand for case FB with $a_3 = 0.03a_{\uparrow\downarrow}$. The error bars are larger in the latter case because of the larger statistical noise induced by the nodal surface imposed by the Fermi statistics.

the true ground state of three dimers. The lower "attractive" state formally existing for these values of a_2 and a_3 in the zero-range model is an artifact since it does not satisfy the zero-range applicability condition. The three-dimer interaction is an effective finite-range repulsion which supports no bound states.

Conclusion

In conclusion, we obtain an analytical expression for the ground and excited trimer energies for one-dimensional bosons interacting via zero-range two- and three-body forces. We argue that since in one dimension the three-body energy correction scales logarithmically with the three-body scattering length a_3, three-body effects are observable even for exponentially small a_3, which significantly simplifies the task of engineering three-body-interacting systems in one dimension. We demonstrate that Bose-Bose or Fermi-Bose dimers, previously shown to be tunable to the dimer-dimer zero crossing, exhibit a noticeable three-dimer repulsion. We can now be certain that the ground state of many such

dimers slightly below the dimer-dimer zero crossing is a liquid in which the two-body attraction is compensated by the three-body repulsion [15].

Our results have implications for quasi-one-dimensional mixtures. We mention particularly the ^{40}K-^{41}K Fermi-Bose mixture which emerges as a suitable candidate for exploring the liquid state of fermionic dimers. Here the intraspecies ^{41}K-^{41}K background interaction is weakly repulsive (the triplet ^{41}K-^{41}K scattering length equals 3.2nm [93]) and the interspecies one features a wide Feshbach resonance at 540G [86]. Let us identify $\uparrow$ with ^{40}K, $\downarrow$ with ^{41}K, and assume the radial oscillator length $l_0 = 56$nm, which corresponds to the confinement frequency $2\pi \times 80$kHz. Under these conditions the effective coupling constants equal $g_{\sigma\sigma'} \approx 2a^{(3D)}_{\sigma\sigma'}/l_0^2$ [44] and the dimer-dimer zero crossing at $g_{\downarrow\downarrow} = 0.575|g_{\uparrow\downarrow}|$ is realized for the three-dimensional scattering lengths $a^{(3D)}_{\downarrow\downarrow} \approx 3.2$nm and $a^{(3D)}_{\uparrow\downarrow} \approx -5.6$nm. The dimer size is then ≈ 560nm and dimer binding energy corresponds to $\approx 2\pi \times 800$Hz placing the system in the one-dimensional regime. For the rightmost (next to rightmost) blue circle in Fig. 3.7, the tetramer is approximately 20 (10) times larger than the dimer and 800 (200) times less bound. Moving left in this figure is realized by increasing $|a^{3D}_{\uparrow\downarrow}|$ and thus getting deeper in the region $g_{\downarrow\downarrow} < 0.575|g_{\uparrow\downarrow}|$. Note, however, that this also pushes the system out of the one-dimensional regime and effects of transversal modes [89–91] become important. Note that while completing this work, we became aware of another work [94] reporting the solution of the three-boson problem with zero-range interactions.

Chapter 4

A perturbative approach for bosons near a two-body zero crossing

Contents

4.1 Few-body perturbative approach 55

4.2 Applications 59

4.2.1 Double-Gaussian potential 59

4.2.2 Yukawa-plus-delta potential 60

4.2.3 Quasi-two-dimensional dipoles 61

4.2.4 Quasi-one-dimensional dipoles 66

4.3 Bogoliubov theory 69

4.4 Conclusions 71

Let us take two particles interacting through a weak two-body potential at $T = 0$: what happens for the system's energy if we had a third particle (assuming only two-body potentials between particles)? A MF naive approach would result in multiplying the initial MF energy by 3, by considering the new possible pairwise interactions. But what if the MF value of the two-body potential vanishes (i.e., when its *shape* permits to fulfill this condition, without totally vanishing in amplitude)? How could one extend the results to the many-body case?

In this Chapter, we reconcile the first-quantized few-body approach with the Bogoliubov perturbation theories in the particular case of a two-body potential of zero mean value [defined by $\int V(\mathbf{r})d^D r = 0$ in the pure D-dimensional case and by Eq. (4.18) in quasi-low-dimensional geometries] calculating the ground-state energy up to terms $\propto V^3$. We find that up to this order, the result is an analytic function of the density and contains two-body corrections $\propto V^2 n^2$ and $\propto V^3 n^2$ as well as an effective three-body term $\propto V^3 n^3$. We present closed-form integral expressions for the corresponding coefficients in pure dimensions and in quasi-low-dimensional geometries and discuss their general consequences. We apply our formalism to bosons interacting by the double-Gaussian potential and by the Yukawa potential in pure dimensions, noticing that the emergent three-body interaction is repulsive (attractive) when the long-range tail of the underlying two-body potential is attractive (repulsive). We then calculate the three-body and two-body energy shifts for quasi-low-dimensional dipoles as a function of their tilt angle θ with respect to the confinement cylindrical symmetry axis. We find that the three-body force for quasi-two-dimensional dipoles changes from attraction to repulsion with increasing θ. For one-dimensional dipoles, the dominant three-body force is attractive and second-order in V except when they are aligned along the axis ($\theta = 0$). In all these quasi-low-dimensional cases the confinement-induced shift of the two-body coupling constant is found to be positive as a result of a renormalization procedure.

The Chapter is organized as follows. In Sec. 4.1 we use the standard perturbation theory to derive the interaction energy shift for N atoms in free space and in quasi-low-dimensional geometries. In Sec. 4.2 we apply the obtained general formulas to the cases of double-Gaussian and Yukawa-plus-delta potentials in pure dimensions. Sections 4.2.3 and 4.2.4 are devoted, respectively, to the quasi-two-dimensional and quasi-one-dimensional tilted dipoles. In Sec. 4.3 we make connections to the many-body case and show how our results can be obtained from the Bogoliubov theory. We conclude in Sec. 4.4.

4.1 Few-body perturbative approach

We consider the system of N distinguishable atoms [1] characterized by the Hamiltonian (we assume unit mass and $\hbar = 1$)

$$\hat{H} = \sum_{i=1}^{N} -\partial^2_{\mathbf{x}_i}/2 - \partial^2_{\mathbf{y}_i}/2 + U(\mathbf{y}_i) + \sum_{i>j} V(\mathbf{x}_i - \mathbf{x}_j, \mathbf{y}_i - \mathbf{y}_j), \tag{4.1}$$

where $U(\mathbf{y})$ is the confining potential and $\mathbf{x}$ and $\mathbf{y}$ denote the sets of single-particle coordinates in the unconfined and confined directions, respectively. For example, in the quasi-two-dimensional geometry $\mathbf{x}$ is the two-dimensional in-plane position vector and $\mathbf{y} = y$ is the coordinate perpendicular to the confinement direction. The unconfined space is assumed to be a cube of unit volume with periodic boundary conditions and we write the single-particle eigenstates of the noninteracting part of Eq. (4.1) as

$$\phi_{\mathbf{q},\boldsymbol{\nu}}(\mathbf{x}, \mathbf{y}) = e^{i\mathbf{q}\mathbf{x}} \psi_{\boldsymbol{\nu}}(\mathbf{y}), \tag{4.2}$$

where each component of $\mathbf{q}$ is an integer divided by 2π and $\boldsymbol{\nu}$ is the set of quantum numbers labeling the eigenstates $\psi_{\boldsymbol{\nu}}(\mathbf{y})$ for the single-particle motion in the confined direction, $\epsilon_{\boldsymbol{\nu}}$ being the corresponding spectrum which we count relative to the ground state (such that $\epsilon_{\mathbf{0}} = 0$).

Assuming the last term on the right-hand side of Eq. (4.1) as a perturbation and applying the standard perturbation theory we write the ground-state energy of the N-body system as

$$E[N] = E^{(1)}[N] + E^{(2)}[N] + E^{(3)}[N] + ..., \tag{4.3}$$

where $E^{(i)}[N]$ denotes the i-th order term in powers of V. In Eq. (4.3) we have already used the fact that by construction $E^{(0)}[N] = 0$ (all particles are in the state $\{\boldsymbol{q}, \boldsymbol{\nu}\} = \mathbf{0}$). We will restrict ourselves to perturbation order $i \leq 3$ and use the general expressions for the energy corrections available up to this order in Ref. [13]. Let us reproduce these general formulas for reference. Denoting the noninteracting multiparticle states by symbols with the bar $\bar{n} = \{\mathbf{k}_1, \boldsymbol{\nu}_1; ...; \mathbf{k}_N, \boldsymbol{\nu}_N\}$, the corresponding multiparticle energies by $\omega_{\bar{n}}$, their differences by $\omega_{\bar{n}\bar{m}} = \omega_{\bar{n}} - \omega_{\bar{m}}$, and the whole interacting part of the Hamiltonian (4.1) by $\bar{V}$, energy corrections to state $\bar{n}$ read [13]

$$E^{(1)}_{\bar{n}} = \bar{V}_{\bar{n}\bar{n}}, \tag{4.4}$$

$$E^{(2)}_{\bar{n}} = -{\sum_{\bar{m}}}' |\bar{V}_{\bar{m}\bar{n}}|^2 / \omega_{\bar{m}\bar{n}}, \tag{4.5}$$

$$E^{(3)}_{\bar{n}} = {\sum_{\bar{k}}}' {\sum_{\bar{m}}}' \frac{\bar{V}_{\bar{n}\bar{m}} \bar{V}_{\bar{m}\bar{k}} \bar{V}_{\bar{k}\bar{n}}}{\omega_{\bar{m}\bar{n}} \omega_{\bar{k}\bar{n}}} - E^{(1)}_{\bar{n}} {\sum_{\bar{m}}}' \frac{|\bar{V}_{\bar{m}\bar{n}}|^2}{\omega^2_{\bar{m}\bar{n}}}, \tag{4.6}$$

where the primes mean that the state $\bar{n}$ is excluded from the summations.

[1] Distinguishable atoms have the same ground state as identical bosons.

Our task thus reduces to counting multi-particle excited states and calculating $\bar{V}_{\bar{n}\bar{m}}$. To this end we introduce the two-body matrix elements

$$\begin{aligned} V^{\boldsymbol{\zeta\eta}}_{\boldsymbol{\mu\nu}}(\mathbf{k}) &= [V^{\boldsymbol{\eta\zeta}}_{\boldsymbol{\nu\mu}}(-\boldsymbol{k})]^* = V^{\boldsymbol{\mu\nu}}_{\boldsymbol{\zeta\eta}}(-\boldsymbol{k}) \\ &= \int d\mathbf{y} d\mathbf{y}' d\mathbf{x} e^{i\mathbf{kx}} V(\mathbf{x}, \mathbf{y}-\mathbf{y}') \psi^*_{\boldsymbol{\zeta}}(\mathbf{y}) \psi^*_{\boldsymbol{\mu}}(\mathbf{y}') \psi_{\boldsymbol{\eta}}(\mathbf{y}) \psi_{\boldsymbol{\nu}}(\mathbf{y}'), \end{aligned} \tag{4.7}$$

where the equalities in the first line follow from $V(\mathbf{r}) = [V(\boldsymbol{r})]^* = V(-\boldsymbol{r})$, assumed to be valid throughout the chapter. In terms of these matrix elements the first correction to the N-body ground-state energy reads

$$E^{(1)}[N] = g_2^{(1)} \binom{N}{2} = V^{\mathbf{00}}_{\mathbf{00}}(\mathbf{0}) \binom{N}{2} \tag{4.8}$$

and the second one can be written as

$$E^{(2)}[N] = g_2^{(2)} \binom{N}{2} + g_3^{(2)} \binom{N}{3}, \tag{4.9}$$

where

$$g_2^{(2)} = -\sum_{\mathbf{k},\boldsymbol{\nu},\boldsymbol{\mu}} \frac{|V^{\mathbf{0\nu}}_{\mathbf{0\mu}}(\mathbf{k})|^2}{k^2 + \epsilon_{\boldsymbol{\nu}} + \epsilon_{\boldsymbol{\mu}}} \tag{4.10}$$

and

$$g_3^{(2)} = -6 \sum_{\boldsymbol{\nu}} \frac{|V^{\mathbf{00}}_{\mathbf{0\nu}}(\mathbf{0})|^2}{\epsilon_{\boldsymbol{\nu}}}. \tag{4.11}$$

In Eqs. (4.10) and (4.11) the summations exclude terms with vanishing denominators [equivalent to the prime in Eq. (4.5)]. Equation (4.10) is just the second-order interaction correction for a single pair. It corresponds to (virtual) excitations of two atoms which, in the first interaction event, get excited into states $\{\boldsymbol{\nu}, -\mathbf{k}\}$ and $\{\boldsymbol{\mu}, \mathbf{k}\}$ and, in the second interaction event, get back to their ground states.

Equation (4.11) represents an effective three-body attraction, which appears in confined geometries for weak two-body interactions of the usual type [for which, in particular, $V^{\mathbf{00}}_{\mathbf{0\nu}}(\mathbf{0}) \neq 0$]. It has been discussed in the context of quasi-one-dimensional [89, 91] and lattice bosons [95]. It can also be obtained by solving the Gross-Pitaevskii equation for the condensate wave function [89]. Accordingly, this term is absent in pure dimensions (in our derivation this follows from the fact that there are no transversal excitations and thus no summation over $\boldsymbol{\nu}$). The emergence of this term in our first-quantization analysis can be understood by going back to Eq. (4.10) and reconsidering virtual excitations where only one particle is promoted to $\boldsymbol{\nu} \neq 0$ (in this case $\mathbf{k}$ should vanish because of the momentum conservation in the unconfined directions). Then the amplitude $V^{\mathbf{00}}_{\mathbf{0\nu}}(\mathbf{0})$ should be replaced by $(N-1)V^{\mathbf{00}}_{\mathbf{0\nu}}(\mathbf{0})$, since the atom can be excited by interacting with $N-1$ other atoms, not just one as implied in Eq. (4.10). In addition, in Eq. (4.10) these special one-particle events should be counted ony once per atom. The equation Eq. (4.9)

comes then from the following procedure,

$$E^{(2)}[N] = g_2^{(2)}\binom{N}{2} - \Big[\frac{N(N-1)}{2} 2\sum_{\boldsymbol{\nu}} \frac{|V_{\mathbf{0}\boldsymbol{\nu}}^{\mathbf{00}}(\mathbf{0})|^2}{-\epsilon_{\boldsymbol{\nu}}}\Big] + N\sum_{\boldsymbol{\nu}} \frac{|(N-1)V_{\mathbf{0}\boldsymbol{\nu}}^{\mathbf{00}}(\mathbf{0})|^2}{-\epsilon_{\boldsymbol{\nu}}}, \quad (4.12)$$

where we removed the terms which are counted in the wrong way in the second term of the right hand side of Eq. (4.12) (since μ and ν play a symmetric role, there is a factor 2 which appears) and we added the correct counting and amplitude for those one particle events.

Equation (4.11) is meant to compensate for these "errors" in Eq. (4.10) when $N > 2$. In Sec. 4.3 we present a many-body approach to this problem based on the second quantization, where Eq. (4.11) emerges in a more natural manner.

Proceeding to the calculation of the third-order correction let us represent it as

$$E^{(3)}[N] = g_3^{(3)}\binom{N}{3} + g_2^{(3)}\binom{N}{2} + \delta^{(3)} + \sigma^{(3)}. \quad (4.13)$$

In Eq. (4.13)

$$g_3^{(3)} = 6\sum_{\mathbf{k},\boldsymbol{\nu},\boldsymbol{\mu},\boldsymbol{\eta}} \frac{V_{\mathbf{0}\boldsymbol{\nu}}^{\mathbf{0}\boldsymbol{\eta}}(\mathbf{k}) V_{\boldsymbol{\eta}\mathbf{0}}^{\mathbf{0}\boldsymbol{\mu}}(\mathbf{k}) V_{\boldsymbol{\mu}\mathbf{0}}^{\boldsymbol{\nu}\mathbf{0}}(\mathbf{k})}{(k^2+\epsilon_{\boldsymbol{\nu}}+\epsilon_{\boldsymbol{\eta}})(k^2+\epsilon_{\boldsymbol{\nu}}+\epsilon_{\boldsymbol{\mu}})}, \quad (4.14)$$

where the summation extends to indices satisfying the constraint $\mathbf{k} \neq \mathbf{0} \vee (\boldsymbol{\nu} \neq \mathbf{0} \wedge \boldsymbol{\mu} \neq \mathbf{0} \wedge \boldsymbol{\eta} \neq \mathbf{0})$ ($\vee$ and $\wedge$ are boolean OR and AND, respectively). The term (4.14) accounts for the following sequence of virtual excitations of three different atoms. The first and the second atoms interact with each other and get excited into states $\{\boldsymbol{\nu}, -\mathbf{k}\}$ and $\{\boldsymbol{\mu}, \mathbf{k}\}$, respectively. Then, the second interaction event results in the second atom getting back to the ground state and the third atom being excited to state $\{\boldsymbol{\eta}, \mathbf{k}\}$. Finally, the first and the third atoms interact with each other both going down to the ground state. The constraint on the summation indices mentioned above is imposed in order to count in Eq. (4.14) only genuine three-body events and not two-body or one-body ones, which we will now discuss.

We write the coefficient in the second term on the right-hand side of Eq. (4.13) in the form

$$g_2^{(3)} = \sum_{\boldsymbol{\nu},\boldsymbol{\mu},\boldsymbol{\eta},\boldsymbol{\zeta},\mathbf{k},\mathbf{q}} \frac{V_{\mathbf{0}\boldsymbol{\eta}}^{\mathbf{0}\boldsymbol{\zeta}}(-\mathbf{q}) V_{\boldsymbol{\eta}\boldsymbol{\nu}}^{\boldsymbol{\zeta}\boldsymbol{\mu}}(\mathbf{q}-\mathbf{k}) V_{\boldsymbol{\nu}\mathbf{0}}^{\boldsymbol{\mu}\mathbf{0}}(\mathbf{k})}{(k^2+\epsilon_{\boldsymbol{\nu}}+\epsilon_{\boldsymbol{\mu}})(q^2+\epsilon_{\boldsymbol{\eta}}+\epsilon_{\boldsymbol{\zeta}})}, \quad (4.15)$$

where the sum is constrained only by the requirement of nonvanishing denominator [equivalent to the primes in Eq. (4.6) or, mathematically, to $(\mathbf{k} \neq \mathbf{0} \vee \boldsymbol{\nu} \neq \mathbf{0} \vee \boldsymbol{\mu} \neq \mathbf{0}) \wedge (\mathbf{q} \neq \mathbf{0} \vee \boldsymbol{\eta} \neq \mathbf{0} \vee \boldsymbol{\zeta} \neq \mathbf{0})$]. Equation (4.15) is nothing else than the first term on the right-hand side of the general formula Eq. (4.6) calculated for a single pair of atoms. However, similarly to Eq. (4.10), Eq. (4.15) does not properly account for some two-body excitations when $N > 2$. We will show that a higher-order compensation term is required [denoted by $\delta^{(3)}$ in Eq. (4.13)] which, however, vanishes when $V_{\boldsymbol{\mu}\boldsymbol{\nu}}^{\boldsymbol{\zeta}\boldsymbol{\eta}}(\mathbf{0}) = 0$. Arguments for

this are rather technical because of the chosen first-quantization technique. We present them for completeness in the next paragraph, which the reader can skip, if not interested.

Consider virtual-excitation sequences implied by Eq. (4.15), for which at least one of the atoms changes its state less than three times. In the sum of Eq. (4.15) this happens when one of the matrix elements is of the form $V^{\gamma\gamma}_{\alpha\beta}(\mathbf{0})$ or $V^{\alpha\beta}_{\gamma\gamma}(\mathbf{0})$, i.e., we are dealing with an interaction event where only one atom changes its transversal state from $\boldsymbol{\beta}$ to $\boldsymbol{\alpha}$ leaving its momentum unchanged as well as the state of all other atoms. This transition can be triggered not only by the interaction with the second atom in state γ, but also with any of the other $N-2$ atoms. In order to account for this type of transitions in Eq. (4.15) one can replace matrix elements $V^{\gamma\delta}_{\alpha\beta}(\mathbf{k})$, characterizing the interaction of two atoms in vacuum, by

$$\begin{aligned}\tilde{V}^{\gamma\delta}_{\alpha\beta}(\mathbf{k}) = V^{\gamma\delta}_{\alpha\beta}(\mathbf{k}) + \delta_{\mathbf{k},\mathbf{0}}\Big[&(N-2)\delta_{\alpha,\beta}V^{\gamma\delta}_{00}(\mathbf{0}) \\ &+ (N-2)\delta_{\gamma,\delta}V^{00}_{\alpha\beta}(\mathbf{0}) + \binom{N-2}{2}\delta_{\alpha,\beta}\delta_{\gamma,\delta}V^{00}_{00}(\mathbf{0})\Big],\end{aligned} \tag{4.16}$$

which corresponds to the same transition but in the presence of $N-2$ other atoms in the ground state. In Eq. (4.16) $\delta_{\boldsymbol{k},\boldsymbol{k}'}$ and $\delta_{\boldsymbol{\nu},\boldsymbol{\nu}'}$ are Kronecker deltas. An additional modification is needed when only one atom is excited throughout the whole sequence of the three interaction events in Eq. (4.15). This happens for $(\boldsymbol{\mu} = \boldsymbol{\zeta} = \mathbf{0} \vee \boldsymbol{\nu} = \boldsymbol{\eta} = \mathbf{0}) \wedge \mathbf{k} = \mathbf{q} = \mathbf{0}$. In this case not only the matrix elements should be corrected as explained above, but, in addition, the whole contribution of such terms should be divided by $N-1$ as in Eq. (4.15) each of these "one-body" excitation sequences is counted twice for every pair [with subsequent multiplication by $\binom{N}{2}$ in Eq. (4.13)], whereas they should be counted only once per atom, illustrating basically the same idea we developed in Eq. (4.12) . These patches of Eq. (4.15) can be cast in the form of a compensation term which we call $\delta^{(3)}$ but do not write explicitly as, for purposes of this chapter, it is sufficient to understand that it vanishes when $V^{\boldsymbol{\zeta\eta}}_{\boldsymbol{\mu\nu}}(\mathbf{0}) = 0$.

Finally, the term $\sigma^{(3)}$ in Eq. (4.13) corresponds to the last term in the general formula Eq. (4.6). This term can be written explicitly by noting its resemblance to Eq. (4.5). However, we observe that it is also proportional to Eq. (4.8), which vanishes when $V^{\mathbf{00}}_{\mathbf{00}}(\mathbf{0}) = 0$. We should note that if $V^{\boldsymbol{\zeta\eta}}_{\boldsymbol{\mu\nu}}(\mathbf{0}) \neq 0$, the sum $\delta^{(3)} + \sigma^{(3)}$ can be expressed in the form of three terms, two of which correct the constants (4.14) and (4.15), and the third one corresponds to an effective four-body interaction. We have checked that five-body terms cancel out.

In pure dimensions we have explicitly

$$E^{(3)}[N] = \binom{N}{2}\sum_{\mathbf{q},\mathbf{k}}\frac{V(-\mathbf{q})V(\mathbf{q}-\mathbf{k})V(\mathbf{k})}{k^2q^2} + 6\binom{N}{3}\sum_{\mathbf{k}}\frac{V^3(\mathbf{k})}{k^4}, \tag{4.17}$$

where states with $\mathbf{k} = \mathbf{0}$, $\mathbf{q} = \mathbf{0}$ or $\mathbf{q} = \mathbf{k}$ are excluded from the summation.

We observe that under the assumption

$$\int d\mathbf{x} V(\mathbf{x}, \mathbf{y}) = 0 \tag{4.18}$$

we have $V^{\zeta\eta}_{\mu\nu}(\mathbf{0}) = 0$ for any set $\{\boldsymbol{\mu}, \boldsymbol{\nu}, \boldsymbol{\zeta}, \boldsymbol{\eta}\}$ [see Eq. (4.7)]. Then, the energy of the N-body system, up to terms of order V^3, equals the renormalized two-body part $[g_2^{(2)} + g_2^{(3)}]\binom{N}{2}$ plus the leading nonpairwise part (an effective three-body interaction) given by $g_3^{(3)}\binom{N}{3}$.

Note that the renormalized two-body interaction scales asymptotically (for $V \to 0$) as V^2. Therefore, slightly softening the condition Eq. (4.18) by allowing the Born integral be of order $\propto V^2$ gives us more flexibility in controlling the renormalized two-body interaction. In particular, one can make it weakly repulsive, weakly attractive, or vanishing. In the latter case the three-body term $g_3^{(3)} \propto V^3$ becomes the leading interaction correction as all other terms scale at least as V^4 [this follows from the scaling $V^{\nu\mu}_{\eta\zeta}(\mathbf{0}) \propto V^2$ for the matrix elements at zero momenta].

This brings us to one of the main statements of this section. In a sufficiently narrow vicinity of a two-body zero crossing, reached by a fine-tuned compensation, expressed by Eq. (4.18), of the attractive and repulsive parts of the interaction potential, the dominant effective three-body interaction is third order in V and is characterized by the coupling constant given by Eq. (4.14). Note that this effective interaction can be repulsive or attractive depending on the shape of the two-body potential and on the confining geometry. In the next Section we calculate this term explicitly for a few academically and practically relevant cases.

4.2 Applications

4.2.1 Double-Gaussian potential

Gaussian potentials, although not very realistic, are very frequently used as model potentials for solving few-body and many-body problems. They are smooth, characterized by regular effective-range expansions, and allow one to calculate quite a few things analytically. Thus, the first example that we will consider is the sum of two Gaussians in pure dimensions, one attractive and one repulsive, with different ranges,

$$V(\mathbf{x}) = v_0 e^{-\lambda_0 x^2} + v_1 e^{-\lambda_1 x^2}. \tag{4.19}$$

The condition (4.18) applied to (4.19) fixes the ratio v_1/v_0 as a function of $\alpha = \lambda_0/\lambda_1$ and dimension D, namely $v_1/v_0 = -\alpha^{-D/2}$. Then, the potential (4.19) leads to the following three-body coupling constant in different dimensions

$$g_3^{(3)}(D=1) = \frac{3\pi}{2}\frac{{v_0}^3}{{\lambda_0}^3}\left[\sqrt{3}(1-\alpha^{3/2}) - (2+\alpha)^{3/2} + (1+2\alpha)^{3/2}\right], \tag{4.20}$$

$$g_3^{(3)}(D=2) = \frac{9\pi^2}{8}\frac{{v_0}^3}{{\lambda_0}^4}\Big[-2\ln(2+\alpha) - \alpha\ln(3\alpha^2+6\alpha) + 2\alpha\ln(1+2\alpha) + \ln(3+6\alpha)\Big], \tag{4.21}$$

and

$$g_3^{(3)}(D=3) = \frac{3\pi^4}{4}\frac{{v_0}^3}{{\lambda_0}^5}\Big[-\sqrt{3} + \sqrt{3\alpha} + 3\sqrt{2+\alpha} - 3\sqrt{1+2\alpha}\Big]. \tag{4.22}$$

In all these cases the configuration of the potential where it has a repulsive central part and attractive tail ($v_0 > 0$ and $\alpha > 1$ or $v_0 < 0$ and $\alpha < 1$) leads to a three-body repulsion (see Fig. 4.1). This phenomenon has been noticed in Ref. [96]. In our perturbative analysis it follows from the fact that the Fourier transform of $V(x)$ is positive for any momentum. By contrast, the repulsive tail case leads to a three-body attraction.

Note also that the momentum integral in Eq. (4.14) is converging at small momenta since $V(k) \propto k^2$ with the main contribution to the integral coming from momenta comparable to the inverse interaction range. We can thus say that the effective three-body term is characterized by the same range as the two-body potential.

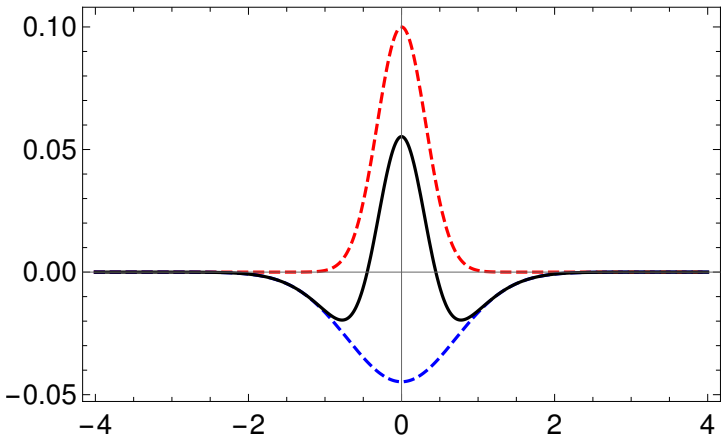

Figure 4.1: The double Gaussian potential (in black) is the sum of two Gaussian potential (in red and blue). The ratio of their amplitude is fixed by the condition Eq. (4.18). We show here the attractive tail case with $v_0 > 0$ and $\alpha > 1$ which leads to $g_3^{(3)} > 0$, i.e a three-body effective repulsion.

4.2.2 Yukawa-plus-delta potential

We now consider the case of an attractive Yukawa potential compensated by a repulsive delta potential. A concrete realization of this model can be achieved by placing bosonic impurities (species $\downarrow$) in a Bose-Einstein condensate of another species ($\uparrow$) [97, 98]. For simplicity, we assume that $m_\downarrow = 1 \gg m_\uparrow$ so that we can integrate out the host-gas dynamics in the adiabatic Born-Oppenheimer approximation. In this manner the phonon exchange in the host gas leads to a static induced Yukawa attraction between the im-

purities and their direct interaction can be tuned in order to reach the condition (4.18). This is attained at the phase-separation threshold $g_{\uparrow\downarrow} = \sqrt{g_{\uparrow\uparrow} g_{\downarrow\downarrow}}$, where $g_{\sigma\sigma'}$ are the two-body interaction coupling constants. In this case, the Fourier transform of the effective interaction (exchange plus direct) between two $\downarrow$ impurities is given by

$$V(\mathbf{k}) = v - \frac{v/\xi^2}{k^2 + 1/\xi^2} = \frac{vk^2}{k^2 + 1/\xi^2}, \tag{4.23}$$

with $v = g_{\downarrow\downarrow} = g_{\uparrow\downarrow}^2/g_{\uparrow\uparrow}$ and $\xi = 1/\sqrt{4m_\uparrow g_{\uparrow\uparrow} n_\uparrow}$ [97, 98].

Substituting Eq. (4.23) into Eq. (4.14) leads to the three-body coupling constant

$$g_3 = S_D v^3 \xi^{4-D}, \tag{4.24}$$

where $S_1 = 3/8$, $S_2 = 3/(4\pi)$ and $S_3 = 9/(16\pi)$. Similarly to the double-Gaussian case, the attractive Yukawa tail corresponds to an effective three-body repulsion since v and $V(k)$ are positive. One can also notice that the main contribution to the effective three-body interaction term comes from $k \sim 1/\xi$ since the integral in Eq. (4.14) converges and there is no other momentum scale.

By analyzing the double-Gaussian potential, the Yukawa-plus-delta potential, and a few other relatively simple two-body potentials satisfying Eq. (4.18) we have observed that the signs of their long-range tails are inversely correlated with the sign of the emergent effective three-body interactions. It is important to mention that this does not hold in general. As a counterexample consider a double-Gaussian potential with, say, attractive tail, to which we add a very weak Yukawa-plus-delta potential with repulsive tail. The three-body interaction in this case is dominated by the double-Gaussian part and is repulsive. However, since the Gaussian-law decay is faster than Yukawa, no matter how weak the Yukawa part is, it will dominate the long-range behavior of the resulting two-body potential. We have just constructed a two-body potential satisfying Eq. (4.18), for which the two-body tail and the three-body effective interaction are both repulsive.

4.2.3 Quasi-two-dimensional dipoles

We now consider quasi-two-dimensional dipoles in the geometry defined by $\mathbf{r} = \{x_1, x_2, y\}$, where $\mathbf{x} = \{x_1, x_2\}$ and y are the in-plane and transverse coordinates, respectively. The external confinement potential is harmonic

$$U(y) = \frac{y^2}{2l^4} - \frac{1}{2l^2}, \tag{4.25}$$

where l is the confinement oscillator length. The transversal eigenfunctions equal $\psi_\nu(y) = e^{-y^2/(2l^2)} H_\nu(y/l)/\sqrt{l\sqrt{\pi} 2^\nu \nu!}$ and correspond to $\epsilon_\nu = \nu/l^2$. The dipole moments are assumed to be in the $\{x_1, y\}$ plane tilted by the angle θ with respect to the y-axis (see Fig. 4.3). The corresponding two-body interaction potential is the sum of the dipole-

dipole and zero-range (pseudo)potentials [99]

$$V(\mathbf{r}) = r_* \frac{r^2 - 3(x_1 \sin\theta + y\cos\theta)^2}{r^5} + 4\pi a \delta(\mathbf{r}) \tag{4.26}$$

with the Fourier transform

$$V(\mathbf{k}, p) = 4\pi r_* \left[\frac{(k_1 \sin\theta + p\cos\theta)^2}{k^2 + p^2} - \frac{1}{3} + \frac{a}{r_*} \right], \tag{4.27}$$

where r_* is the dipolar length proportional to the square of the dipole moment, $\mathbf{k} = \{k_1, k_2\}$, and $k = |\mathbf{k}|$. Equation (4.18) for this tilted-dipole setup translates to the condition [100–102]

$$a = a_* = (1/3 - \cos^2\theta) r_*, \tag{4.28}$$

which marks the point where $V(\mathbf{0}, p) = 0$.

Equation (4.26) should be understood as an effective mean-field potential valid in the limit of zero momenta and energies. The short-range coupling constant $4\pi a$ is defined by postulating that the N-body interaction energy shift in the limit of extremely large l scales as

$$E[N] = \binom{N}{2} \frac{1}{\sqrt{2\pi} l} 4\pi (a - a_*). \tag{4.29}$$

This formulation of the zero-momentum limit avoids problems associated with the fact that this limit in Eq. (4.27) is not well defined, which, in particular, makes Eq. (4.8) useless in the strictly uniform three-dimensional space. For the same reason a cannot be called the scattering length since the zero-momentum limit of the scattering amplitude depends on the direction of the momentum. In spite of this peculiarity of the potential (4.26) it could be treated perturbatively in the same manner as the ordinary isotropic pseudopotential $4\pi a \delta(\mathbf{r})$. The ultraviolet cutoff implicit in Eq. (4.26) may or may not be important for a given observable (here we have in mind energy shifts or coupling constants $g_n^{(i)}$) depending on whether the corresponding momentum integral is ultraviolet divergent or not.

The matrix elements of the potential (4.27) of interest to us can be written as [2]

$$V_{\mu 0}^{\nu 0}(\mathbf{k}) = V_{\mu 0}^{0\nu}(\mathbf{k}) = V_{0\mu}^{0\nu}(\mathbf{k}) = \int_{-\infty}^{\infty} \frac{dp}{2\pi} V(\mathbf{k}, p) \lambda_\nu(p) \lambda_\mu(-p), \tag{4.30}$$

where

$$\lambda_\nu(p) = \int_{-\infty}^{\infty} \psi_\nu(y) \psi_0(y) e^{ipy} dy = (-1)^{\nu/2} (lp)^\nu e^{-p^2 l^2/4} / \sqrt{2^\nu \nu!}. \tag{4.31}$$

[2] Our derivation of the matrix elements follows the procedure of Edler *et al.* [103] who discussed quasi-one-dimensional dipoles aligned along the symmetry axis.

Integrating over p in Eq. (4.30) then gives

$$\begin{aligned} V_{\mu 0}^{\nu 0}(\mathbf{k}) = V_{\mu 0}^{0\nu}(\mathbf{k}) = V_{0\mu}^{0\nu}(\mathbf{k}) &= \frac{(-1)^{\mu+s/2}}{2^{(s-1)/2}}\sqrt{\frac{\pi}{\nu!\mu!}}\frac{a-a_*}{l}[1+(-1)^s](s-1)!! \\ &\quad - \frac{(-1)^{\mu+s/2}}{2^s}\sqrt{\frac{\pi}{\nu!\mu!}}\frac{r_*}{l}(kl)^{s+1}e^{k^2l^2/2} \\ \times \Bigg\{ &[1+(-1)^s](s-1)!!\,\Gamma\left(\frac{1-s}{2},\frac{k^2l^2}{2}\right)\left(\cos^2\theta - \frac{k_1^2}{k^2}\sin^2\theta\right) \\ &+ \frac{1-(-1)^s}{\sqrt{2}}s!!\,\Gamma\left(-\frac{s}{2},\frac{k^2l^2}{2}\right)\frac{k_1}{k}\sin 2\theta\Bigg\} \\ \xrightarrow[s\gg 1]{} &\sqrt{\frac{s!}{\nu!\mu!}}\frac{1}{2^{s/2+5/4}\pi^{3/4}s^{1/4}l}[(-1)^{\mu+s/2}V(\mathbf{k},\sqrt{s}/l)+(-1)^{\nu+s/2}V(\mathbf{k},-\sqrt{s}/l)], \end{aligned} \tag{4.32}$$

where $\Gamma(j,\sigma)$ is the incomplete Gamma function and we have denoted $s=\nu+\mu$. The last line in Eq. (4.32) is an approximate expression valid for large s and obtained by observing that the product $\lambda_\nu(p)\lambda_\mu(-p)$ in this limit is essentially the sum of two delta peaks at $p=\pm\sqrt{s}/l$.

Substituting Eq. (4.32) into Eq. (4.14) and setting $a=a_*$ we obtain

$$g_3^{(3)} = \frac{r_*^3}{l}[C_0F_0(\theta)+C_1F_1(\theta)], \tag{4.33}$$

where

$$F_0(\theta) = \frac{1+3\cos 2\theta}{4}\frac{31+12\cos 2\theta+21\cos 4\theta}{64}, \tag{4.34}$$

$$F_1(\theta) = \frac{1+7\cos 2\theta}{8}\sin^2 2\theta, \tag{4.35}$$

and the numerical coefficients $C_0=-141.1$ and $C_1=-10.7$. The solid line in Fig. 4.2 shows $C_0F_0(\theta)+C_1F_1(\theta)$ as a function of θ. It equals C_0 for $\theta=0$, i.e., for dipoles aligned perpendicularly to the plane we arrive at a three-body attraction (assuming positive r_*). Again, we observe that the three-body attraction is correlated with the repulsive tail. By contrast, for dipoles in the plane $C_0F_0(\pi/2)+C_1F_1(\pi/2)=-5C_0/16$ and we predict a three-body repulsion.

That the sum in Eq. (4.14) converges at large momenta and energies can be understood by considering the purely three-dimensional version of Eq. (4.14) for dipoles. In this case, $V(\mathbf{k})=O(|k|^0)$ and the integral over the three-dimensional momentum is converging at large k as $\int d^3k/k^4$. A cutoff at $k\sim 1/r_0$ would produce an effective-range correction to g_3 on the order of $\delta g_3 \sim r_0 r_*^3/l^2$ [3]. Assuming $r_0\sim r_*$, this gives the "natural" scaling $\delta g_3 \sim r_*^4/l^2$ for the three-dimensional three-body interaction coupling constant $\propto r_*^4$ projected to the transversal ground state of the trap. This is to say that the three-body interaction (4.33) is enhanced by the factor $l/|r_*|\gg 1$ compared to the

[3] Introducing a cutoff $\epsilon_c \propto 1/r_0^2$ for excitation energies in Eq. (4.14) we clearly observe the scaling $g_3(\epsilon_c)-g_3(\infty)\propto 1/\sqrt{\epsilon_c}$. We use this scaling for calculating C_0, C_1 in Eq. (4.33).

"natural" three-dimensional scale. Nevertheless, it remains much weaker than the "natural" two-dimensional scaling $g_3 \propto l^2$ for a nonperturbative two-dimensional potential of range l.

The quasi-two-dimensional model at hand is often reduced to a purely two-dimensional one by projecting the interaction potential on the transversal Gaussian ground state [60, 100, 102, 104–109]. In our case this projection means that in Eq. (4.14) we retain only terms with $\boldsymbol{\nu} = \boldsymbol{\mu} = \boldsymbol{\eta} = \mathbf{0}$. This approximation gives $C_0 = -127.4$ and $C_1 = 0$ in Eq. (4.33) and is rather accurate (see the dashed line in Fig. 4.2). This curious fact is consistent with the above-mentioned convergence of the sum in Eq. (4.14) at high energies. As we will now show, the two-body energy correction requires a more accurate treatment.

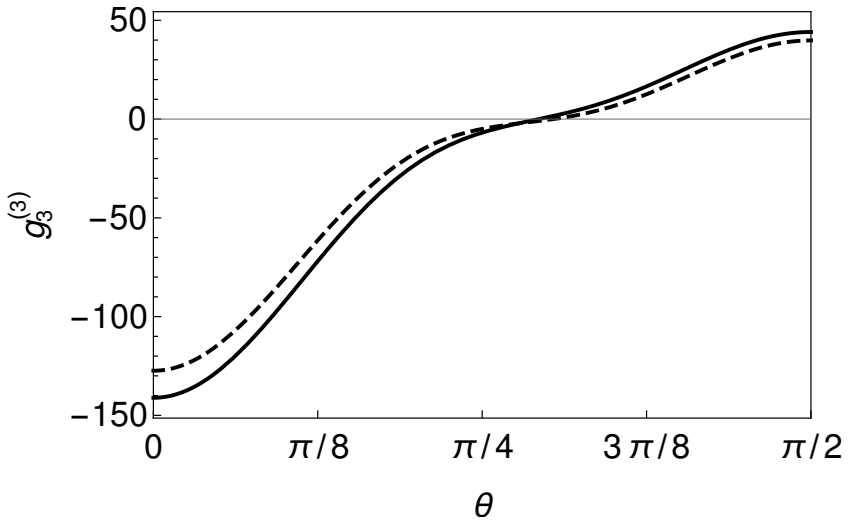

Figure 4.2: $g_3^{(3)}$ in units of r_*^3/l as a function of the tilt angle θ for the case of quasi-two-dimensional dipoles. The solid line is obtained by evaluating the sum in Eq. (4.14) with all excited states of the trap taken into account. The dashed line includes only the transverse ground state ($\nu = \mu = \eta = 0$). Assuming $r_* > 0$ the effective three-body interaction monotonically changes from attractive when dipoles are perpendicular to the plane ($\theta = 0$) to repulsive when they are in the plane ($\theta = \pi/2$). The change of sign takes place at $\theta \approx 0.29\pi$.

Let us now discuss the confinement-induced correction to the two-body interaction, given by Eq. (4.10), for $a = a_*$. Under this condition the sum in Eq. (4.10) converges at small momenta and we do not have to deal with the logarithmic infrared divergence, typical for the "ordinary" two-dimensional scattering (see, for instance, §45 in [13]). On the other hand, Eq. (4.10) does feature an ultraviolet diverging part

$$-\frac{1}{\sqrt{2\pi}l}\sum_{s,\boldsymbol{k}}\frac{V^2(\mathbf{k},\sqrt{s}/l)+V^2(\mathbf{k},-\sqrt{s}/l)}{4\pi l\sqrt{s}(k^2+s/l^2)}, \tag{4.36}$$

which is obtained by substituting the large-s asymptote given by the last line in Eq. (4.32) into Eq. (4.10) and using the fact that $\sum_{\nu,\mu}(\nu!\mu!)^{-1}\delta_{\nu+\mu,s} = 2^s/s!$. By identifying $s =$

$(lp)^2$ and passing from summation over s to integration over p Eq. (4.36) transforms into

$$-\frac{1}{\sqrt{2\pi}l}\int_{-\infty}^{\infty}\frac{dp}{2\pi}\int\frac{d^2k}{(2\pi)^2}\frac{V^2(\mathbf{k},p)}{k^2+p^2}, \tag{4.37}$$

which is nothing else than the second-order Born correction calculated for $V(\mathbf{k},p)$ in free space and averaged over the transversal density profile [4]. This piece renormalizes the short-range coupling constant $4\pi a$ and has to be formally thrown away since it has already been taken into account in Eq. (4.29). The regularized sum in Eq. (4.10) for $a=a_*$ then equals

$$g_2^{(2)}=\frac{r_*^2}{l^2}\left(B_0\frac{3+10\cos 2\theta+19\cos^2 2\theta}{32}+B_1\frac{\sin^2 2\theta}{4}\right), \tag{4.38}$$

where the coefficients $B_0=0.55$ and $B_1=1.5$ are obtained by extrapolating the numerical summation to infinite cutoff. The second-order correction Eq. (4.38) is positive (because of the renormalization) and monotonically decays from $B_0(r_*/l)^2$ for $\theta=0$ (dipoles perpendicular to the plane) to $(3/8)B_0(r_*/l)^2$ for $\theta=\pi/2$ (dipoles in the plane). This means that in order to stay at the two-body zero crossing while increasing the confinement, one has to tune the short-range interaction coupling constant to the value $4\pi a\approx 4\pi a_*-\sqrt{2\pi}g_2^{(2)}l$ (valid up to second order in r_*/l). We do not calculate $g_2^{(3)}$ limiting our discussion to the leading-order two-body and three-body corrections.

We should note that the positivity of the renormalized $g_2^{(2)}$ may be specific to the considered confinement and interaction potentials. Zin and co-workers [110], using essentially the same renormalization scheme but for dipoles under periodic boundary conditions, arrived at a negative $g_2^{(2)}$.

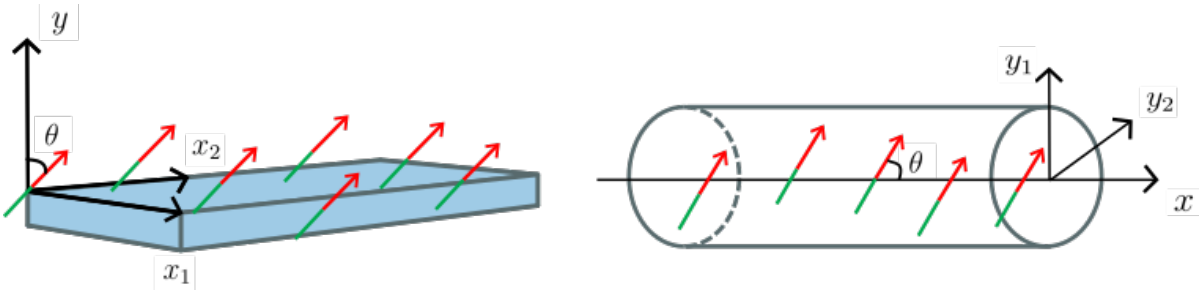

Figure 4.3: To the left, the quasi-two dimensional case where the dipole moments (in red and green) are assumed to be in the $\{x_1,y\}$ plane tilted by the angle θ with respect to the y-axis. To the right, the quasi-one dimensional case where the dipole moments are assumed to be in the $\{x,y_1\}$ plane tilted by the angle θ with respect to the longitudinal x-axis.

[4] Averaging over the density profile means multiplying by $\int\psi_0^4(y)dy=1/(\sqrt{2\pi}l)$ and by $\int\psi_{0,0}^4(\mathbf{y})d^2y=1/(2\pi l^2)$, respectively, in the quasi-two-dimensional and quasi-one-dimensional cases.

4.2.4 Quasi-one-dimensional dipoles

We now proceed to discussing the quasi-one-dimensional model of tilted dipoles, wich has recently been realized experimentally with Dy [111]. In spite of their formal analogy, the quasi-two-dimensional and quasi-one-dimensional models of tilted dipoles have an interesting difference which concerns the effective three-body interaction. Let us define the quasi-one-dimensional model by the coordinates $\mathbf{r} = \{x, \boldsymbol{y}\} = \{x, y_1, y_2\}$, the external confinement potential is assumed cylindrically symmetric,

$$U(\mathbf{y}) = \frac{y^2}{2l^4} - \frac{1}{l^2}. \tag{4.39}$$

The single-particle eigenfunctions $\psi_{\boldsymbol{\nu}}(\mathbf{y})$ satisfy $[-\partial_{\mathbf{y}}^2/2 + U(\mathbf{y})]\psi_{\nu,m} = \epsilon_{\nu,m}\psi_{\nu,m}$, where $\epsilon_{\nu,m} = (2\nu + |m|)/l^2$. We have used the cylindrical symmetry of the potential (4.39) to write $\boldsymbol{\nu} = \{\nu, m\}$, where the integers $\nu \geq 0$ and $-\infty < m < \infty$ are the radial and angular quantum numbers, respectively. The eigenfunctions read

$$\psi_{\nu,m}(\boldsymbol{y}) = e^{im\phi}\frac{(-1)^\nu}{l\sqrt{\pi}}\sqrt{\frac{\nu!}{(\nu+|m|)!}}\left(\frac{y}{l}\right)^{|m|} L_\nu^{|m|}\left(\frac{y^2}{l^2}\right) e^{-y^2/2l^2}, \tag{4.40}$$

where $L_\nu^{|m|}$ is the Laguerre polynomial and $\phi = \arg(y_1 + iy_2)$.

The dipole moments are assumed to be in the $\{x, y_1\}$ plane tilted by the angle θ with respect to the longitudinal x-axis (see Fig. 4.3). The interaction (pseudo)potential is then given by

$$V(\mathbf{r}) = r_*\frac{r^2 - 3(x\cos\theta + y_1\sin\theta)^2}{r^5} + 4\pi a\delta(\mathbf{r}), \tag{4.41}$$

which can also be obtained from Eq. (4.26) by replacing $x_1 \to y_1$, $x_2 \to y_2$, and $y \to x$. Accordingly, the Fourier transform $V(k, \mathbf{p})$ of (4.41) is obtained from Eq. (4.27) by replacing $k_1 \to p_1$, $k_2 \to p_2$, and $p \to k$.

In contrast to the quasi-two-dimensional case, for quasi-one-dimensional dipoles with tilt, Eq. (4.18) cannot in general be satisfied for all $\mathbf{y}$. Indeed, one can check that

$$\int dx V(x, \mathbf{y}) = 4\pi(a - a_*)\delta(\mathbf{y}) + 2r_*\sin^2\theta\frac{y_2^2 - y_1^2}{y^4}, \tag{4.42}$$

where

$$a_* = \left(\frac{1}{3} - \frac{\sin^2\theta}{2}\right) r_*. \tag{4.43}$$

From Eq. (4.42) we see that the condition $V_{\mathbf{00}}^{\mathbf{00}}(\mathbf{0}) = 0$ requires $a = a_*$ (this condition corresponds to $\epsilon_{\rm dd} = 1$ in notations of Ref. [103]). However, the matrix elements $V_{\boldsymbol{\mu\nu}}^{\boldsymbol{\zeta\eta}}(\mathbf{0})$ involving excited states all vanish only if $a = a_*$ and $\sin\theta = 0$. Therefore, for a finite tilt angle the dominant nonpairwise interaction correction is given by $g_3^{(2)}$ Eq. (4.11) and corresponds to an effective three-body attraction. We will calculate it for arbitrary θ. As far as $g_3^{(3)}$ is concerned, it can become dominant only at (or sufficiently close to) the

point $\theta = 0$.

The relevant matrix elements needed for these calculations can be written as [5]

$$\begin{aligned} V^{\mathbf{0}\{\nu,m\}}_{\mathbf{0}\{\mu,m'\}}(k) &= V^{\mathbf{0}\{\nu,m\}}_{\{\mu,-m'\}\mathbf{0}}(k) = V^{\{\nu,-m\}\mathbf{0}}_{\mathbf{0}\{\mu,m'\}}(k) = V^{\{\nu,m\}\mathbf{0}}_{\mathbf{0}\{\mu,-m'\}}(k) \\ &= \int \frac{d^2p}{(2\pi)^2} V(k,\mathbf{p})\lambda_{\nu,m}(\boldsymbol{p})\lambda_{\mu,m'}(-\boldsymbol{p}), \end{aligned} \tag{4.44}$$

where

$$\begin{aligned} \lambda_{\nu,m}(\boldsymbol{p}) &= \int \psi_0(\boldsymbol{y})\psi_{\nu,m}(\boldsymbol{y})e^{i\boldsymbol{p}\boldsymbol{y}}d^2y \\ &= \frac{(-1)^{\nu+|m|/2}}{\sqrt{\nu!(\nu+|m|)!}}\left(\frac{lp}{2}\right)^{2\nu+|m|} e^{-p^2l^2/4}\left(\frac{p_1+ip_2}{p}\right)^m. \end{aligned} \tag{4.45}$$

Then, integrating in Eq. (4.44) over $\boldsymbol{p}$ gives

$$\begin{aligned} V^{\mathbf{0}\{\nu,m\}}_{\mathbf{0}\{\mu,m'\}}(k) &= \frac{(-1)^s 2^{-s-1}s!}{\sqrt{\nu!(\nu+|m|)!\mu!(\mu+|m'|)!}} \frac{4(a-a_*)\delta_{m+m',0} + r_*\delta_{|m+m'|,2}\sin^2\theta}{l^2} \\ &+ \frac{r_*(-1)^s(kl/2)^{2s+2}e^{k^2l^2/2}}{l^2\sqrt{\nu!(\nu+|m|)!\mu!(\mu+|m'|)!}} \\ &\times \{s!\Gamma(-s,k^2l^2/2)[\delta_{m+m',0}(4-6\sin^2\theta) - \delta_{|m+m'|,2}\sin^2\theta] \\ &+ 2(s+1/2)!\Gamma(-s-1/2,k^2l^2/2)\delta_{|m+m'|,1}\sin 2\theta\}, \end{aligned} \tag{4.46}$$

where $s = \nu + \mu + (|m| + |m'|)/2$.

Substituting Eq. (4.46) and more precisely, its particular case:

$$V^{\mathbf{00}}_{\mathbf{0}\{\nu,m\}}(0) = \frac{(-1)^\nu}{2^{\nu-1}}\left(\frac{a-a_*}{l^2}\delta_{m,0} - \frac{r_*\sin^2\theta}{8l^2}\sqrt{\frac{\nu+1}{\nu+2}}\delta_{|m|,2}\right), \tag{4.47}$$

into Eq. (4.11), we get

$$g_3^{(2)} = -12\ln\frac{4}{3}\left(\frac{a-a_*}{l}\right)^2 + \left(\frac{3}{2} - 6\ln\frac{4}{3}\right)\left(\frac{r_*}{l}\right)^2\sin^4\theta. \tag{4.48}$$

The first term on the right-hand side of Eq. (4.48) recovers the result of Refs. [89, 91] obtained for $r_* = 0$. By tuning to $a = a_*$ this term vanishes simultaneously with the leading two-body energy shift $g_2^{(1)} = V^{\mathbf{00}}_{\mathbf{00}}(0)$. Nevertheless, Eq. (4.48) predicts that the three-body attraction persists for any finite tilt angle even if $a = a_*$. Tilted dipoles can thus realize a model of one-dimensional bosons with three-body attraction, interesting for some applications (see, for example, Ref. [78]). Curiously, $g_3^{(2)}$ remains finite also for the "magic" angle given by $\cos\theta = 1/\sqrt{3}$, a characteristic point where $V(x,\boldsymbol{y})$ looses its long-range dipolar tail in the x direction.

As we have mentioned, for $\theta = 0$ and $a = a_*$ the second-order term $g_3^{(2)}$ vanishes.

[5] Our derivation of the matrix elements follows the procedure of Edler *et al.* [103] who discussed quasi-one-dimensional dipoles aligned along the symmetry axis.

The three-body interaction in this case emerges in the third order and can be repulsive. Evaluating Eq. (4.14) and using Eq. (4.46) with $\theta = 0$ and $a = a_*$, we obtain [6]

$$g_3^{(3)} = 4.65(r_*/l)^3. \tag{4.49}$$

We see that the attractive long-range tail (corresponding to $r_* > 0$) is correlated with a three-body repulsion. As in the quasi-two-dimensional case we can compare the full quasi-one-dimensional model with the purely one-dimensional one obtained by projecting the interaction potential $V(\mathbf{r})$ to the radial ground state. The calculation of $g_3^{(3)}$ then proceeds by restricting the sum in Eq. (4.14) to $\boldsymbol{\nu} = \boldsymbol{\mu} = \boldsymbol{\eta} = 0$ and gives $g_3^{(3)} = 3.57(r_*/l)^3$.

Finally, let us come back to the case of finite θ and mention the confinement-induced correction $g_2^{(2)}$. For $a = a_*$ Eq. (4.10) contains no infrared divergences and the ultraviolet one has the same origin and is treated in the same manner as in the quasi-two-dimensional case. Performing a very similar analysis of the large-s asymptote of $V_{\mathbf{0}\{\mu,m'\}}^{\mathbf{0}\{\nu,m\}}(k)$ we arrive at the diverging integral of the type (4.37) for the function $V^2(k,\mathbf{p})$ with the prefactor $1/(2\pi l^2)$ instead of $1/(\sqrt{2\pi}l)$ (see Sec.4.2.3). When calculating Eq. (4.10) we subtract this diverging contribution and arrive at

$$g_2^{(2)} = \frac{r_*^2}{l^3}(D_0 + D_1 \sin^2\theta + D_2 \sin^4\theta) \tag{4.50}$$

with the numerical coefficients $D_0 = 0.081$, $D_1 = 0.35$ and $D_2 = -0.2$. The correction (4.50) is always positive.

We can try to calculate $g_2^{(2)}$ by projecting to the transversal ground state, i.e., integrating over k in Eq. (4.10) with $\boldsymbol{\nu} = \boldsymbol{\mu} = 0$. In this manner we obtain $g_2^{(2)} = -0.94(r_*^2/l^3)[1 - (3/2)\sin^2\theta]^2$, which is actually quite different from Eq. (4.50), indicating that the correct renormalization procedure is important. In fact, Edler and coworkers [103] have calculated the BMF energy density for quasi-one-dimensional dipoles with $\theta = 0$ and $a = a_*$ by using the projected value of $g_2^{(2)}$ as the low-density reference point for their Hugenholtz-Pines approach. We agree with them on the effective three-body repulsion in this case, but disagree on g_2. This, however, does not qualitatively change the conclusion of Ref. [103] on the existence of self-bound states in this system since one can always tune g_2 by modifying a. Nevertheless, it would be interesting to perform the BMF crossover analysis using Eq. (4.50) as the low-density reference point.

[6] Again, we use the scaling $g_3(\epsilon_c) - g_3(\infty) \propto 1/\sqrt{\epsilon_c}$ after the introduction of a cutoff $\epsilon_c \propto 1/r_0^2$ for excitation energies in Eq. (4.14). We use this scaling for calculating the numerical coefficient in Eq. (4.49).

4.3 Bogoliubov theory

The standard perturbation theory of Sec. 4.1 requires that the interaction shifts be smaller than the level spacing in the non-interacting system of N particles. In principle, one can always reach this regime by decreasing V while keeping the volume fixed. The fixed volume maintains a low-momentum cutoff, avoiding possible infrared divergences in the integrals, and leads to the regular expansion of the energy in integer powers of V.

The problem of infrared divergences can also be solved in the thermodynamic limit by turning to the Bogoliubov theory which accounts for a nonperturbative change in the system behavior at length scales comparable or larger than the healing length $\xi \propto 1/\sqrt{V_{\mathbf{00}}^{\mathbf{00}}(\mathbf{0})n}$. The Bogoliubov theory thus effectively introduces an infrared density-dependent cutoff at $k \sim 1/\xi$, which, in particular, leads to the nonanalyticity of the energy as a function of n (and V).

In all examples of Sec. 4.2 the infrared divergences are eliminated by the condition (4.18) [7]. Our theory thus predicts the regular expansion of the energy in integer powers of n, characterized by the effective few-body coupling constants g_2 and g_3, which are "local" BMF contributions involving virtual excitations with wave lengths comparable to the interaction range.

The perturbation theory of Sec. 4.1 is basically the Born series expansion for which the typical value of $|V|$ (in real space) multiplied by the square of its range should be small [13]. This small parameter is density independent. By contrast, the Bogoliubov theory relies on the relative smallness of the non-condensed fraction, which depends on the density. It is then interesting to figure out how the hierarchy of the Bogoliubov theory (the mean-field term, the leading-order BMF contribution, the beyond-Bogoliubov terms) is related to our expansion in powers of V. In the remaining part of this section we show how the perturbative results obtained in Sec. 4.1 can be deduced from the Bogoliubov theory.

The Hamiltonian (4.1) in the second quantization reads

$$\begin{aligned}\hat{H} &= \sum_{\boldsymbol{q},\boldsymbol{\nu}} (q^2/2 + \epsilon_{\boldsymbol{\nu}}) \hat{a}^\dagger_{\boldsymbol{q},\boldsymbol{\nu}} \hat{a}_{\boldsymbol{q},\boldsymbol{\nu}} \\ &+ \frac{1}{2} \sum_{\boldsymbol{q}_1,\boldsymbol{q}_2,\boldsymbol{k},\boldsymbol{\nu},\boldsymbol{\mu},\boldsymbol{\eta},\boldsymbol{\zeta}} V^{\boldsymbol{\zeta\eta}}_{\boldsymbol{\mu\nu}}(\mathbf{k}) \hat{a}^\dagger_{\boldsymbol{q}_2+\boldsymbol{k},\boldsymbol{\mu}} \hat{a}^\dagger_{\boldsymbol{q}_1-\boldsymbol{k},\boldsymbol{\zeta}} \hat{a}_{\boldsymbol{q}_2,\boldsymbol{\nu}} \hat{a}_{\boldsymbol{q}_1,\boldsymbol{\eta}}.\end{aligned} \tag{4.51}$$

Following the standard Bogoliubov procedure we assume the macroscopic occupation of the ground state replacing $\hat{a}_{\mathbf{0},\mathbf{0}}$ and $\hat{a}^\dagger_{\mathbf{0},\mathbf{0}}$ by $\sqrt{n_0}$ and then expanding $\hat{H} = H_0 + \hat{H}_{sp} + \sum_{i=1}^4 \hat{H}_i$, where

$$H_0 = V_{\mathbf{00}}^{\mathbf{00}}(\mathbf{0}) n_0^2/2, \tag{4.52}$$

[7] There are, of course, examples featuring infrared divergences on the one hand, and satisfying Eq. (4.18) on the other. Consider, for instance, the low-momentum scaling $V(k) \propto |k|^\gamma$ with small positive γ.

$$\hat{H}_{sp} = \sum_{\boldsymbol{q},\boldsymbol{\nu}} (q^2/2 + \epsilon_{\boldsymbol{\nu}}) \hat{a}^\dagger_{\boldsymbol{q},\boldsymbol{\nu}} \hat{a}_{\boldsymbol{q},\boldsymbol{\nu}}, \tag{4.53}$$

$$\hat{H}_1 = n_0^{3/2} {\sum_{\boldsymbol{\nu}}}' V^{\boldsymbol{00}}_{\boldsymbol{\nu 0}}(\mathbf{0}) \hat{a}^\dagger_{\mathbf{0},\boldsymbol{\nu}} + V^{\boldsymbol{00}}_{\mathbf{0}\boldsymbol{\nu}}(\mathbf{0}) \hat{a}_{\mathbf{0},\boldsymbol{\nu}}, \tag{4.54}$$

$$\begin{aligned} \hat{H}_2 = \frac{n_0}{2} {\sum_{\boldsymbol{\nu},\boldsymbol{\mu},\boldsymbol{k}}}' & V^{\boldsymbol{\nu 0}}_{\boldsymbol{\mu 0}}(\mathbf{k}) \hat{a}^\dagger_{\boldsymbol{k},\boldsymbol{\mu}} \hat{a}^\dagger_{-\boldsymbol{k},\boldsymbol{\nu}} + V^{\boldsymbol{0\nu}}_{\boldsymbol{0\mu}}(\mathbf{k}) \hat{a}_{-\boldsymbol{k},\boldsymbol{\mu}} \hat{a}_{\boldsymbol{k},\boldsymbol{\nu}} \\ & + 2[V^{\boldsymbol{00}}_{\boldsymbol{\mu\nu}}(\mathbf{0}) + V^{\boldsymbol{0\nu}}_{\boldsymbol{\mu 0}}(\mathbf{k})] \hat{a}^\dagger_{\boldsymbol{k},\boldsymbol{\mu}} \hat{a}_{\boldsymbol{k},\boldsymbol{\nu}}, \end{aligned} \tag{4.55}$$

$$\begin{aligned} \hat{H}_3 = \sqrt{n_0} {\sum_{\boldsymbol{q},\boldsymbol{k},\boldsymbol{\nu},\boldsymbol{\mu},\boldsymbol{\eta}}}' & V^{\boldsymbol{\mu\eta}}_{\boldsymbol{\nu 0}}(\mathbf{k}) \hat{a}^\dagger_{\boldsymbol{k},\boldsymbol{\nu}} \hat{a}^\dagger_{\boldsymbol{q},\boldsymbol{\mu}} \hat{a}_{\boldsymbol{q}+\mathbf{k},\boldsymbol{\eta}} \\ & + V^{\boldsymbol{0\nu}}_{\boldsymbol{\eta\mu}}(\mathbf{k}) \hat{a}^\dagger_{\boldsymbol{q}+\mathbf{k},\boldsymbol{\eta}} \hat{a}_{\boldsymbol{k},\boldsymbol{\nu}} \hat{a}_{\boldsymbol{q},\boldsymbol{\mu}}, \end{aligned} \tag{4.56}$$

and

$$\hat{H}_4 = \frac{1}{2} {\sum_{\boldsymbol{q}_1,\boldsymbol{q}_2,\boldsymbol{k},\boldsymbol{\nu},\boldsymbol{\mu},\boldsymbol{\eta},\boldsymbol{\zeta}}}' V^{\boldsymbol{\zeta\eta}}_{\boldsymbol{\mu\nu}}(\mathbf{k}) \hat{a}^\dagger_{\boldsymbol{q}_2+\boldsymbol{k},\boldsymbol{\mu}} \hat{a}^\dagger_{\boldsymbol{q}_1-\boldsymbol{k},\boldsymbol{\zeta}} \hat{a}_{\boldsymbol{q}_2,\boldsymbol{\nu}} \hat{a}_{\boldsymbol{q}_1,\boldsymbol{\eta}}. \tag{4.57}$$

In Eqs. (4.54-4.57) the primes indicate that the corresponding sum excludes terms involving creation or annihilation operators of condensate particles.

Equation (4.52) is the usual mean-field term. As far as the linear part Eq. (4.54) is concerned, it appeared because we skipped one step of the standard Bogoliubov method. Namely, we just took the single-particle ground state $\phi_{\mathbf{0},\mathbf{0}}(\mathbf{x},\mathbf{y})$ [see Eq. (4.2)] for the condensate mode instead of solving the mean-field Gross-Pitaevskii equation, which, in general, leads to a different profile in the confined direction (see, for example, [105]). The inconvenience of having this linear term is compensated by the fact that the matrix elements $V^{\boldsymbol{\zeta\eta}}_{\boldsymbol{\mu\nu}}(\mathbf{k})$ do not depend on the density and other parameters through the outcome of the Gross-Pitaevskii equation. In fact, this equation may not even always have a solution if the system is unstable from the mean-field viewpoint. It is also interesting to observe that tuning $V^{\boldsymbol{00}}_{\boldsymbol{00}}(\mathbf{0})$ to zero does not necessarily mean $\hat{H}_1 = 0$ since matrix elements of the type $V^{\boldsymbol{00}}_{\boldsymbol{\nu 0}}(\mathbf{0})$ can still remain finite. A particular example of this phenomenon is quasi-one-dimensional dipoles with finite tilt discussed in Sec. 4.2.4. In such cases, one can treat $\hat{H}_1$ as a perturbation on top of the single-particle Hamiltonian $\hat{H}_{sp}$ given by Eq. (4.53). The second-order correction to the energy calculated in this manner equals $g_3^{(2)} n_0^3/6$, with $g_3^{(2)}$ given by Eq. (4.11).

In what follows we proceed under the assumption (4.18), which means $H_0 = \hat{H}_1 = 0$. Among remaining terms the sum $\hat{H}_{sp} + \hat{H}_2$ is the quadratic Bogoliubov Hamiltonian, the zero-point energy of which gives the leading-order BMF contribution to the energy density. The diagonalization of this Hamiltonian consists of solving the linear Bogoliubov-de Gennes equations and can be done analytically in some cases (for instance, for flat condensates with periodic boundary conditions [110]). Otherwise, and this is the case of harmonic confinement, this procedure requires a numerical diagonalization of a $2M \times 2M$ matrix, where M is the size of the discretized $\boldsymbol{\nu}$-space [103]. This is however, not necessary for our purposes. We just note that for small V or n_0 we can treat $\hat{H}_2$ as a

perturbation to $\hat{H}_{sp}$ and proceed with the standard perturbation theory. It is then easy to see that the first-order energy shift vanishes, and the second and third-order corrections are given by $g_2^{(2)} n_0^2/2$ and $g_3^{(3)} n_0^3/6$, respectively, where the coupling constants are given by Eqs. (4.10) and (4.14). On the other hand, the third-order correction to the two-body constant Eq. (4.15) is not recovered, which is understandable since $\hat{H}_2$ does not include interactions between excited atoms.

In our search for all third-order corrections we thus have to formally go beyond the Bogoliubov approximation and consider $\hat{H}_3$ and $\hat{H}_4$. Note that these operators do not perturb the ground state of $\hat{H}_{sp}$ in any order. They can thus only react on the ground state already perturbed by $\hat{H}_2$ leading to corrections of order V^3 or higher. Indeed, the ground state of $\hat{H}_{sp} + \hat{H}_2$, calculated to the first order in $\hat{H}_2$, reads

$$|1\rangle = -\frac{n_0}{2} \sum_{\boldsymbol{\nu},\boldsymbol{\mu},\boldsymbol{k}}{}' \frac{V_{\boldsymbol{\mu 0}}^{\boldsymbol{\nu 0}}(\mathbf{k})}{k^2 + \epsilon_{\boldsymbol{\nu}} + \epsilon_{\boldsymbol{\mu}}} \hat{a}_{\boldsymbol{k},\boldsymbol{\mu}}^\dagger \hat{a}_{-\boldsymbol{k},\boldsymbol{\nu}}^\dagger |0\rangle , \tag{4.58}$$

where $|0\rangle$ is the vacuum of excitations of $\hat{H}_{sp}$, i.e., pure condensate with density n_0. We then observe that $\langle 1| \hat{H}_3 |1\rangle = 0$ and the leading-order beyond-Bogoliubov contribution equals

$$\langle 1| \hat{H}_4 |1\rangle = g_2^{(3)} n_0^2/2, \tag{4.59}$$

where $g_2^{(3)}$ is given by Eq. (4.15). Finally, we note that the leading-order noncondensed density equals

$$\delta n = \langle 1| \sum_{\boldsymbol{q},\boldsymbol{\nu}} \hat{a}_{\boldsymbol{q},\boldsymbol{\nu}}^\dagger \hat{a}_{\boldsymbol{q},\boldsymbol{\nu}} |1\rangle = n_0^2 \sum_{\mathbf{k},\boldsymbol{\nu},\boldsymbol{\mu}} \frac{|V_{\boldsymbol{0\mu}}^{\boldsymbol{0\nu}}(\mathbf{k})|^2}{(k^2 + \epsilon_{\boldsymbol{\nu}} + \epsilon_{\boldsymbol{\mu}})^2}, \tag{4.60}$$

and, to the order V^3, for all the above mentioned energy corrections we can take n_0 to be equal to the total density. We have thus established the consistency of the second-quantized Bogoliubov approach with the standard first-quantized approach of Sec. 4.1 up to the order V^3. Note, however, that Eq. (4.60) features an infrared logarithmic divergence for quasi-two-dimensional dipoles since $V_{\boldsymbol{0\mu}}^{\boldsymbol{0\nu}}(\mathbf{k}) \propto k$. This divergence leads to the scaling $\delta n \propto V^2 \ln V$, which does not change our conclusion, but signals that at higher orders a nonperturbative treatment of the quadratic Bogoliubov Hamiltonian is necessary in this case.

4.4 Conclusions

In conclusion, we have developed a perturbation approach for calculating interaction energy shifts for bosons with the interaction potential V tuned close to the condition (4.18). Under this assumption the leading nonpairwise energy correction is a third-order effect manifesting itself in the form of an effective three-body interaction. Whether this interaction is attractive or repulsive is determined by the shape of $V(\mathbf{k})$ through Eq. (4.14). For simple two-body potentials the sign of g_3 is systematically anticorrelated

with the sign of the long-range tail of the two-body potential, but this does not hold in general (see a counterexample in the end of Sec. 4.2.2).

We have applied our theory to a few particular shapes of V in pure dimensions (double-Gaussian and Yukawa-plus-delta potentials) and in quasi-low-dimensional geometries where we have considered tilted dipoles. For the latter systems we have fully characterized the leading two-body and three-body energy corrections as a function of the tilt angle. In particular, we have found that dipoles under harmonic quasi-two-dimensional confinement are characterized by an effective three-body attraction when aligned perpendicularly to the plane and by a three-body repulsion, if aligned in the plane (see Fig. 4.2). It remains to be seen if this repulsion can stabilize dilute supersolid stripe phases of tilted dipoles, so far predicted to be stable only in the dense regime [112,113]). The three-body repulsion for dipoles aligned in the plane has also been found by Zin *et al.* [110], although in their case the quasi-two-dimensional confinement is achieved by imposing the periodic boundary condition.

Our analysis of quasi-one-dimensional dipoles has revealed a strong (second-order) three-body attraction for any finite tilt angle and a weaker (third-order) three-body repulsion when the dipoles are aligned along the unconfined axis. This latter observation is in agreement with the BMF calculations of Ref. [103]. We however disagree on the leading-order two-body correction $g_2^{(2)}$, positive in our case and negative in Ref. [103] (see our comment in the end of Sec. 4.2.4). We argue that our results can be used to improve the Hugenholtz-Pines analysis by providing the low-density reference point for quasi-low-dimensional tilted dipoles.

Chapter 5

Three-body interaction near a narrow two-body zero crossing

Contents

5.1 Mean-field analysis 74

5.1.1 Application to two-dimensional dipoles 76

5.1.2 Inelastic losses 77

5.2 Regularized model and two-body problem 77

5.3 Three-body problem 80

5.3.1 One dimension 85

5.3.2 Two dimensions 87

5.3.3 Three dimensions 88

5.4 Discussion and conclusions 89

How can one engineer an effective three-body repulsive force?

How can it stabilize quasi-two-dimensional dipolar atoms in the pursuit of the supersolid phase?

In this Chapter, we analyze a simple mechanism for the emergence of an effective three-body interaction. Namely, we consider bosons interacting with each other by a potential tuned to a zero-crossing near a narrow Feshbach resonance, where the conversion amplitude from atoms to closed-channel dimers is small and where the two-body scattering amplitude is characterized by a large effective range R_e. The effective three-body force appears in this model when one takes into account the interaction between atoms and closed-channel dimers, characterized by the coupling strength g_{12}. We find that the three-body coupling constant g_3 in D dimensions is proportional to $R_e^D g_{12}$ and can thus be enhanced near narrow two-body zero crossings.

The Chapter is organized as follows. In Sec. 5.1 we introduce the two-channel model and perform its mean-field analysis. In the dilute limit, the density of closed-channel dimers in the system scales as $R_e^D n^2 \ll n$ and the effective three-body interaction emerges simply as the atom-dimer mean-field interaction energy $\propto R_e^D g_{12} n^3$. We show that this simple mechanism, applied to two-dimensional dipoles, generates conditions for observing supersolid phases predicted in Ref. [114].

In Secs. 5.2 and 5.3 we turn to the few-body perspective and perform a detailed nonperturbative analysis of the two-body (Sec. 5.2) and three-body (Sec. 5.3) problems with zero-range potentials. In particular, the three-body scattering length near a narrow two-body zero crossing is found for an arbitrary atom-dimer interaction strength in any dimension.

5.1 Mean-field analysis

We start with the two-channel model described by the Hamiltonian [115]

$$\begin{aligned}\hat{H} = \int_{\mathbf{r}} \Big\{ &- \hat{\psi}_1^\dagger(\mathbf{r}) \frac{\nabla^2}{2} \hat{\psi}_1(\mathbf{r}) + \hat{\psi}_2^\dagger(\mathbf{r}) \left(-\frac{\nabla^2}{4} + \nu_0 \right) \hat{\psi}_2(\mathbf{r}) \\ &- \frac{\alpha}{2} [\hat{\psi}_1^\dagger(\mathbf{r}) \hat{\psi}_1^\dagger(\mathbf{r}) \hat{\psi}_2(\mathbf{r}) + \text{h.c.}] + \sum_{\sigma\sigma'} \frac{g_{\sigma\sigma'}}{2} \hat{n}_\sigma(\mathbf{r}) \hat{n}_{\sigma'}(\mathbf{r}) \Big\},\end{aligned} \tag{5.1}$$

where $\hat{\psi}_1$ and $\hat{\psi}_2$ are, respectively, the annihilation operators of atoms and dimers, $\hat{n}_\sigma$ are the corresponding density operators, ν_0 is the detuning parameter, $g_{\sigma\sigma'}$ are interaction constants, α is the atom-dimer conversion amplitude (without loss of generality assumed real and positive), and we have set $\hbar$ and atom mass equal to 1. Hereafter, $\int_{\mathbf{r}}$ denotes $\int d^D r$.

In the mean-field description of (5.1) we assume pure atomic and molecular condensates $\hat{\psi}_\sigma = \sqrt{n_\sigma}$ with the same phase (which corresponds to the energy minimum for

$\alpha > 0$) [115]. We arrive at the energy density

$$E/L^D = \nu_0 n_2 - \alpha n_1 \sqrt{n_2} + \sum_{\sigma\sigma'} g_{\sigma\sigma'} n_\sigma n_{\sigma'}/2, \tag{5.2}$$

which we minimize with respect to n_2 (or n_1) keeping the total density $n = n_1 + 2n_2$ constant. For positive ν_0 and small n the dimer population behaves quadratically in n

$$n_2 = \left(\frac{\alpha n}{2\nu_0}\right)^2 \left(1 + \frac{4g_{11}\nu_0 - 2g_{12}\nu_0 - 3\alpha^2}{\nu_0^2} n\right) + O(n^4) \tag{5.3}$$

and the energy density reads

$$\frac{E}{L^D} = \left(\frac{g_{11}}{2} - \frac{\alpha^2}{4\nu_0}\right)\left(n^2 - \frac{\alpha^2}{\nu_0^2} n^3\right) + \frac{g_{12}\alpha^2}{4\nu_0^2} n^3 + O(n^4). \tag{5.4}$$

The two-body zero crossing occurs at the detuning $\nu_0 = \alpha^2/2g_{11}$ where the first term in the right-hand side of Eq. (5.4) vanishes. One can then see that the residual three-body energy shift originates from the direct mean-field interaction of atoms with dimers. It equals $g_{12} n_1 n_2 \approx g_3 n^3/3!$ with

$$g_3 = 6 g_{12} g_{11}^2/\alpha^2 = 3 g_{12} R_e^D. \tag{5.5}$$

The effective volume $R_e^D = 2g_{11}^2/\alpha^2$ introduced in Eq. (5.5) characterizes the closed-channel population. Indeed, the density of dimers can be written as

$$n_2 \approx R_e^D n^2/2 \tag{5.6}$$

meaning that each pair of atoms is found in the closed-channel dimer state with probability $(R_e/L)^D$.

If $g_{\sigma\sigma'}$ are of the same order of magnitude $\sim g$, the expansion (5.4) is in powers of $R_e^D n$, which we assume small. Then, at the zero crossing the three-body term gives the leading contribution to the energy density $\sim g n^2 (R_e^D n)^1$ and we neglect subleading terms such as, for instance, the dimer-dimer interaction $\sim g_{22}\alpha^4 n^4/\nu_0^4 \sim g n^2 (R_e^D n)^2$. On the other hand, it may be interesting to keep a small but finite effective two-body interaction $g_{\text{eff}} = g_{11} - \alpha^2/2\nu_0 \sim g(R_e^D n) \ll g$, so that it can compete with the three-body term. It is also useful to note that the effective two-body interaction depends on the collisional momentum as $g_{\text{eff}}(k) = g_{\text{eff}}(0) - R_e^D k^2$ (see [116] and Sec. 5.2). However, if $k \ll \sqrt{gn}$, the corresponding effective-range correction gives a contribution to (5.4) much smaller than $g n^2 (R_e^D n)^1$. We thus conclude that on this level of expansion we reduce (5.1) to the model of scalar bosons with local effective two-body and three-body interactions.

5.1.1 Application to two-dimensional dipoles

Having in mind supersolid phases, which require a three-body repulsive force [114], let us perform the same mean-field analysis in the case of two-dimensional dipoles oriented perpendicular to the plane. Instead of pointlike interactions characterized by the momentum-independent constants $g_{\sigma\sigma'}$ we now assume momentum-dependent pseudopotentials [114, 117]

$$\tilde{V}_{\sigma\sigma'}(|\mathbf{k}-\mathbf{k}'|) = g_{\sigma\sigma'} - 2\pi d_\sigma d_{\sigma'}|\mathbf{k}-\mathbf{k}'|, \tag{5.7}$$

where $\mathbf{k}$ and $\mathbf{k}'$ are the incoming and outgoing relative momenta and d_1 and d_2 are dipole moments of atoms and dimers, respectively. The pseudopotential (5.7) is an effective potential valid only for the leading-order mean-field analysis at low momenta. Its coordinate representation

$$V_{\sigma\sigma'}(\mathbf{r}-\mathbf{r}') = \int \frac{d^2q}{(2\pi)^2}\tilde{V}_{\sigma\sigma'}(q)e^{i\mathbf{q}(\mathbf{r}-\mathbf{r}')} \tag{5.8}$$

has the long-distance asymptote $d_\sigma d_{\sigma'}/r^3$ with the characteristic range $r^*_{\sigma\sigma'} = 2\mu_{\sigma\sigma'}d_\sigma d_{\sigma'}$, where $\mu_{11} = 1/2$ and $\mu_{12} = 2/3$ are the atom-atom and atom-dimer reduced masses, respectively.

Obviously, for homogeneous condensates the momentum-dependent part of (5.7) plays no role and our previous analysis holds. Namely, we arrive at the energy density $E/L^2 = g_{\rm eff}n^2/2 + g_3n^3/6$, where $g_{\rm eff} = g_{11} - \alpha^2/2\nu_0$ is tuned to be small and g_3 is given by Eq. (5.5). Let us now assume that the atomic and dimer condensates are spatially modulated with a characteristic momentum k (in the supersolid phase the modulation is periodic). Then, the most important new terms in Eqs. (5.2) and (5.4) are the kinetic energy of the atomic component $\sim nk^2$ and the momentum-dependent part of the atom-atom interaction $\sim -r^*_{11}kn^2$. Minimizing their sum with respect to k gives a contribution $\epsilon_{\rm mod} \sim -r^{*2}_{11}n^3$ to the energy density and the optimal modulation momentum $k_{\rm min} \sim r^*_{11}n$ [114]. One can check that other momentum-dependent terms are subleading. For instance, the kinetic energy of dimers $\sim n_2k^2$ and the momentum-dependent atom-dimer interaction $\sim r^*_{12}knn_2$ carry an additional factor $R_{\rm e}^2n \ll 1$. It is important to mention that the density of dimers satisfies Eq. (5.6) locally, i.e., $n_2(\mathbf{r}) \approx R_{\rm e}^2n^2(\mathbf{r})/2$. Deviations from this relation, which follows from minimizing the first two terms in the right-hand side of Eq. (5.2), are energetically too costly. A change of n_2 by, say, a factor of two compared to the optimal value would cost $\sim g_{11}n^2 \gg gn^2(R_{\rm e}^2n)$ in the energy density.

This analysis leads us to the model of two-dimensional dipoles characterized by an effective two-body pseudopotential $\tilde{V}(k) = g_{\rm eff} - 2\pi d_1^2k$ and local three-body term $g_3\delta(\mathbf{r}_1-\mathbf{r}_2)\delta(\mathbf{r}_2-\mathbf{r}_3)$. The mean-field phase diagram of this model has been worked out in Ref. [114]. It has been shown that the stability of the system with respect to collapse is ensured by the repulsive three-body interaction term compensating the effec-

tively attractive $\epsilon_{\rm mod}$, which also scales as n^3. The supersolid stripe, honeycomb and triangular phases are predicted when these two terms are comparable and $g_{\rm eff} < 0$. To give a concrete example, the four-critical point where the three supersolid phases meet with one another and with the uniform phase (this is also the point where the roton minimum touches zero) is characterized by $g_{12}R_{\rm e}^2 = 2(\pi r_{11}^*)^2$ and $nR_{\rm e}^2 = |g_{\rm eff}|/g_{12}$.

5.1.2 Inelastic losses

Collisions of atoms with closed-channel dimers can lead to the relaxation to more deeply bound molecular states. The rate of this process in a unit volume is given by $\alpha_{\rm r} n_1 n_2$, where $\alpha_{\rm r}$ is the relaxation rate constant. In our model this corresponds to the atom loss rate $\dot{n} = -(3/2)\alpha_{\rm r} R_{\rm e}^D n^3$, and we see that this effective three-body loss gets enhanced with increasing $R_{\rm e}$ in the same manner as the elastic three-body interaction (5.5). In fact, the atom-dimer relaxation can be mathematically modeled by allowing g_{12} to be complex. Shotan and co-workers [116] have measured the three-body loss rate constant near a two-body zero crossing in three dimensions. They argue that this quantity is proportional to $R_{\rm e}^4$. Here we claim a slightly different scaling ($\propto R_{\rm e}^3$), valid when $R_{\rm e}$ is much larger than the van der Waals range.

For Feshbach molecules of the size of the van der Waals length $\alpha_{\rm r}$ is typically of the same order of magnitude as g_{12}. The lifetime of the sample is thus comparable to the timescale associated with the elastic three-body energy shift. There are, however, ways of overcoming this problem. For dipoles oriented perpendicular to the plane in the quasi-two-dimensional geometry inelastic processes are suppressed by the predominantly repulsive dipolar tail. For instance, for Dy the atom-dimer dipolar length r_{12}^* can reach about 50 nm depending on the magnetic moment of the closed-channel dimer. The confinement of frequency $\omega = 2\pi\times 100$ kHz for this system gives the oscillator length $\sqrt{\hbar/2\mu_{12}\omega} \approx 21$ nm. Under these conditions one expects a noticeable reduction of the relaxation rate [118–120]. This mechanism may work also for dipolar molecules where larger values of r_{12}^* can be reached.

A different approach to this problem is to consider closed-channel dimers which are weakly-bound and have a halo character, i.e., well extended beyond the support of the potential. A specific way of generating three-body interactions in this manner has been proposed by one of us in Ref. [20]; two atoms in state 1 collide and both go to another internal state $1'$ where they form an extended molecular state. The effective three-body force is then due to a repulsive mean-field interaction between atoms $1'$ and a third atom in state 1. In this case, the relaxation is slow since the dimer is not "preformed".

5.2 Regularized model and two-body problem

We now go back to the model (5.1), try to analyze it from the few-body viewpoint, and characterize the three-body interaction beyond the mean-field result (5.5) (also trying

to determine its validity regime). Clearly, at some point the strength of the background atom-atom interaction becomes a relevant parameter (not just the ratio g_{11}/α). One also observes that the pointlike interaction and conversion terms in Eq. (5.1) lead to divergences and have to be regularized in dimensions $D > 1$, which necessitates an additional parameter (a short-range or high-momentum cutoff).

In order to regularize the model (5.1) we use the delta-shell pseudopotential representation [121, 122] with a finite range r_0. Namely, we rewrite Eq. (5.1) as

$$\begin{aligned}\hat{H} = &\int_{\mathbf{r}} -\hat{\psi}_1^\dagger(\mathbf{r})\frac{\nabla^2}{2}\hat{\psi}_1(\mathbf{r}) + \hat{\psi}_2^\dagger(\mathbf{r})\left(-\frac{\nabla^2}{4}+\nu_0\right)\hat{\psi}_2(\mathbf{r}) \\ &+\sum_{\sigma\sigma'}\frac{g_{\sigma\sigma'}}{2}\int_{\mathbf{r}}\int_{\mathbf{y}}\tilde{\delta}_{r_0}(\mathbf{y})\hat{n}_\sigma(\mathbf{r}+\mathbf{y}/2)\hat{n}_{\sigma'}(\mathbf{r}-\mathbf{y}/2) \\ -\frac{\alpha}{2}\int_{\mathbf{r}}\int_{\mathbf{y}}&\tilde{\delta}_{r_0}(\mathbf{y})[\hat{\psi}_1^\dagger(\mathbf{r}+\mathbf{y}/2)\hat{\psi}_1^\dagger(\mathbf{r}-\mathbf{y}/2)\hat{\psi}_2(\mathbf{r})+\text{h.c.}],\end{aligned} \tag{5.9}$$

where $\tilde{\delta}_{r_0}(\mathbf{y}) = \delta(|\mathbf{y}|-r_0)/S_D(r_0)$ is the normalized delta shell with $S_1(r_0) = 2$, $S_2(r_0) = 2\pi r_0$, and $S_3(r_0) = 4\pi r_0^2$. The range r_0 should be understood as the smallest lengthscale in our problem. It does not enter in the final formulas and it is just a convenient way to regularize the problem without using zero-range pseudopotentials, which have different forms in different dimensions. In the one-dimensional case r_0 can be set to zero from the very beginning, but we keep it finite in order to use the same formalism for the cases with different D. Note also that we do not intend to consider effects of scattering with angular momenta $l \neq 0$. This is to say that, as r_0 is decreased, the coupling constants $g_{\sigma\sigma'}$ and α are tuned to reproduce desired (physical) R_e and $a_{\sigma\sigma'}$ only for the s-wave channel. Then, in the limit $r_0 \to 0$, the terms $g_{\sigma\sigma'}\tilde{\delta}_{r_0}(\mathbf{y})$ and $\alpha\tilde{\delta}_{r_0}(\mathbf{y})$ are too weak to induce any scattering for $l > 0$.

A stationary two-body state with zero center-of-mass momentum and $l = 0$ in the two-channel models (5.1) or (5.9) is represented by

$$\int_{\mathbf{c}}\int_{\mathbf{y}}\Psi(y)\hat{\psi}_1^\dagger(\mathbf{c}+\mathbf{y}/2)\hat{\psi}_1^\dagger(\mathbf{c}-\mathbf{y}/2)\,|0\rangle + \int_{\mathbf{c}}\phi\hat{\psi}_2^\dagger(\mathbf{c})\,|0\rangle\,, \tag{5.10}$$

where $|0\rangle$ is the vacuum state. Acting on (5.10) by the operator $\hat{H}-E$, and requiring that the result vanish, we get the coupled Schrödinger equations at energy E,

$$[-\nabla_{\mathbf{y}}^2 - E + g_{11}\tilde{\delta}_{r_0}(y)]\Psi(y) = \alpha\tilde{\delta}_{r_0}(y)\phi/2, \tag{5.11}$$

$$(\nu_0 - E)\phi = \alpha\Psi(r_0), \tag{5.12}$$

which, upon eliminating the closed-channel amplitude ϕ, become

$$[-\nabla_{\mathbf{y}}^2 - E + g_\text{eff}(E)\tilde{\delta}_{r_0}(y)]\Psi(y) = 0 \tag{5.13}$$

with

$$g_{\rm eff}(E) = g_{11} + \frac{1}{2}\frac{\alpha^2}{E-\nu_0}. \tag{5.14}$$

The zero crossing condition at zero energy thus reads

$$\nu_0 = \alpha^2/2g_{11}. \tag{5.15}$$

We also introduce the effective range by the formula

$$R_{\rm e}^D = \alpha^2/2\nu_0^2 > 0, \tag{5.16}$$

which characterizes the small-E asymptote $g_{\rm eff}(E) = g_{\rm eff}(0) - R_{\rm e}^D E + O(E^2)$ (cf. [116]). At the crossing Eq. (5.16) is consistent with our earlier definition of $R_{\rm e}$ introduced in Eq. (5.5). As we have mentioned, $R_{\rm e}^D$ is also related to the closed-channel occupation. Indeed, from the normalization integral of Eq. (5.10) one finds that the closed-channel to open-channel probability ratio equals $|\phi|^2/\int_{\mathbf{y}} 2|\Psi(y)|^2 = |\phi|^2/(2L^D|\Psi(r_0)|^2)$ where we have used the fact that at the crossing $\Psi(y) = \Psi(r_0)$. On the other hand, from Eq. (5.12) one obtains $|\phi|^2 = 2R_{\rm e}^D|\Psi(r_0)|^2$ for $|E| \ll |\nu_0|$, which gives the result claimed in Sec. 5.1. Namely, the probability for two atoms to be in the closed-channel dimer state equals $(R_{\rm e}/L)^D$.

Eventually, we will need to express our results in terms of the scattering lengths $a_{\sigma\sigma'}$ and the effective range $R_{\rm e}$ rather than in terms of the bare r_0-dependent quantities $g_{\sigma\sigma'}$, α, and ν_0. Relations between $g_{\sigma\sigma'}$ and $a_{\sigma\sigma'}$ are obtained by solving the scattering problem at zero collision energy and by looking at the long-distance asymptote of the two-body wave function. Namely, the zero-energy Schrödinger equation reads

$$[-\nabla_{\mathbf{y}}^2 + 2\mu_{\sigma\sigma'}g_{\sigma\sigma'}\tilde{\delta}_{r_0}(y)]\Psi(y) = 0. \tag{5.17}$$

In one dimension the (unnormalized) solution is

$$\Psi(y) = \begin{cases} 1, & |y| < r_0 \\ 1 + \mu_{\sigma\sigma'}g_{\sigma\sigma'}(|y| - r_0), & |y| > r_0, \end{cases} \tag{5.18}$$

from which we see that

$$a_{\sigma\sigma'} = r_0 - 1/\mu_{\sigma\sigma'}g_{\sigma\sigma'}. \tag{5.19}$$

In the limit $r_0 \to 0$ we recover the usual relation $g_{\sigma\sigma'} = -1/\mu_{\sigma\sigma'}a_{\sigma\sigma'}$. In two dimensions the solution of Eq. (5.17) reads

$$\Psi(\mathbf{y}) = \begin{cases} 1, & |\mathbf{y}| < r_0 \\ 1 + \mu_{\sigma\sigma'}g_{\sigma\sigma'}\ln(|\mathbf{y}|/r_0)/\pi, & |\mathbf{y}| > r_0 \end{cases} \tag{5.20}$$

and one has

$$\mu_{\sigma\sigma'} g_{\sigma\sigma'} = \pi / \ln(r_0/a_{\sigma\sigma'}). \tag{5.21}$$

In three dimensions

$$\Psi(\mathbf{y}) = \begin{cases} 1, & |\mathbf{y}| < r_0 \\ 1 - \mu_{\sigma\sigma'} g_{\sigma\sigma'}/2\pi|\mathbf{y}| + \mu_{\sigma\sigma'} g_{\sigma\sigma'}/2\pi r_0, & |\mathbf{y}| > r_0, \end{cases} \tag{5.22}$$

from which we obtain

$$1/a_{\sigma\sigma'} = 2\pi/\mu_{\sigma\sigma'} g_{\sigma\sigma'} + 1/r_0. \tag{5.23}$$

We now analyze conditions for having two-body bound states at the two-body zero crossing, in particular, having in mind the three-body recombination to these states when considering the three-body problem. We just note that solutions of Eq. (5.13) at distances $|y| \ll 1/\sqrt{|E|}$ in different dimensions are given, respectively, by Eqs. (5.18), (5.20), and (5.22) with $\sigma = \sigma' = 1$ and with g_{11} substituted by $g_{\rm eff}(E)$. We then match these asymptotes with the decaying solutions $\Psi^{(D=1)}(y) \propto \exp(\kappa|y|)$, $\Psi^{(D=2)}(y) \propto K_0(\kappa|\mathbf{y}|)$, and $\Psi^{(D=3)}(y) \propto \exp(-\kappa|\mathbf{y}|)/|\mathbf{y}|$, where $\kappa = \sqrt{-E}$. This matching procedure gives the following equations for the determination of κ ($\gamma \approx 0.577$ is the Euler constant),

$$(\kappa R_{\rm e})^2 (a_{11}/R_{\rm e}) - \kappa R_{\rm e} = 2, \qquad D = 1, \tag{5.24}$$

$$(\kappa R_{\rm e})^2 \ln(\kappa a_{11} e^{\gamma}/2) = 2\pi, \qquad D = 2, \tag{5.25}$$

$$(\kappa R_{\rm e})^3 - (\kappa R_{\rm e})^2 (R_{\rm e}/a_{11}) = 4\pi, \qquad D = 3. \tag{5.26}$$

Analyzing these equations we find that in one dimension there is no two-body bound state, if $a_{11} < 0$ (or $g_{11} > 0$). In higher dimensions we always have a bound state, but it becomes deep in the limit of small positive a_{11} ($E \propto -1/a_{11}^2$). In principle, the case of a weak repulsive background atom-atom interaction can also be realized by a finite-range repulsive potential (in the mean-field spirit of Sec. 5.1). Then, the dimer states given by Eqs. (5.24-5.26) are spurious, consistent with the fact that the zero-range theory can no longer be used at such high momenta.

5.3 Three-body problem

Similar to Eq. (5.10) a stationary state of three atoms with zero center-of-mass momentum can be written in the form

$$\begin{aligned} &\int_{\mathbf{c}} \int_{\mathbf{x}} \int_{\mathbf{y}} \Psi(\mathbf{x},\mathbf{y}) \hat{\psi}_1^\dagger(\mathbf{c} - \mathbf{x}/2\sqrt{3} - \mathbf{y}/2) \hat{\psi}_1^\dagger(\mathbf{c} - \mathbf{x}/2\sqrt{3} + \mathbf{y}/2) \hat{\psi}_1^\dagger(\mathbf{c} + \mathbf{x}/\sqrt{3}) \, |0\rangle \\ &+ \int_{\mathbf{c}} \int_{\mathbf{x}} \phi(\mathbf{x}) \hat{\psi}_2^\dagger(\mathbf{c} - \mathbf{x}/2\sqrt{3}) \hat{\psi}_1^\dagger(\mathbf{c} + \mathbf{x}/\sqrt{3}) \, |0\rangle \, , \end{aligned} \tag{5.27}$$

where $\mathbf{c}$ is the center-of-mass coordinate and the relative Jacobi coordinates are

$$\begin{aligned}\mathbf{x} &= (2\mathbf{r}_1 - \mathbf{r}_2 - \mathbf{r}_3)/\sqrt{3},\\ \mathbf{y} &= \mathbf{r}_3 - \mathbf{r}_2.\end{aligned} \tag{5.28}$$

Let us introduce operators $\hat{P}_+$ and $\hat{P}_-$ which exchange the first atom with the second and the third, respectively. Acting by these operators on an arbitrary function $F(\mathbf{x},\mathbf{y})$ results in

$$\hat{P}_\pm F(\mathbf{x},\mathbf{y}) = F(-\mathbf{x}/2 \mp \sqrt{3}\mathbf{y}/2, -\sqrt{3}\mathbf{x}/2 \pm \mathbf{y}/2). \tag{5.29}$$

The open-channel wave function $\Psi(\mathbf{x},\mathbf{y})$ is invariant with respect to these permutations.

The coupled Schrödinger equations for Ψ and ϕ read

$$[-\nabla^2_{\mathbf{x}} - \nabla^2_{\mathbf{y}} - E + g_{11}(1 + \hat{P}_+ + \hat{P}_-)\tilde{\delta}_{r_0}(y)]\Psi(\mathbf{x},\mathbf{y}) = \alpha(1 + \hat{P}_+ + \hat{P}_-)\tilde{\delta}_{r_0}(y)\phi(\mathbf{x})/2, \tag{5.30}$$

$$[-\nabla^2_{\mathbf{x}} - \nu_0 - E + g_{12}\tilde{\delta}_{r_0}(\sqrt{3}x/2)]\phi(\mathbf{x}) = \alpha\Psi(\mathbf{x}, r_0), \tag{5.31}$$

where $\Psi(\mathbf{x}, r_0)$ in the right-hand side of Eq. (5.31) denotes the projection on the s-wave channel in the coordinate $\mathbf{y}$, i.e., the angular average $\langle\Psi(\mathbf{x}, r_0\hat{y})\rangle_{\hat{y}}$. The difference between $\Psi(\mathbf{x}, r_0\hat{y})$ and $\Psi(\mathbf{x}, r_0)$, which accounts for non-s-wave scattering channels, vanishes in the limit $r_0 \to 0$ and we will thus make the replacement $\tilde{\delta}_{r_0}(y)\Psi(\mathbf{x},\mathbf{y}) \to \tilde{\delta}_{r_0}(y)\Psi(\mathbf{x}, r_0)$ in Eq. (5.30). Then, it is convenient (the reason will become clear below) to introduce an auxiliary function $f(\mathbf{x})$ such that

$$\Psi(\mathbf{x}, r_0) = -f(\mathbf{x})/g_{11} + \alpha\phi(\mathbf{x})/2g_{11}. \tag{5.32}$$

We now eliminate Ψ from Eqs. (5.30) and (5.31) in favor of f and thus derive coupled equations for f and ϕ. To this end we note that with the use of (5.32) Eq. (5.30) becomes

$$(-\nabla^2_{\mathbf{x}} - \nabla^2_{\mathbf{y}} - E)\Psi(\mathbf{x},\mathbf{y}) = (1 + \hat{P}_+ + \hat{P}_-)\tilde{\delta}_{r_0}(y)f(\mathbf{x}). \tag{5.33}$$

Equation (5.33) can now be solved with respect to Ψ by using the Green function $G_E^{(2D)}$ of the $2D$-dimensional Helmholtz operator in the left-hand side (see, for example, Ref. [123]). This procedure gives

$$\begin{aligned}\Psi(\mathbf{x}, r_0) = \Psi_0(\mathbf{x}, 0) + \int_{\mathbf{x}'} \Bigg\{ & G_E^{(2D)}[\sqrt{(\mathbf{x} - \mathbf{x}')^2 + r_0^2}] \\ & + \sum_{\pm} G_E^{(2D)}(\sqrt{x^2 \pm \mathbf{x}\mathbf{x}' + x'^2}) \Bigg\} f(\mathbf{x}'),\end{aligned} \tag{5.34}$$

where $\Psi_0(\mathbf{x},\mathbf{y})$ is any solution of $(-\nabla^2_{\mathbf{x}} - \nabla^2_{\mathbf{y}} - E)\Psi_0(\mathbf{x},\mathbf{y}) = 0$. In Eq. (5.34) we have already taken the limit $r_0 \to 0$, where it exists. With the use of Eq. (5.34) the function $\Psi(\mathbf{x}, r_0)$ can now be eliminated from Eqs. (5.32) and (5.31). Here we explicitly

write down the resulting coupled equations for f and ϕ at the two-body zero crossing ($\nu_0 = \alpha^2/2g_{11}$) and at zero energy ($E = 0$, $\Psi_0 = 1$),

$$\hat{L}f(\mathbf{x}) + f(\mathbf{x})/g_{11} = \phi(\mathbf{x})/\sqrt{2R_e^D} - 1, \tag{5.35}$$
$$[-\nabla_{\mathbf{x}}^2 + g_{12}\tilde{\delta}_{r_0}(\sqrt{3}x/2)]\phi(\mathbf{x}) = -\sqrt{2/R_e^D}f(\mathbf{x}), \tag{5.36}$$

where $\hat{L}$ is the integral operator in the right-hand side of Eq. (5.34) with $E = 0$. We will use the following forms of the zero-energy Green functions

$$G_0^{(2)}(\rho) = -\ln(\rho/R_e)/2\pi, \tag{5.37}$$
$$G_0^{(4)}(\rho) = 1/4\pi^2\rho^2, \tag{5.38}$$
$$G_0^{(6)}(\rho) = 1/4\pi^3\rho^4. \tag{5.39}$$

Equations (5.35) and (5.36) conserve angular momentum and parity. We will be interested in the case of positive parity (for $D = 1$) and zero angular momentum (for $D > 1$) so that $f(\mathbf{x}) = f(x)$ and $\phi(\mathbf{x}) = \phi(x)$. Note also that if $g_{12} = 0$, the solution of Eqs. (5.35) and (5.36) is $f(x) = 0$ and $\phi(x) = \sqrt{2R_e^D}$ indicating the absence of two-body and three-body interactions.

The quantity that we want to extract from solving Eqs. (5.35) and (5.36) is $\tilde{f}(0) = \int_{\mathbf{x}} f(x)$, which is proportional to the three-body scattering amplitude. Indeed, at large hyperradii $\rho = \sqrt{x^2 + y^2}$ Eq. (5.34) gives $\Psi \approx 1 + 3\tilde{f}(0)G_0^{(2D)}(\rho)$ or, explicitly,

$$\Psi = \begin{cases} 1 - 3\tilde{f}(0)\ln(\rho/R_e)/2\pi & \propto \ln(\rho/a_3), \ D = 1, \\ 1 + 3\tilde{f}(0)/4\pi^2\rho^2 & \propto 1 - S_3/\rho^2, \ D = 2, \\ 1 + 3\tilde{f}(0)/4\pi^3\rho^4 & \propto 1 - \Upsilon_3/\rho^4, \ D = 3, \end{cases} \tag{5.40}$$

where we have introduced the three-body scattering length a_3 in one dimension, surface S_3 in two dimensions, and hypervolume Υ_3 in three dimensions which read

$$a_3 = R_e \exp\left[2\pi/3\tilde{f}(0)\right], \qquad D = 1, \tag{5.41}$$
$$S_3 = -3\tilde{f}(0)/4\pi^2, \qquad D = 2, \tag{5.42}$$
$$\Upsilon_3 = -3\tilde{f}(0)/4\pi^3, \qquad D = 3. \tag{5.43}$$

It is useful to note that for $D = 2, 3$ the three-body potential $g_3\delta(\sqrt{3}\mathbf{x}/2)\delta(\mathbf{y})$ with [1]

$$g_3 = -3(\sqrt{3}/2)^D\tilde{f}(0) \tag{5.44}$$

treated in the first Born approximation would produce the same scattered wave as Eqs. (5.40). Equations (5.42), (5.43), and (5.44) relate the three-body coupling constant

[1] The prefactor $\sqrt{3}/2$ here [and also in Eqs. (5.36), (5.47-5.49)] comes from our definition of the Jacobi coordinates (5.28), according to which the atom-dimer distance equals $\sqrt{3}x/2$.

g_3 to the three-body scattering surface and hypervolume. The corresponding contribution to the energy density of a three-body-interacting condensate equals $g_3 n^3/6$ in the weakly interacting regime, which is defined by $|S_3|n \ll 1$ in two dimensions and by $|\Upsilon_3|n^{4/3} \ll 1$ for $D = 3$. The quantity g_3/L^{2D} gives the energy shift for three (condensed) atoms in a large volume L^D. By solving the three-body problem nonperturbatively we calculate the exact g_3, which can then be compared to the mean-field result given by Eq. (5.5).

The relation between a_3 and the three-body energy shift in the case $D = 1$ is slightly more subtle. Pastukhov [124] has recently shown that the ground-state energy density of a three-body-interacting one-dimensional Bose gas can be expanded in half-integer powers of the small parameter

$$g_3(n) = \sqrt{3}\pi/\ln(1/a_3 n) \ll 1, \tag{5.45}$$

with the leading-order term equal to $E/L = g_3(n)n^3/6$. Although, g_3 given by Eq. (5.45) depends on n, one can replace $1/n$ by another density-independent length scale l. If this scale is not exponentially different from $1/n$, the two small parameters are equivalent since they differ only by a higher-order term $\sim g_3^2$. By computing a_3 we can thus compare Eqs. (5.5) and (5.45) which we expect to approach each other in the limit $R_\mathrm{e}/a_{12} \to 0$ (at fixed n). Equivalently, one can say that in this limit Eq. (5.5) predicts the leading exponential dependence of the one-dimensional three-body scattering length

$$a_3 \propto \exp\left(\frac{\pi}{\sqrt{3}}\frac{\mu_{12}a_{12}}{R_\mathrm{e}}\right) = \exp\left(\frac{2\pi}{3\sqrt{3}}\frac{a_{12}}{R_\mathrm{e}}\right) \tag{5.46}$$

leaving, however, the preexponential factor unknown.

Returning to the task of determining $\tilde{f}(0)$ from Eqs. (5.35) and (5.36) we note that the three-body problem in hand admits a zero-range description parametrized by a_{11}, a_{12}, and R_e (see, however, Sec. 5.3.3). Indeed, the sum $\hat{L}f(x) + f(x)/g_{11}$ in Eq. (5.35) is well behaved in the limit $r_0 \to 0$ since the singularity of $\hat{L}f(x)$ gets canceled by the r_0-dependent term in $1/g_{11}$ [see Eqs. (5.21) and (5.23)]. The parameter r_0 thus drops out from Eq. (5.35), g_{11} being conveniently eliminated in favor of a_{11}. As far as Eq. (5.36) is concerned, one can just substitute the interaction term $g_{12}\tilde{\delta}_{r_0}(\sqrt{3}x/2)$ by the Bethe-Peierls boundary conditions at $x \to 0$

$$\phi(x) \propto |x| - 2a_{12}/\sqrt{3}, \qquad D = 1, \tag{5.47}$$

$$\phi(x) \propto \ln\left(\sqrt{3}x/2a_{12}\right), \qquad D = 2, \tag{5.48}$$

$$\phi(x) \propto 1 - 2a_{12}/\sqrt{3}x, \qquad D = 3. \tag{5.49}$$

In other words, Eq. (5.36) is equivalent to

$$-\nabla_{\mathbf{x}}^2\phi(\mathbf{x}) = -\sqrt{2/R_\mathrm{e}^D}f(\mathbf{x}) \tag{5.50}$$

supplemented by the boundary conditions (5.47)-(5.49).

From now on, for brevity, we choose to measure all distances in units of R_e. The function $\tilde{f}(0)$ then depends on a_{11} and a_{12} (measured in units of R_e) and its dimension is clear from Eq. (5.40).

The idea of solving Eqs. (5.35) and (5.47)-(5.50) is to eliminate ϕ by inverting the Laplacian in Eq. (5.50) and then deal with a single integral equation for f. We perform this procedure in momentum space [the Fourier transform is defined by $\tilde{F}(p) = \int_{\mathbf{x}} F(x)e^{-i\mathbf{px}}$] where Eq. (5.50) formally transforms into $p^2\tilde{\phi}(p) = -\sqrt{2}\tilde{f}(p)$. Note, however, that we can always add to $\phi(\mathbf{x})$ a general solution of the Laplace equation $-\nabla^2_{\mathbf{x}}\phi = 0$, possibly singular at the origin. The solution of Eq. (5.50) in momentum space is thus $-\sqrt{2}\tilde{f}(p)/p^2$ plus any linear combination of $\delta(\mathbf{p})$ and $1/p^2$. The freedom of choosing the corresponding coefficients is removed by Eq. (5.35) and the boundary conditions (5.47)-(5.49). The passage to momentum space in Eq. (5.35) is realized by rewriting the Fourier-space version of the operator

$$(\hat{L} + 1/g_{11})\tilde{f}(p) = \left(\frac{2}{\sqrt{3}}\right)^{D-2} \sum_{\pm} \int \frac{\tilde{f}(q)}{p^2 \pm \mathbf{pq} + q^2} \frac{d^D q}{(2\pi)^D} + \tilde{f}(p) \times \begin{cases} 1/2|p| - a_{11}/2, & D = 1, \\ -(1/2\pi)\ln(pa_{11}e^{\gamma}/2), & D = 2, \\ -p/4\pi + 1/4\pi a_{11}, & D = 3. \end{cases} \tag{5.51}$$

We now proceed to reformulating the boundary conditions (5.47)-(5.49) in momentum space. To this end let us first study the large-x behavior of $\phi(x)$ and $f(x)$ and check that these functions indeed possess well-defined Fourier transforms. When two atoms are far away from the third one (large x), the function ϕ is approximately proportional to Ψ due to Eq. (5.12), which is equivalent to having small f in Eq. (5.32). Thus, the large-x asymptotic behavior of $\phi(x)$ is given by Eq. (5.40) and, by calculating the second derivative of these asymptotes and using Eq. (5.50), we obtain the large-x scaling $f(x) \propto x^{-2D}$. We conclude that the passage to momentum representation is straightforward for $D > 1$ where $f(x)$ and $\phi(x)$ are well behaved. By contrast, in one dimension $\phi(x) \propto \ln|x|$ should be understood in the generalized sense by using a limit of a series of Fourier-transformable functions. In particular, we can use the relation $K_0(\sqrt{\epsilon}|x|) \approx -\ln\frac{\sqrt{\epsilon}|x|e^{\gamma}}{2}$ valid for small $\epsilon > 0$ and define a generalized Fourier transform of $\ln|x|$ as

$$-\frac{\pi}{|p|} = \lim_{\epsilon\to+0}\left[-\frac{\pi}{\sqrt{p^2+\epsilon}} - 2\pi\delta(p)\ln\frac{\sqrt{\epsilon}e^{\gamma}}{2}\right]. \tag{5.52}$$

An immediate application of this formalism is the reformulation of the Bethe-Peierls boundary condition (5.47) in momentum space. Namely, for small x we have

$$\phi(x) = \int \tilde{\phi}(p)\frac{dp}{2\pi} - \frac{|x|}{2}\lim_{p\to\infty} p^2\tilde{\phi}(p) + o(x), \tag{5.53}$$

where the integral is convergent, the singularity $\tilde{\phi}(p) \propto 1/|p|$ being understood in the sense of Eq. (5.52). Comparing Eq. (5.53) with (5.47) and denoting $C = \lim_{p\to\infty} p^2\tilde{\phi}(p)$ gives us the Bethe-Peierls boundary condition in momentum space

$$\int \frac{\tilde{\phi}(p)}{C}\frac{dp}{2\pi} = \frac{a_{12}}{\sqrt{3}}. \tag{5.54}$$

Repeating the same procedure in two dimensions Eq. (5.48) transforms into

$$\int \left[\frac{\tilde{\phi}(p)}{C} - \frac{1}{p^2+\sigma}\right]\frac{d^2p}{(2\pi)^2} = \frac{1}{2\pi}\ln\frac{a_{12}\sqrt{\sigma}e^{\gamma}}{\sqrt{3}}, \tag{5.55}$$

where σ is any positive number. In the case $D = 3$, Eq. (5.49) becomes

$$\int \left[\frac{\tilde{\phi}(p)}{C} - \frac{1}{p^2}\right]\frac{d^3p}{(2\pi)^3} = -\frac{\sqrt{3}}{8\pi a_{12}}. \tag{5.56}$$

The task of reformulating our problem in momentum space is thus over.

We now write the solution of Eq. (5.50) in the form

$$\tilde{\phi}(p) = \sqrt{2}(2\pi)^D\delta(\mathbf{p}) + \frac{C - \sqrt{2}\tilde{f}(p)}{p^2}. \tag{5.57}$$

Equation (5.57) is consistent with the definition of C (which is still unknown) and the coefficient in front of $\delta(\mathbf{p})$ is dictated by Eq. (5.35) and by the fact that the operator (5.51) does not give rise to a delta function. We now eliminate $\tilde{\phi}(p)$ by substituting Eq. (5.57) into Eqs. (5.35) and (5.54)-(5.56) and after simple manipulations we obtain the following results.

5.3.1 One dimension

In one dimension we arrive at

$$\tilde{f}(0) = \frac{1}{a_{12}/\sqrt{3} + I^{(1)}(a_{11})}, \tag{5.58}$$

where the function $I^{(1)}(a_{11}) = \int \frac{\chi(p)-1}{p^2}\frac{dp}{2\pi}$ is defined through the solution of

$$\frac{\sqrt{3}}{2}\sum_{\pm}\int \frac{\chi(q)}{p^2 \pm pq + q^2}\frac{dq}{2\pi} + \left(\frac{1}{2|p|} + \frac{1}{p^2} - \frac{a_{11}}{2}\right)\chi(p) = \frac{1}{p^2}, \tag{5.59}$$

$C = \sqrt{2}\tilde{f}(0)$, and $\tilde{f}(p) = \tilde{f}(0)\chi(p)$. Substituting Eq. (5.58) into Eq. (5.41) a_3 factorizes into (we restore the dimensions here)

$$a_3 = R_e \exp\left(\frac{2\pi}{3\sqrt{3}}\frac{a_{12}}{R_e}\right) \exp\left[\frac{2\pi}{3} I^{(1)}\left(\frac{a_{11}}{R_e}\right)\right], \tag{5.60}$$

consistent with Eq. (5.46) in the limit of small R_e/a_{12}.

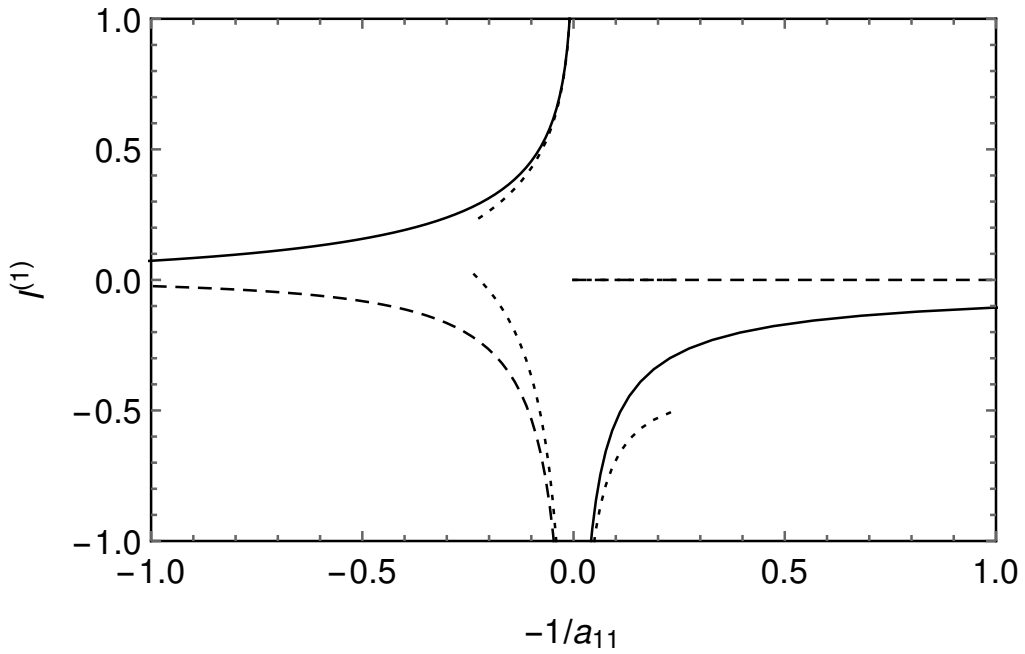

Figure 5.1: Functions $\mathrm{Re}I^{(1)}$ (solid) and $\mathrm{Im}I^{(1)}$ (dashed) characterizing the dependence of the effective three-body interaction on a_{11} in one dimension [see Eqs. (5.58) and (5.40)]. a_{11} is measured in units of R_e. The dotted curves correspond to the large-a_{11} asymptote [Eq. (5.62)]. For $a_{11} \to \pm 0$ one has $I^{(1)} \approx -0.03$.

Let us now discuss the function $I^{(1)}$. For large a_{11} (weak atom-atom interaction) this function can be expanded in powers of $\sqrt{-1/a_{11}}$. In order to see this we rescale the momentum $p = \sqrt{-1/a_{11}}z$ and rewrite Eq. (5.59) in the form

$$\chi(z) = \frac{1}{1+z^2/2} - \frac{1}{\sqrt{-a_{11}}}\frac{z^2}{1+z^2/2}\left[\frac{\sqrt{3}}{2}\sum_{\pm}\int \frac{\chi(y)}{z^2 \pm yz + y^2}\frac{dy}{2\pi} + \frac{\chi(z)}{2|z|}\right], \tag{5.61}$$

which we then solve iteratively. In particular, the first iteration gives $\chi(z) = 1/(1+z^2/2)$ and provides the leading order term $I^{(1)} \approx -\sqrt{-a_{11}/8}$. The second iteration results in

$$I^{(1)} = -\sqrt{-\frac{a_{11}}{8}} + \frac{9 + 5\sqrt{3}\pi + 27\ln(-a_{11}e^{-2\gamma}/2)}{36\pi} + o(1). \tag{5.62}$$

The solid and dashed lines in Fig. 5.1 show, respectively, the real and imaginary parts of $I^{(1)}$ as a function of $-1/a_{11}$ ($= g_{11}/2$) obtained numerically. The dotted lines indicate the real and imaginary parts of the large-a_{11} asymptote (5.62).

For negative a_{11} the solution is real and $\mathrm{Im}I^{(1)} \equiv 0$. By contrast, for $a_{11} > 0$ the function $\chi(p)$ is characterized by simple poles at $p = \pm(\kappa + i0)$, where $\kappa > 0$ is defined by Eq. (5.24) [this is also the point where the term in round brackets in Eq. (5.59) vanishes]. These poles correspond to the three-body recombination to a dimer state, which, as found in Sec. 5.2, exists only for positive a_{11}. One sees that $I^{(1)}$ and, therefore, $\tilde{f}(0)$ become complex reflecting the three-body loss. Technically, as one passes from positive to negative $-1/a_{11}$, the choice of the correct branch of the square root and logarithm in Eq. (5.62) is ensured by keeping $-1/a_{11}$ just below the real axis.

5.3.2 Two dimensions

The solution in the two-dimensional case can be written as

$$\tilde{f}(0) = \frac{2\pi}{\ln\left(a_{12}e^{\gamma}/\sqrt{3}\right) + 2\pi I^{(2)}(a_{11})}, \tag{5.63}$$

where $I^{(2)}(a_{11}) = \int \frac{\chi(p)-1/(p^2+1)}{p^2}\frac{d^2p}{(2\pi)^2}$ and χ satisfies

$$\sum_{\pm}\int \frac{\chi(q)}{p^2 \pm \mathbf{pq} + q^2}\frac{d^2q}{(2\pi)^2} + \left(\frac{1}{p^2} - \frac{1}{2\pi}\ln\frac{a_{11}pe^{\gamma}}{2}\right)\chi(p) = \frac{1}{p^2}. \tag{5.64}$$

The three-body scattering surface is proportional to $\tilde{f}(0)$ [see Eq. (5.42)] and the mean-field result (5.5) is recovered for weak attractive or repulsive atom-dimer interactions (small or large a_{12}). As in the one-dimensional case we see that the dependence on a_{12} is analytic and for the complete solution of the problem one needs to know only $I^{(2)}(a_{11})$.

For a weak atom-atom background interaction (small or large a_{11}), introducing the small parameter $\lambda = 1/\ln(1/a_{11})$, we can proceed iteratively in exactly the same manner as in the one-dimensional case. Namely, using the momentum rescaling $p = \sqrt{\lambda}z$ one can see that to the leading order $\chi(z) \approx 1/(1 + z^2/2\pi)$ and after two iterations we have

$$I^{(2)} = \frac{\ln(2\pi\lambda)}{4\pi} + \lambda\frac{\ln(C\lambda)}{8\pi} + o(\lambda), \tag{5.65}$$

where $C \approx 0.013$.

In Fig. 5.2 we plot the real (solid) and imaginary (dashed) parts of $I^{(2)}$ versus λ together with the asymptote (5.65) (dotted). In the two-dimensional case $\mathrm{Im}I^{(2)}$ is always finite since there is always a dimer bound state available for the recombination (see Sec. 5.2). However, for small positive λ the dimer is exponentially deep and small (its energy is proportional to $1/a_{11}^2 = e^{-1/\lambda}$) so that the recombination in this limit is

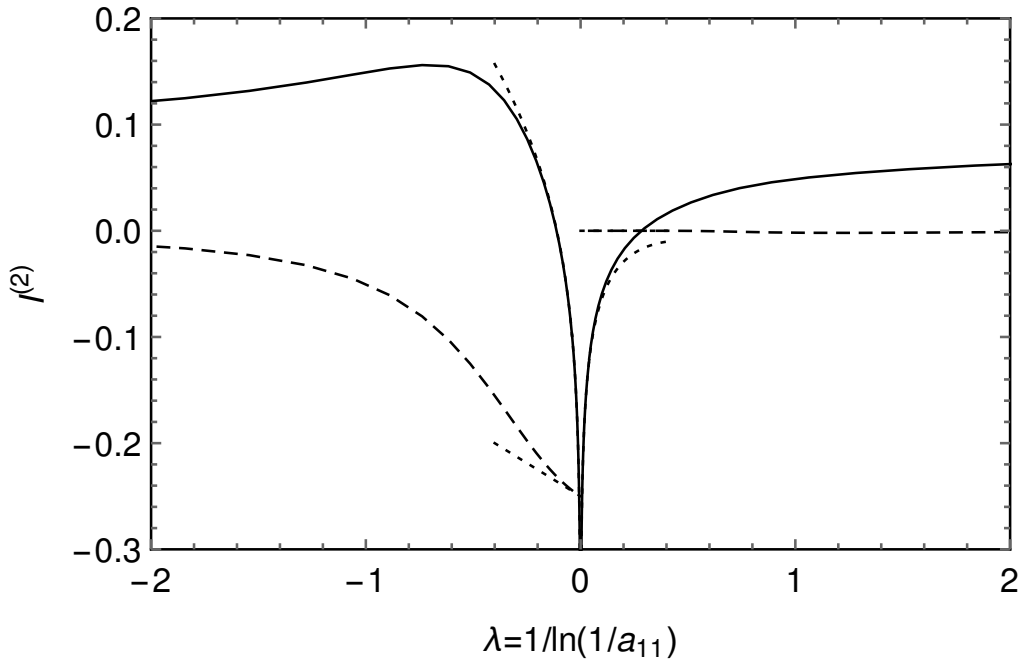

Figure 5.2: Real and imaginary parts of $I^{(2)}$ in the two-dimensional case. We use the same notations as in Fig. 5.1.

not captured by the power expansion Eq. (5.65).

Note that for small λ the characteristic momentum involved in the solution $\chi(p)$ is $\sqrt{\lambda}$. Therefore, the asymptotic expansion (5.65) is also valid if, instead of the zero-range atom-atom interaction, we have a potential of a finite but sufficiently small range $\ll 1/\sqrt{\lambda} = \sqrt{|\ln(1/a_{11})|}$, characterized by the same scattering length a_{11}. In particular, one can have a purely repulsive potential which does not lead to a dimer state in our problem.

5.3.3 Three dimensions

In three dimensions we have

$$\tilde{f}(0) = \frac{1}{-\sqrt{3}/8\pi a_{12} + I^{(3)}(a_{11})}, \tag{5.66}$$

where $I^{(3)}(a_{11}) = \int \frac{\chi(p)}{p^2} \frac{d^3p}{(2\pi)^3}$ with χ satisfying

$$\frac{2}{\sqrt{3}} \sum_{\pm} \int \frac{\chi(q)}{p^2 \pm \mathbf{pq} + q^2} \frac{d^3q}{(2\pi)^3} + \left(\frac{1}{p^2} - \frac{p}{4\pi} + \frac{1}{4\pi a_{11}} \right) \chi(p) = \frac{1}{p^2}. \tag{5.67}$$

Here we also manage to separate the dependencies on the atom-dimer and atom-atom interactions. The mean-field solution (5.5) is retrieved for $a_{12} \to 0$. Calculating $I^{(3)}$ is, however, more subtle than in the low-dimensional cases. Indeed, small hyperradii effec-

tively correspond to high collision momenta and energies where the two-body scattering length is approximated by its background value a_{11}. Thus, at $\rho \ll a_{11}$ we deal with the Efimovian three-boson system which requires a three-body parameter or a cutoff momentum. Mathematically, this can be seen from Eq. (5.67) at momenta $p \gg 1/a_{11}$, where the dominant terms are the integral and $-p\chi(p)/4\pi$. The corresponding large-momentum behavior of $\chi(p)$ is a linear combination of Efimov waves $p^{\pm is_0-2}$ with $s_0 \approx 1.00624$ [125]. The coefficients in this linear combination are fixed by introducing an external (three-body) parameter, phase, or momentum. Namely, one can set

$$\chi \propto \frac{\sin[s_0 \ln(p/p_0)]}{p^2} \tag{5.68}$$

as the asymptotic boundary condition for $p \gg 1/a_{11}$. Accordingly, the quantity $I^{(3)}$ is, in fact, a function of a_{11} and the three-body parameter p_0. However, for small a_{11} the leading-order contribution to $I^{(3)}$ is universal, i.e., independent of p_0. Indeed, for small a_{11} and momenta $p \ll 1/|a_{11}|$ Eq. (5.67) reduces to $(1/p^2 + 1/4\pi a_{11})\chi(p) = 1/p^2$. The corresponding solution $\chi = 1/(1 + p^2/4\pi a_{11})$ is characterized by the typical momentum $\sqrt{a_{11}} \ll 1/a_{11}$ and leads to

$$I^{(3)} \approx \sqrt{a_{11}/4\pi}. \tag{5.69}$$

In order to estimate the next-order term we match $\chi(p)$ with the Efimov wave (5.68) at momentum $p \sim 1/|a_{11}|$ obtaining a contribution to $I^{(3)}$ of the order of a_{11}^2.

It makes sense to study the case of larger a_{11} ($\gtrsim R_e$) within our zero-range model, if we deal with a zero crossing near a narrow Feshbach resonance (large R_e) which, in turn, lies in the vicinity of a broader Feshbach resonance (large a_{11}). At the same time it is interesting to have a significant atom-dimer interaction (large a_{12}) such that the two terms in the denominator of Eq. (5.66) are comparable. Then, in order to find the effective three-body force we also need to know the three-body and inelasticity parameters (or, equivalently, the real and imaginary parts of p_0), which could be known from the Efimov loss spectroscopy near the broad resonance. Given the large number of parameters in this problem we just give a prescription for calculating $I^{(3)}$. Namely, one has to solve Eq. (5.67) with the boundary condition (5.68) at $p \to \infty$ also requiring $\chi \propto 1/(p - \kappa - i0)$ near the pole given by Eq. (5.26).

5.4 Discussion and conclusions

In this chapter we have expanded the idea that the bosonic model with a Feshbach-type atom-dimer conversion (5.1) near a two-body zero crossing can be reduced to a purely atomic model with an effective three-body interaction, which strongly depends on the atom-dimer conversion amplitude. As a particular example, we show that this mechanism of generating three-body forces can be used for stabilizing supersolid phases of two-dimensional dipoles.

Sections 5.2 and 5.3 have been devoted to constructing a zero-range regularized version of the model (5.1) with a minimal set of parameters (a_{11}, a_{12}, and R_e). We have solved this model nonperturbatively in the two-body and three-body cases in all dimensions at the two-body zero crossing. Formulas (5.58), (5.63), and (5.66) give analytic dependencies of the three-body scattering amplitude on a_{12} in different dimensions. The dependence on a_{11} is found numerically and also analytically for weak atom-atom background interactions. In the three-dimensional case, our three-body zero-range model is Efimovian and requires an additional three-body parameter. We find, however, that for small $|a_{11}|/R_e$, effects associated with the Efimov physics are subleading.

These results show that for comparable and weak atom-dimer and atom-atom interactions (characterized by g_{12} and g_{11}, respectively), the three-body interaction is mostly influenced by g_{12}, consistent with the mean-field result (5.5). However, the convergence is not always uniform. For example, in the two-dimensional case, one can simultaneously decrease g_{12} and g_{11}, keeping both terms in the denominator of Eq. (5.63) comparable to (or even canceling) each other (resulting in a diverging three-body scattering surface). In the same spirit, we can use the nonperturbative three-dimensional formula Eq. (5.66) and predict a three-body resonance at $\sqrt{3}R_e/8\pi a_{12} \approx \sqrt{a_{11}/4\pi R_e} \ll 1$.

Inelastic three-body events manifest themselves through the appearance of an imaginary part of $\tilde{f}(0)$, which, in turn, comes from the complex $I^{(D)}$ or complex atom-dimer scattering length a_{12}. The former reflects the three-body recombination to a dimer state and the latter the relaxation process in collisions of atoms with closed-channel dimers.

Several proposals on how to observe elastic three-body interactions experimentally are based on the following ideas. A repulsive three-body force could stabilize a system with attractive two-body interactions and make it self-trapped [15]. The structure and energies of few-body bound states, detectable spectroscopically, are also influenced by these forces [78, 92, 94, 126]. Collective-mode frequency shifts in a trapped gas could be another experimentally observable signature of three-body interactions [127].

Conclusion and perspectives

The last couple of years clearly show that it is unnecessary to go into the strongly interacting limit to observe interesting quantum effects. Indeed, the study of systems where one looks at a regime where the leading pairwise MF contribution is made weak, thus enhancing BMF effects, offers a very rich and interesting physics. This domain developed recently, thanks to an active dialog between theorists and experimentalists [34].

In this thesis, we started the journey by introducing the LHY correction in systems exhibiting a competition between attractive and repulsive forces (namely, BB mixture with repulsive intraspecies and attractive interspecies interactions, and dipolar gases with repulsive contact interactions), which can be controlled independently from the MF term. Dramatic effects of this correction have been observed experimentally in both systems, essentially via the formation of an exotic phase of matter, the dilute quantum droplet, constituting then a direct proof of the existence and importance of BMF terms.

A first question arises naturally: what other physical systems can exhibit such peculiar quantum properties, and if so, what are the main differences with the systems previously presented?

As the reader may have seen, most of the results in this manuscript have been developed through few-body approaches [2]. In particular, it turned out that we focused on BMF effects which can be encapsulated in local effective three-body interactions of different origins, where the LHY correction is not anymore the leading BMF term.

Indeed, in Chapter 3, where we studied the one-dimensional BB mixture, we showed the appearance of a three-dimer repulsion close to the dimer-dimer zero crossing line, which stabilizes the collapsing system into a liquid-like droplet. This effective three-body force arises from virtual excitations of internal and external degrees of freedom of the system. We actually largely explored the kinematic equivalence of the three-body scattering in one dimension with the two-body scattering in two dimensions. We showed that taking into account the existence of this effective three-body force has a big impact on the one-dimensional three-body problem with two-body contact interactions, even if this force is extremely weak. In Chapter 4, using a common perturbation theory scheme, we derived in every pure and quasi-low dimensional configuration an explicit expression

[2] One of the main motivations is that it offers to venture into both the weakly and strongly-interacting regime, i.e., in the regime not tractable on the Bogoliubov level.

for the three-body coupling constant associated with a weak two-body potential of vanishing MF value. Finally, in Chapter 5, we presented a way to engineer a three-body force in a one-component Bose gas, finding its origin in an atom-dimer interaction close to a two-body zero-crossing near a narrow Feshbach resonance.

In all the present systems, we proposed ways to verify our theoretical results experimentally. Although the result of the last chapter can be typically used to stabilize the supersolid phase in quasi-2D [114], engineering such many-body force also has other applications. We recall here that a local repulsive g_{k+1} contact interaction is the *parent* Hamiltonian of the k-th state of the Read-Rezayi series of quantum Hall states, which supports topologically protected states useful for quantum computing (maximizing the value g_{k+1} actually increase the protection of these desired states) [128].

Interestingly, we note that adding an effective three-body interaction in weakened MF systems can sometimes be cast via another picture that takes into account the finite physical range of two-body interactions [129]. More work on the equivalence and differences of these approaches is necessary to understand BMF physics better.

An obvious continuation of our work would be to switch to a many-body viewpoint and to perform a generalization of the Bogoliubov theory where one adds a short-range three-body force in every dimension, expressing the results in terms of *universal* parameters. This problem is not trivial since the interaction requires a renormalization scheme which is different from the two-body-interacting case, typically requiring to go beyond the standard Bogoliubov approach.

As the reader might expect, there is still a lot of open problems to better understand these systems where BMF terms play a crucial role. For the MF unstable BB mixture and dipolar gases system, there are still indeed a lot of theoretical challenges:

The inhomogeneous problem (associated, for example, with the implementation of the external potential necessary to first trap and cool down the atoms) has yet to be more explored, particularly when the LDA is no more valid. Indeed the approximation may fail to describe the system for a low number of particles or for typical regimes of particle interactions and trapping parameters.

Moreover, although the usual description through the extended Gross-Pitaevskii equation of these systems is in good agreement with experiments, by its nature, it fails to understand what happens in the nonperturbative regime (in this sense, we made progress for the one dimensional BB mixture in Chapter 3). In general, more work is still needed to understand the dynamics of these many-body systems better. In this direction, we mention a recent work using the diagrammatic Beliaev approach, which permits to get rid of the instabilities [130] encountered with a Bogoliubov approach of the MF collapsing BB mixture. We also mention two studies about the dimensional crossover for the BMF correction associated with the formation of droplets in BB mixture [110, 131]. For dipolar gases, the pursuit of supersolidity with quantum droplets makes appear a really

complex phase diagram where not all the phase transitions have been fully understood theoretically [34]. Moreover, finite temperature effects have also to be more explored: for example, experimentally wise, the quantum droplet in the BB mixture still suffer from a too-short lifetime to observe its collective excitations.

In conclusion, looking at systems where the BMF terms are of the order of the usual leading MF terms (eventually becoming the dominant one) offers a wonderful platform to appreciate the large panel of interactions at play in a system, from its fundamental and effective few-body ones to its emerging collective excitations of pure quantum nature, and ultimately redefine our classic conception of states of matter.

Appendix A

Detailed derivation of Eq.(3.18)

Extended STM equation

To a integrable function $f : \mathbb{R}^3 \to \mathbb{C}$, we define its Fourier transform $\tilde{f}$ as

$$\tilde{f}(p_1, p_2, p_3) = \int e^{-ip_1x_1} e^{-ip_2x_2} e^{-ip_3x_3} f(x_1, x_2, x_3). \tag{A.1}$$

Let us assume three particles in one dimension of position x_i of mass m interacting via two-body contact potential of coupling constant $g = -2/ma_2$, and a three-body δ-potential. The idea is to perform a STM approach of this three-body problem. Let us see the three-body wavefunction $\Psi(x_1, x_2, x_3)$ as the Green's function solution of the equation

$$\Big[-\frac{1}{2m} \sum_{i=1}^{3} \frac{\partial^2}{\partial x_i^2} - E \Big] \Psi(x_1, x_2, x_3) = -g \sum_{i<j} \delta(x_{ij}) \Psi(x_1, x_2, x_3) + \frac{1}{m} \delta(x_{12}) \delta(x_{13}), \tag{A.2}$$

where $x_{ij} = x_i - x_j$ and we set $\hbar = 1$.

We Fourier transform Eq.(A.2), which leads to

$$\tilde{\Psi}(p_1, p_2, p_3) = \frac{-g \Big[\mathcal{F}_{12}(p_3; Q) + \mathcal{F}_{13}(p_2; Q) + \mathcal{F}_{23}(p_1; Q) \Big] + 2\pi\delta(Q)/m}{\dfrac{p_1^2 + p_2^2 + p_3^2}{2m} - E}, \tag{A.3}$$

where $Q = p_1 + p_2 + p_3$ is the center-of-mass momentum, and $\mathcal{F}_{ij}(p_k; Q)$ corresponds to the Fourier transform of $\delta(x_{ij})\Psi(x_1, x_2, x_3)$.

Since we are working on the problem of three identical bosons, we find $\mathcal{F}_{ij}(p; Q) = \mathcal{F}(p; Q)$ which reads

$$\mathcal{F}(p; Q) = \int \tilde{\Psi}(q_1, q_2, p) \delta(q_1 + q_2 - Q + p) \frac{dq_1 dq_2}{2\pi}. \tag{A.4}$$

To have the *extended* STM equation (i.e. with a three-body term), we insert Eq.(A.3) into Eq.(A.4) and we obtain

$$\mathcal{F}(p_3;Q) = \int \left\{ \frac{-g\Big[\mathcal{F}(p_3;Q)+\mathcal{F}(q_2;Q)+\mathcal{F}(q_1;Q)\Big]}{\frac{q_1^2+q_2^2+p_3^2}{2m}-E} + \frac{2\pi\delta(Q)/m}{\frac{q_1^2+q_2^2+p_3^2}{2m}-E} \right\} \delta(q_1+q_2-Q+p)\frac{dq_1 dq_2}{2\pi}. \tag{A.5}$$

We then insert the ansatz for the total wavefunction $\tilde{\Psi}(p_1,p_2,p_3) = 2\pi\delta(Q)\tilde{\psi}(p_1,p_2,p_3)$ according to a zero value of the center of mass momentum. We hence define the function $\tilde{F}$ such that

$$\mathcal{F}(p;Q) = \frac{a_2}{2}2\pi\delta(Q)\tilde{F}(p) \quad , \quad \tilde{F}(p) = \frac{2}{a_2}\int \tilde{\psi}(p,q,-p-q)\frac{dq}{2\pi}. \tag{A.6}$$

We insert Eq.(A.6) into Eq.(A.5) and use the symmetry between q_1 and q_2. We integrate over q_2 and recalling $q_1 = q$ and $p_3 = p$ and using $g = -2/ma_2$ we finally end up with

$$\tilde{F}(p) = \tilde{F}(p)I(p) + \int \frac{2\tilde{F}(q)}{p^2+q^2+pq-mE}\frac{dq}{2\pi} + I(p), \tag{A.7}$$

where

$$I(p) = \int \frac{1}{p^2+q^2+pq-mE}\frac{dq}{2\pi} = \frac{1}{\sqrt{3p^2-4mE}}. \tag{A.8}$$

We put Eq.(A.7) in a more condensed form, namely

$$(\hat{L}-a_2/2)\tilde{F} = \frac{-1}{\sqrt{3p^2-4mE}}, \tag{A.9}$$

where $\hat{L}$ is an operator which satisfies

$$\hat{L}\tilde{F}(p) = \frac{\tilde{F}(p)}{\sqrt{3p^2-4mE}} + \int \frac{2\tilde{F}(q)}{p^2+q^2+pq-mE}\frac{dq}{2\pi}. \tag{A.10}$$

Remark that comparing

$$F(x) = \int e^{ipx}\tilde{F}(p)\frac{dp}{2\pi} = \frac{2}{a_2}\int e^{ipx}\tilde{\psi}(p,q,-p-q)\frac{dpdq}{(2\pi)^2} \tag{A.11}$$

with the wavefunction Ψ which satisfies

$$\Psi(x_1,x_2,x_3) = \int e^{ipx_{31}}e^{iqx_{32}}\tilde{\psi}(p,q,-p-q)\frac{dpdq}{(2\pi)^2}, \tag{A.12}$$

we find by identification

$$F(x) = \frac{2}{a_2}\Psi(-2x/3, x/3, x/3), \tag{A.13}$$

in good agreement with the function F defined in the short version of the calculation in Chapter 3.

Boundary conditions for the three-body term

We now have to introduce the three-body scattering length a_3 in our problem. To do this, we study the wave function in real space. We hence Fourier transform back Eq.(A.3), and thanks to symmetry between p_1, p_2, p_3, we end up with

$$\Psi(x_1, x_2, x_3) = \int e^{iqx_{31}} e^{ipx_{32}} \left[\frac{3\tilde{F}(q)}{p^2+q^2+pq-mE}\right] \frac{dpdq}{(2\pi)^2} + K_0(\sqrt{-mE}\rho), \tag{A.14}$$

where $\rho = \sqrt{2/3}\sqrt{x_{12}^2 + x_{13}^2 + x_{23}^2}$ is the hyper-radius and K_0 the Bessel decaying function.

Since a_3 is defined as the position of the extrapolated node of the zero-energy wave function, we take the limit of the previous equation when $\rho \to 0$ and obtain

$$-\frac{1}{\sqrt{3}\pi}\ln(\rho/a_3) = 3\int \frac{\tilde{F}(q)}{\sqrt{3q^2-4mE}}\frac{dq}{2\pi} - \frac{1}{\sqrt{3}\pi}\ln\frac{\sqrt{-mE}\rho e^{\gamma}}{2}, \tag{A.15}$$

where we developed $K_0(x)$ up to order one and the Euler's constant γ appears in the result. Note that the exponentials in the integral disappeared leading us to use Eq.(A.8). After small rearrangements we find

$$\ln\frac{\sqrt{-mE}a_3 e^{\gamma}}{2} = 3\sqrt{3}\pi\int \frac{\tilde{F}(q)}{\sqrt{3q^2-4mE}}\frac{dq}{2\pi}. \tag{A.16}$$

From STM to the Final Equation

The idea is now to understand how from the two following Eq.(A.9) and Eq.(A.16) we arrive, introducing $\kappa = \sqrt{-mE}a_2/2$, to the final equation

$$\ln\frac{a_3\kappa e^{\gamma}}{a_2} = \frac{2}{\kappa^2-1}\left[\frac{\pi}{3\sqrt{3}} + \frac{3\kappa^2-1}{\sqrt{4\kappa^2-1}}\arctan\sqrt{\frac{2\kappa+1}{2\kappa-1}}\right]. \tag{A.17}$$

Briefly, we eliminate $\tilde{F}$ from Eq.(A.16). To do so, we have to extract the expression of $\tilde{F}$ thanks to the extended STM equation Eq.(A.9).

In the following, we use the definition of the following hermitian inner product

$$\forall\ f, g\ \ \langle f|g\rangle = \frac{1}{2\pi}\int_{-\infty}^{+\infty} f^* g. \tag{A.18}$$

Hence, Eq.(A.16) reads

$$\ln \frac{a_3 \kappa e^{\gamma}}{a_2} = 3\sqrt{3}\pi \, \langle \frac{1}{\sqrt{3q^2 - 4mE}} | \tilde{F} \rangle \, , \tag{A.19}$$

whereas using Eq.(A.9) we get

$$\tilde{F} = \left(\hat{L} - a_2/2\right)^{-1} \frac{-1}{\sqrt{3q^2 - 4mE}}, \tag{A.20}$$

Therefore, we can write

$$\langle \frac{1}{\sqrt{3q^2 - 4mE}} | \tilde{F} \rangle = \left\langle \frac{1}{\sqrt{3q^2 - 4mE}} \middle| \left(\hat{L} - a_2/2\right)^{-1} \middle| \frac{-1}{\sqrt{3q^2 - 4mE}} \right\rangle , \tag{A.21}$$

The main idea is now to use the diagonal representation of the operator $\left(\hat{L} - a_2/2\right)^{-1}$. Indeed since we are dealing with $E < 0$, the spectrum of $\hat{L}$ contains only the trimer and atom-dimer scattering states which can be both derived. We denote λ_ν the eigenvalue associated to the orthonormal eigenvector $\tilde{F}_\nu$ which satisfies

$$\hat{L}\tilde{F}_\nu = \lambda_\nu \tilde{F}_\nu \quad , \quad \left\langle \tilde{F}_\nu \middle| \left(\hat{L} - a_2/2\right)^{-1} \middle| \tilde{F}_\mu \right\rangle = \frac{\delta_{\nu\mu}}{\lambda_\nu - a_2/2}. \tag{A.22}$$

We can then rewrite Eq.(A.21) such that

$$\langle \frac{1}{\sqrt{3q^2 - 4mE}} | \tilde{F} \rangle = -\sum_\nu \langle \frac{1}{\sqrt{3q^2 - 4mE}} | \tilde{F}_\nu \rangle \, \frac{1}{\lambda_\nu - a_2/2} \, \langle \tilde{F}_\nu | \frac{1}{\sqrt{3q^2 - 4mE}} \rangle \, , \tag{A.23}$$

Using the definition of the operator $\hat{L}$ Eq.(A.10) we remark that

$$\langle 1 | \hat{L}\tilde{F}_\nu \rangle = 3 \, \langle \frac{1}{\sqrt{3q^2 - 4mE}} | \tilde{F} \rangle \, , \tag{A.24}$$

Moreover, thanks to Eq.(A.22), and the definition of the inverse Fourier transform we have

$$\langle 1 | \hat{L}\tilde{F}_\nu \rangle = \lambda_\nu \, \langle 1 | \tilde{F}_\nu \rangle = \lambda_\nu F_\nu(x=0), \quad \text{where} \quad F_\nu(x) = \int \tilde{F}_\nu(p) e^{ipx} \frac{dp}{2\pi}. \tag{A.25}$$

Using Eq.(A.24) and Eq.(A.25) we can replace inner products of the sum in Eq.(A.23) by a function of $\{\lambda_\nu, F_\nu(0), F_\nu^*(0)\}$, such that we can rewrite Eq.(A.19) as

$$\ln \frac{a_3 \kappa e^{\gamma}}{a_2} = -\frac{\pi}{\sqrt{3}} \sum_\nu \frac{\lambda_\nu^2}{(\lambda_\nu - a_2/2)} |F_\nu(x=0)|^2. \tag{A.26}$$

We now separate the spectrum of $\hat{L}$ that contains the McGuire trimer state F_{MG} (see

Ref. [77]) and the atom-dimer scattering states F_k, where k is the relative atom-dimer momentum, namely

$$\ln\frac{a_3\kappa e^\gamma}{a_2} = -\frac{\pi}{\sqrt{3}}\Big[\frac{\lambda_{\rm MG}^2}{(\lambda_{\rm MG}-a_2/2)}|F_{\rm MG}(0)|^2 + \sum_k \frac{\lambda_k^2}{(\lambda_k - a_2/2)}|F_k(0)|^2\Big]. \tag{A.27}$$

Using $\lambda_{\rm MG} = 1/\sqrt{-mE}$ and $F_{\rm MG}(p) = \frac{2(-mE)^{-1/4}}{(1-p^2/mE)}$ consistent with Ref. [77], we take care of the first term in the sum.

Let us consider now the atom-dimer scattering states. According to the relation $E = 3k^2/4m - 1/ma_2^2$ in the absence of three-body force, and requiring that $\lambda_k = a_2/2$ in this case (thanks to Eq.(A.9) with no right-hand side), we find that $\lambda_k = (3k^2 - 4mE)^{-1/2}$. Thanks to a Bethe Ansatz formalism detailed in the next subsection, we obtain

$$|F_k(0)|^2 = \frac{1}{2}\frac{3k^2 - mE}{k^2 - mE}, \tag{A.28}$$

and using the correspondence $\sum_k \to \frac{1}{2\pi}\int dk$ we find

$$\sum_k \frac{\lambda_k^2}{(\lambda_k - a/2)}|F_k(0)|^2 = \frac{1}{4\pi}2\sqrt{3}I(\kappa), \tag{A.29}$$

where I is defined as

$$I(\kappa) = \frac{1}{\sqrt{3}}\int_0^{+\infty} dp \frac{3p^2+1}{(p^2+1)\big[\sqrt{3p^2+4} - \kappa(3p^2+4)\big]}. \tag{A.30}$$

We then do the change of variable $3p^2 = 4\sinh^2(z)$, leading to

$$I(\kappa) = \int_0^{+\infty} dz \frac{1+4\sinh^2(z)}{(3+\sinh^2(z))(1-2\kappa\cosh(z))}. \tag{A.31}$$

Analytically it follows that

$$I(\kappa) = \frac{\pi}{3\sqrt{3}}\frac{1+3\kappa}{\kappa^2-1} + 2\frac{(1-3\kappa^2)}{(\kappa^2-1)\sqrt{4\kappa^2-1}}\arctan\sqrt{\frac{2\kappa+1}{2\kappa-1}}, \tag{A.32}$$

and we can group the previous terms such that

$$\ln\frac{a_3\kappa e^\gamma}{a_2} = \frac{\pi}{\sqrt{3}}\Big(\frac{\kappa+1}{\kappa^2-1}\Big) - \frac{1}{2}I(\kappa). \tag{A.33}$$

By simple manipulations, we can now rewrite the previous expression such that it gives the final equation

$$\ln\frac{a_3\kappa e^\gamma}{a_2} = \frac{2}{\kappa^2-1}\Big[\frac{\pi}{3\sqrt{3}} + \frac{3\kappa^2-1}{\sqrt{4\kappa^2-1}}\arctan\sqrt{\frac{2\kappa+1}{2\kappa-1}}\Big] \tag{A.34}$$

Three-body Bethe-Ansatz

We give here a quick calculation of the atom-dimer scattering states with the Bethe Ansatz formalism. In the domain $\mathcal{D} = \{x_1 < x_2 < x_3\}$, we write the three-body wavefunction $\Psi(x_1, x_2, x_3)$, where x_i refer to the position of particles in the center-of-mass frame as

$$\begin{aligned}\Psi(x_1,x_2,x_3) = t e^{-\frac{|x_2-x_1|}{a_2}} e^{ik(x_3-\frac{(x_1+x_2)}{2})} + e^{-\frac{|x_3-x_2|}{a_2}} e^{ik(x_1-\frac{(x_3+x_2)}{2})} \\ + c_1 e^{-\frac{|x_3-x_1|}{a_2}} e^{ik(x_2-\frac{(x_1+x_3)}{2})} + c_2 e^{-\frac{|x_3-x_1|}{a_2}} e^{-ik(x_2-\frac{(x_1+x_3)}{2})},\end{aligned} \tag{A.35}$$

where we introduced three coefficients (t,c_1,c_2) we need to calculate. For this, we first rewrite the problem in terms of two variables (x, y) such that

$$x_1 = -\frac{x}{2\sqrt{3}} - \frac{y}{2} \ , \ x_2 = -\frac{x}{2\sqrt{3}} + \frac{y}{2} \ , \ x_3 = \frac{x}{\sqrt{3}}. \tag{A.36}$$

We use the two-body contact conditions between two particles (say here for example, $x_1 = x_2$ i.e. $y = 0$), arising from the δ-potential interaction,

$$\left.\frac{\partial \Psi}{\partial y}\right|_{y=0^+} = -\left.\frac{\Psi}{a_2}\right|_{y=0^+}, \tag{A.37}$$

and we end up with the following identities

$$\begin{cases} c_1 = \dfrac{-6 + i3ka_2}{2 + i3ka_2}, \\ c_2 = 0, \\ t = \dfrac{(-2 + i3a_2k)(-6 + i3a_2k)}{(2 + i3a_2k)(6 + i3a_2k)}, \end{cases} \tag{A.38}$$

$$\Psi(0,0,0) = 1 + c_1 + c_2 + t = \frac{-2 + i3ak}{2 + iak}. \tag{A.39}$$

Using $a_2 = 2\lambda_k = 2(3k^2 - 4mE)^{-1/2}$ and the fact $\langle F_\nu \,|\, F_\nu \rangle = 1$, we find

$$|F_k(0)|^2 = \frac{1}{2}\frac{3k^2 - mE}{k^2 - mE}. \tag{A.40}$$

Appendix B

Synthèse en français

Le traitement des systèmes à petit ou grand nombre de corps en interaction est au cœur d'une grande variété de domaines de la physique. Malheureusement, il apparaît que dès le cas $N = 3$ particules, la solution générale est trop compliquée. À partir de là, il faut se baser activement sur un ensemble d'approximations (toutes associées à diverses approches théoriques), guidées par la valeur typique des paramètres du système en question. Ici, on peut alors se demander :

Existe-t-il une branche particulière de la physique qui offre une bonne plateforme, tant sur le plan théorique qu'expérimental, pour étudier les systèmes en interaction à petit et grand nombre de corps ?

Le domaine des ***gaz ultra-froids***, où l'on travaille avec des gaz d'atomes à très basse température, semble être un très bon candidat. En effet, un très petit nombre de paramètres est nécessaire pour décrire le système en interaction et, de manière tout aussi notable, la plupart de ces paramètres peuvent être réglés avec précision dans les expériences. Ainsi, ce domaine nous offre un formidable terrain de jeu pour mieux comprendre la matière quantique à l'échelle atomique [1]. Ce domaine semble également pouvoir commencer à répondre à d'autres problèmes à plusieurs corps, allant de la matière condensée à l'astrophysique, en jouant le rôle de simulateur quantique, grâce à sa capacité à reproduire artificiellement certains phénomènes difficiles à calculer numériquement [2–4].

Rappelons ici les propriétés de base de ces gaz avant de poursuivre.

Les gaz ultrafroids sont des systèmes très dilués, car ils sont environ 10^5 fois moins denses que l'air ambiant (la densité $n \simeq 10^{14}$ atomes/cm^3). La longueur d'onde atomique de de Broglie $\lambda_T = (2\pi\hbar^2/mk_BT)^{1/2}$ est rendue très grande puisque la température T est typiquement comprise entre 100 nK et 1 μK. A ces échelles typiques, le gaz ne peut plus être considéré comme classique et obéit à des statistiques quantiques, sa nature changeant radicalement selon le caractère bosonique ou fermionique de ses composants. Dans le cas bosonique, on obtient finalement un état remarquable de la matière, appelé condensat de Bose Einstein, où les atomes occupent l'état fondamental du gaz de façon macroscopique. Il a été observé pour la première fois expérimentalement en 1995 [5–7],

et le domaine s'est beaucoup développé depuis cette percée. Les méthodes incroyables pour réaliser de tels systèmes, qui font principalement appel à la physique du laser et à l'utilisation du refroidissement par évaporation, sont présentées dans la Réf. [8].

En fait, la formation d'un condensat de Bose Einstein émerge purement des statistiques quantiques et ne nécessite pas d'interactions, mais celles-ci ont un effet dramatique sur le gaz (sans mentionner leur nécessité dans le refroidissement par évaporation [8], ou dans l'apparition de l'état superfluide [9]). En introduisant R_e, la *portée* du potentiel interatomique (typiquement quelques nm), nous rappelons que dans le régime où $\lambda_T \gg R_e$ (atomes ultrafroids), un seul paramètre est généralement suffisant pour décrire l'interaction à deux corps entre les particules : la dite *longueur de diffusion* a. Ceci conduit à l'équivalence de tous les potentiels à courte portée à deux corps avec la même longueur de diffusion : on parle ici d'*universalité*. À partir de ce paramètre, on définit généralement la *force* g_2 d'un potentiel effectif à deux corps modélisant l'interaction.

Considérons maintenant un système homogène de N atomes qui intéragissent dans un volume V à $T = 0$. Si on suppose que la distance moyenne entre les atomes $l = n^{-1/3}$ satisfait la condition $l \gg R_e$, alors on ne prend généralement en compte que les interactions par paires. Cela conduit à effectuer une analyse du système en champ moyen (MF) : pour obtenir l'énergie d'interaction E_{MF}, nous multiplions l'énergie d'une paire en interaction $\propto g_2$ par le nombre de paires dans le système, ce qui conduit pour un grand nombre d'atomes N à $E_{\mathrm{MF}} = g_2 N^2/2V$. Pour $g_2 > 0$, correspondant à une répulsion globale, le système est en phase gazeuse et se dilate pour minimiser son énergie. Il doit alors être piégé par un potentiel externe de manière à être localisé pour les expériences. Pour $g_2 < 0$, associé à une attraction globale, le système s'effondre sur lui-même. A ce stade, on peut se demander :

Ces deux scénarios (phase gazeuse et effondrement) sont-ils exhaustifs ? Ou est-il possible d'obtenir un état liquide, c'est-à-dire un état lié (et très dilué) en équilibre avec le vide sans potentiel externe ?

Un tel état exigerait que l'énergie totale d'interaction par particule $E_{\mathrm{int}}/N(n)$ présente un minimum non trivial à une certaine densité n_0. Une façon d'obtenir une telle propriété est de prendre en compte l'existence de termes d'énergie ***au-delà du champ moyen*** (BMF) $E_{\mathrm{BMF}} = E_{\mathrm{int}} - E_{\mathrm{MF}}$ pour contrebalancer celui du champ moyen. Habituellement, ces termes BMF correspondent à des corrections d'ordre supérieur de l'énergie totale et ne changent pas vraiment les propriétés du système. Supposons ici que l'ordre principal de ces termes est $\propto g_\alpha n^\alpha$ où $\alpha > 2$ [1] On peut alors écrire l'énergie totale par particule comme suit

$$E_{\mathrm{int}}/N \propto g_2 n + g_\alpha n^{\alpha-1}, \text{ with } \alpha > 2. \tag{B.1}$$

[1] Dans le cas général, et particulièrement pour les faibles dimensions, l'ordre principal des termes BMF peut avoir une dépendance différente et plus compliquée en la densité n. Cependant, le mécanisme possible de stabilisation reste le même.

Pour avoir un minimum à n_0, il faut avoir l'échelle particulière $g_2 \sim g_\alpha n_0^{\alpha-2}$, où les deux termes doivent avoir des signes différents : une attraction de champ moyen étant stabilisée par une répulsion au-delà du champ moyen et inversement. De plus, le gaz doit rester dilué pour ne pas souffrir d'une courte durée de vie due aux collisions inélastiques. En trois dimensions, où $g_2 \propto a$, on peut montrer qu'il est préférable d'avoir simultanément un petit a et un grand g_α avec un petit α. Notons également que l'on peut s'attendre à ce que le terme BMF soit fortement dépendant du terme MF, d'où le fait qu'il n'est a priori pas évident de contrôler ces termes indépendamment.

On peut alors s'interroger sur les différentes options qui s'offrent pour obtenir un tel système "auto"-stable. Abordons le problème d'un point de vue historique. En 1957, Lee, Huang et Yang (LHY) ont dérivé dans le cas d'un gaz de Bose homogène faiblement répulsif (où $na^3 \ll 1$) les deux premiers termes de la densité d'énergie [10, 11] avec la méthode du pseudopotentiel (en accord avec l'approche de Bogoliubov [12, 13]),

$$E/V = \frac{4\pi\hbar^2 a}{m}\frac{n^2}{2}\left(1 + \frac{128}{15\sqrt{\pi}}\sqrt{na^3} + ...\right). \tag{B.2}$$

Dans nos notations, cette correction LHY correspond à un terme $\alpha = 5/2$. Elle est universelle, car elle ne dépend que de la longueur de diffusion ($\propto a^{5/2}$), et une propriété frappante réside dans sa nature purement quantique (car elle correspond à *des fluctuations quantiques*, ou dans une image plus théorique, à l'énergie du point zéro des phonons de Bogoliubov). Cependant, bien que ce terme ait effectivement été observé [14] et puisse être manipulé, on constate que cet effet est perturbatif et que le terme LHY est alors toujours beaucoup plus petit que le terme MF. Par conséquent, nous devons *a priori* chercher ailleurs pour obtenir cet état auto-stable que nous poursuivons.

Près de cinq décennies après LHY, Bulgac s'est posé la question de l'ingénierie des gouttelettes liquides quantiques [15]. Sa proposition réside dans la possibilité d'ajuster finement la longueur de diffusion dans les expériences grâce à un champ magnétique externe par le biais du mécanisme de Feshbach. En suivant le cas résonnant où $|a| \to +\infty$ et impliquant la physique d'Efimov [16, 17], il montre qu'une répulsion à trois corps (c'est-à-dire, $\alpha = 3$ et $g_3 > 0$) peut contribuer à stabiliser un système de bosons en interaction attractive ($g_2 < 0$), conduisant ainsi à un état autolié de densité $n_0 = -2g_2/g_3$ qu'il appelle un *boselet* (une gouttelette de bosons). Bien qu'il s'agisse d'un grand pas théorique, ces gouttelettes semblent difficiles à observer car dans le cas de la résonance, les collisions inélastiques [2] sont vraiment importantes et conduisent à une courte durée de vie de l'échantillon [18, 19].

Cependant, Petrov a présenté en 2014 un moyen de contrôler les interactions à deux corps et à trois corps effectives dans le cas non résonnant [20], ouvrant la voie à l'observation de gouttelettes quantiques auto-liées. En effet, cette proposition repose

[2] Typiquement, dans une collision inélastique à trois corps, deux atomes peuvent former une molécule telle que le troisième atome porte alors un surplus d'énergie cinétique suffisant pour quitter le piège.

sur un système de dipôles dans une géométrie bicouche avec tunnellisation inter-couches, où l'on peut réduire drastiquement les collisions inélastiques.

Un an plus tard, Petrov a réalisé que l'effet tunnel n'était pas nécessaire à la liquéfaction. Il a étudié dans la Réf. [21] une mixture boson-boson ($\uparrow$, $\downarrow$) avec une attraction inter-espèces à deux corps ($g_{\uparrow\downarrow} < 0$) et une répulsion intra-espèces à deux corps ($g_{\uparrow\uparrow}, g_{\downarrow\downarrow} > 0$) près de la région où le champ moyen prédit l'effondrement, définie par la condition $g_{\uparrow\downarrow}^2 > g_{\uparrow\uparrow} g_{\downarrow\downarrow}$ (c'est-à-dire que la *partie attractive* du système surpasse la *partie répulsive*). En analysant la densité d'énergie du mélange jusqu'à la correction LHY pour ce système, il a montré que ce terme peut en fait stabiliser le mélange qui s'effondre avec un réglage fin des interactions, et que le système se transforme plutôt en une gouttelette de liquide dilué. En d'autres termes, le système classique instable (d'un point de vue champ moyen) est stabilisé en " allumant " la mécanique quantique. Ici, la différence fondamentale avec le gaz de bosons à un seul composant est que le terme MF et la correction LHY peuvent être contrôlés indépendamment et donc accordés au même ordre. Diverses propriétés de cette phase exotique (spectre d'excitation, tension de surface, etc...) ont été décrites dans cet article, comme la voie expérimentale pour obtenir un tel état : quelques années plus tard, il a été observé avec succès dans un mélange de potassium (^{39}K, ^{41}K) à l'ICFO à Barcelone [22], puis plus tard au LENS à Florence [23].

Ce nouvel état liquide diffère assez fortement de l'image classique des liquides que nous connaissons, qui est expliquée par la théorie de Van der Waals [24]. En effet, ils sont beaucoup plus dilués (la gouttelette est 10^8 fois moins dense que l'eau !) et le cadre est ici plutôt universel puisque le liquide dépend d'un ensemble de quelques paramètres, contrairement aux liquides classiques où la description dépend des détails des potentiels interatomiques [25].

Parallèlement, des gouttelettes quantiques dipolaires ont été observées par les groupes de Stuttgart et d'Innsbruck à l'aide de gaz dipolaires (respectivement avec des dipôles Dy et Er) [26–29]. Ils s'expliquent par le même mécanisme de stabilisation que le cas de la mixture boson-boson, c'est-à-dire grâce aux fluctuations quantiques (terme LHY). Ici, le terme de champ moyen est affaibli via un équilibre entre une queue dipolaire attractive et une interaction de contact à courte portée répulsive.

Bien que l'observation de cet état de gouttelette semblable à un liquide constitue une avancée majeure car allant au-delà du paradigme de Van der Waals, elle ouvre également la voie à la réalisation d'un état encore plus intriguant : le *supersolide*. Cet état de la matière, qui présente à la fois une structure cristalline et un mouvement sans frottement, a une longue histoire car il a été prédit théoriquement depuis plusieurs décennies sans jamais être observé. Récemment, trois groupes ont apporté la première preuve expérimentale de propriétés supersolides via la formation de réseaux cohérents de gouttelettes dipolaires quantiques, reposant fondamentalement sur les interactions entre

les particules [31–33].

Ces idées maîtresses et les observations expérimentales ont considérablement augmenté l'attention portée aux systèmes avec un terme MF intentionnellement affaibli (augmentant ainsi l'importance des termes BMF) au cours des dernières années. La Ref. [34] est une revue très utile sur ce nouveau domaine.

D'un point de vue théorique, ces systèmes où une partie attractive et une partie répulsive entrent en compétition sont un moyen de mieux apprécier la richesse physique des termes au-delà du champ moyen. Des excitations collectives non-locales (fluctuations quantiques) aux interactions locales effectives entre plusieurs corps, nous voyons maintenant que ces termes ne peuvent plus être réduits à un problème académique car ils peuvent changer radicalement la nature du système. Cela soulève la question suivante :

De quoi dépendent ces termes au-delà du champ moyen ?

Bien sûr, ils sont principalement liés à la forme et à la force des interactions dans le système considéré, ainsi qu'au potentiel de piégeage, mais une de leurs caractéristiques majeures est qu'ils dépendent généralement fortement de la dimension considérée. Par exemple, le terme LHY implique une somme dans l'espace des moments, et sa dépendance à la densité de particules varie donc fortement ($n^{5/2}$ pour $D = 3$, $n^2 \ln n$ pour $D = 2$ et $n^{3/2}$ pour $D = 1$). Cela offre de larges possibilités car les expérimentateurs sont capables de confiner fortement le système dans des directions souhaitées, gelant ainsi certains degrés de liberté des atomes, pour entrer dans des régimes dits de *quasi-basse dimension*. On utilise fréquemment des piège harmoniques, et le système présente souvent une forme de cigare (quasi-1D) ou de crêpe (quasi-2D). Il faut d'ailleurs noter que la réduction du problème à un modèle en pure basse dimension contribue souvent à ajouter des interactions effectives à plusieurs corps dans le système, qui trouvent leur origine dans les excitations virtuelles des atomes dans le piège. D'une manière plus générale, en suivant une approche de théorie effective des champs (EFT), on peut montrer que des forces effectives à plusieurs corps apparaissent *naturellement* lorsqu'on intègre les degrés de liberté gelés dans un système [35].

Dans cette thèse, nous avons l'intention d'étudier les effets au-delà du champ moyen à proximité d'une région où l'interaction de champ moyen est considérablement affaiblie ($g_2 \to 0$) dans divers systèmes, géométries et interactions. Bien que cela va nous amener à naviguer entre les problèmes à petit et grand nombre de corps, l'accent sera mis sur l'approche à petit nombre de corps. Ce manuscrit est divisé en cinq chapitres, les deux premiers servant d'introduction pédagogique.

Dans le **premier chapitre**, nous rappelons les concepts utiles de l'approche à petit nombre de corps qui serviront de blocs de construction pour comprendre tous les chapitres suivants. Nous examinons l'interaction typique entre deux atomes neutres et présentons certaines propriétés de diffusion à deux corps à basse énergie, ainsi que le mécanisme

de Feshbach. Nous introduisons ensuite des potentiels effectifs beaucoup plus faciles à manipuler que les interactions réelles et qui contiennent les propriétés de diffusion à basse énergie du système, en utilisant ce que l'on appelle l'approximation de portée nulle. En particulier, nous présentons la méthode de Skorniakov-Ter-Martirosian, particulièrement pratique pour les problèmes à trois et quatre corps auxquels nous serons confrontés par la suite.

Dans le **second chapitre**, nous entrons dans le monde à grand nombre de corps et présentons plus en détail les motivations principales de cette thèse, à savoir les systèmes où le terme de champ moyen peut être ajusté à une valeur arbitrairement faible, soulignant l'importance des effets au-delà du champ moyen, et menant finalement à de nouveaux états exotiques de la matière. En suivant d'abord l'exemple d'une mixture boson-boson équilibré en masse avec des interactions de contact attractives inter-espèces et répulsives intra-espèces, nous expliquons comment le terme LHY peut stabiliser le système près du régime où l'approximation du champ moyen prédit l'effondrement, conduisant à la formation d'une gouttelette très diluée. La question est abordée dans toutes les dimensions. Nous donnons également un bref aperçu des gaz dipolaires, qui peuvent présenter le même phénomène de stabilisation quantique.

Dans le **troisième chapitre**, nous enrichissons le diagramme de phase du mélange boson-boson 1D défini dans le chapitre précédent. En partant du régime où le système se transforme en un gaz répulsif de dimères, nous résolvons le problème de la diffusion dimère-dimère. Dans le plan paramétré par les rapports des constantes de couplage $g_{\uparrow\uparrow}/|g_{\uparrow\downarrow}|$ et $g_{\downarrow\downarrow}/|g_{\uparrow\downarrow}|$ nous traçons la courbe où l'interaction dimère-dimère passe d'attractive à répulsive. Nous constatons que cette courbe est décalée de manière significative (de plus d'un facteur 2) vers une valeur plus grande de $g_{\sigma\sigma}$ (ou plus petite de $|g_{\uparrow\downarrow}|$) par rapport à la limite de stabilité du champ moyen $g_{\uparrow\uparrow}g_{\downarrow\downarrow} = g_{\uparrow\downarrow}^2$. Pour une faible attraction dimère-dimère, nous prédisons une phase liquide diluée dimérisée stabilisée contre l'effondrement par une force répulsive à trois dimères. Motivés par la vérification de cette prédiction, nous nous tournons vers la résolution du problème de trois bosons avec des interactions de contact à deux et trois corps à une dimension et calculons analytiquement les énergies de l'état fondamental et de l'état excité du trimère. Ce résultat théorique est en soi une étape importante pour comprendre les systèmes bosoniques unidimensionnels. En utilisant la technique de diffusion Monte Carlo, nos collaborateurs ont calculé l'énergie de liaison des trois dimères formés dans le mélange unidimensionnel boson-boson ou fermion-boson précédemment étudié. En combinant ces résultats avec notre analyse à trois corps, nous extrayons la longueur de diffusion des trois dimères à proximité de la région où l'interaction à deux corps dimère-dimère disparaît. Dans les deux cas considérés, l'interaction entre les trois dimères s'avère être répulsive. Nos résultats s'appliquent également aux mélanges boson-fermion unidimensionnels. Ils constituent également une proposition concrète pour obtenir un gaz unidimensionnel avec une pure répulsion à trois corps.

Dans le **quatrième chapitre**, nous développons la théorie des perturbations pour des bosons interagissant via un potentiel à deux corps faible V, dont les parties attractive et répulsive s'annulent. Nous constatons que la principale contribution non relative à une interaction par paires à l'énergie émerge au troisième ordre en V et représente une interaction effective à trois corps, dont le signe dans la plupart des cas (mais pas en général) est anticorrélé avec le signe de la queue à longue portée de V. Nous appliquons notre théorie à quelques potentiels d'interaction à deux corps particuliers et calculons les principales corrections d'interaction à deux et à trois corps pour des dipôles inclinés dans des géométries quasi-basse dimension. Nous montrons qu'à grand nombre de corps, notre approche est cohérente avec le traitement de Bogoliubov.

Dans le **cinquième chapitre**, motivés par certains cas où le terme LHY semble ne pas pouvoir contrebalancer le terme MF instable (gaz de Bose à un seul composant, géométrie de faible dimension, etc ...), nous proposons une façon de concevoir une force effective à trois corps pour assurer cette propriété : pour des bosons interagissant entre eux par un potentiel à deux corps où l'on impose la disparition de l'interaction par paires , nous montrons l'émergence d'une force effective à trois corps que nous calculons en toute dimension. Nous utilisons le modèle standard à deux canaux paramétré par la force de l'interaction atome-atome de fond, l'amplitude du couplage entre canal ouvert et canal fermé, et la force de l'interaction atome-dimère. La force à trois corps provient de l'interaction atome-dimère, mais elle peut être considérablement renforcée pour les croisements étroits, c'est-à-dire pour les petites amplitudes de conversion atome-dimère. Cet effet peut être utilisé pour stabiliser les atomes et molécules dipolaires en quasi-2D.

En conclusion, l'étude de systèmes où les termes au-delà du champ moyen sont de l'ordre du terme de champ moyen (et éventuellement dominants), offre une plateforme merveilleuse pour apprécier la large palette d'interactions en jeu dans un système, nous amenant ultimement à redéfinir notre conception classique des états de la matière.

Bibliography

[1] Immanuel Bloch, Jean Dalibard, and Wilhelm Zwerger. Many-body physics with ultracold gases. *Rev. Mod. Phys.*, 80:885–964, Jul 2008.

[2] I. M. Georgescu, S. Ashhab, and Franco Nori. Quantum simulation. *Rev. Mod. Phys.*, 86:153–185, Mar 2014.

[3] Schäfer Florian, Fukuhara Takeshi, Sugawa Seiji, Takasu Yosuke, and Takahashi Yoshiro. Tools for quantum simulation with ultracold atoms in optical lattices. *Nature Reviews Physics*, 2(8):411–425, 2020.

[4] Hu Jiazhong, Feng Lei, Zhang Zhendong, and Chin Cheng. Quantum simulation of Unruh radiation. *Nature Physics*, 15(8):785–789, 2019.

[5] M. H. Anderson, J. R. Ensher, M. R. Matthews, C. E. Wieman, and E. A. Cornell. Observation of Bose-Einstein Condensation in a Dilute Atomic Vapor. *Science*, 269(5221):198–201, 1995.

[6] C. C. Bradley, C. A. Sackett, J. J. Tollett, and R. G. Hulet. Evidence of bose-einstein condensation in an atomic gas with attractive interactions. *Phys. Rev. Lett.*, 75:1687–1690, Aug 1995.

[7] K. B. Davis, M. O. Mewes, M. R. Andrews, N. J. van Druten, D. S. Durfee, D. M. Kurn, and W. Ketterle. Bose-einstein condensation in a gas of sodium atoms. *Phys. Rev. Lett.*, 75:3969–3973, Nov 1995.

[8] Wolfgang Ketterle and N.J. Van Druten. Evaporative Cooling of Trapped Atoms. volume 37 of *Advances In Atomic, Molecular, and Optical Physics*, pages 181–236. Academic Press, 1996.

[9] Sandro Stringari. Bose–einstein condensation and superfluidity in trapped atomic gases. *Comptes Rendus de l'Académie des Sciences - Series IV - Physics*, 2(3):381–397, 2001.

[10] T. D. Lee and C. N. Yang. Many-body problem in quantum mechanics and quantum statistical mechanics. *Phys. Rev.*, 105:1119–1120, Feb 1957.

[11] T. D. Lee, Kerson Huang, and C. N. Yang. Eigenvalues and eigenfunctions of a bose system of hard spheres and its low-temperature properties. *Phys. Rev.*, 106:1135–1145, Jun 1957.

[12] N. N. Bogoliubov. On the theory of superfluidity. *J. Phys. (USSR)*, 11:23–32, 1947.

[13] L. D. Landau and E. M. Lifshitz. Quantum mechanics. 1999.

[14] Nir Navon, Swann Piatecki, Kenneth Günter, Benno Rem, Trong Canh Nguyen, Frédéric Chevy, Werner Krauth, and Christophe Salomon. Dynamics and thermodynamics of the low-temperature strongly interacting bose gas. *Phys. Rev. Lett.*, 107:135301, Sep 2011.

[15] Aurel Bulgac. Dilute quantum droplets. *Phys. Rev. Lett.*, 89:050402, Jul 2002.

[16] V. Efimov. Energy levels arising from resonant two-body forces in a three-body system. *Physics Letters B*, 33(8):563–564, 1970.

[17] Pascal Naidon and Shimpei Endo. Efimov physics: a review. *Reports on Progress in Physics*, 80(5):056001, Mar 2017.

[18] S. Inouye, M. R. Andrews, J. Stenger, H. J. Miesner, D. M. Stamper-Kurn, and W. Ketterle. Observation of Feshbach resonances in a Bose–Einstein condensate. *Nature*, 392(6672):151–154, 1998.

[19] J. L. Roberts, N. R. Claussen, S. L. Cornish, and C. E. Wieman. Magnetic field dependence of ultracold inelastic collisions near a feshbach resonance. *Phys. Rev. Lett.*, 85:728–731, Jul 2000.

[20] D. S. Petrov. Three-body interacting bosons in free space. *Phys. Rev. Lett.*, 112:103201, Mar 2014.

[21] D.S. Petrov. Quantum mechanical stabilization of a collapsing bose-bose mixture. *Physical Review Letters*, 115(15), Oct 2015.

[22] C. R. Cabrera, L. Tanzi, J. Sanz, B. Naylor, P. Thomas, P. Cheiney, and L. Tarruell. Quantum liquid droplets in a mixture of Bose-Einstein condensates. *Science*, 359(6373):301–304, 2018.

[23] G. Semeghini, G. Ferioli, L. Masi, C. Mazzinghi, L. Wolswijk, F. Minardi, M. Modugno, G. Modugno, M. Inguscio, and M. Fattori. Self-bound quantum droplets of atomic mixtures in free space. *Phys. Rev. Lett.*, 120:235301, Jun 2018.

[24] Rowlinson J. S. Legacy of van der Waals. *Nature*, 244(5416):414–417, 1973.

[25] Petrov Dmitry S. Liquid beyond the van der Waals paradigm. *Nature Physics*, 14(3):211–212, 2018.

[26] Kadau Holger, Schmitt Matthias, Wenzel Matthias, Wink Clarissa, Maier Thomas, Ferrier-Barbut Igor, and Pfau Tilman. Observing the Rosensweig instability of a quantum ferrofluid. *Nature*, 530(7589):194–197, 2016.

[27] Igor Ferrier-Barbut, Holger Kadau, Matthias Schmitt, Matthias Wenzel, and Tilman Pfau. Observation of quantum droplets in a strongly dipolar bose gas. *Phys. Rev. Lett.*, 116:215301, May 2016.

[28] Schmitt Matthias, Wenzel Matthias, Böttcher Fabian, Ferrier-Barbut Igor, and Pfau Tilman. Self-bound droplets of a dilute magnetic quantum liquid. *Nature*, 539(7628):259–262, 2016.

[29] L. Chomaz, S. Baier, D. Petter, M. J. Mark, F. Wächtler, L. Santos, and F. Ferlaino. Quantum-fluctuation-driven crossover from a dilute bose-einstein condensate to a macrodroplet in a dipolar quantum fluid. *Phys. Rev. X*, 6:041039, Nov 2016.

[30] A. J. Leggett. Can a solid be "superfluid"? *Phys. Rev. Lett.*, 25:1543–1546, Nov 1970.

[31] Fabian Böttcher, Jan-Niklas Schmidt, Matthias Wenzel, Jens Hertkorn, Mingyang Guo, Tim Langen, and Tilman Pfau. Transient supersolid properties in an array of dipolar quantum droplets. *Phys. Rev. X*, 9:011051, Mar 2019.

[32] L. Tanzi, E. Lucioni, F. Famà, J. Catani, A. Fioretti, C. Gabbanini, R. N. Bisset, L. Santos, and G. Modugno. Observation of a dipolar quantum gas with metastable supersolid properties. *Phys. Rev. Lett.*, 122:130405, Apr 2019.

[33] L. Chomaz, D. Petter, P. Ilzhöfer, G. Natale, A. Trautmann, C. Politi, G. Durastante, R. M. W. van Bijnen, A. Patscheider, M. Sohmen, M. J. Mark, and F. Ferlaino. Long-lived and transient supersolid behaviors in dipolar quantum gases. *Phys. Rev. X*, 9:021012, Apr 2019.

[34] Fabian Böttcher, Jan-Niklas Schmidt, Jens Hertkorn, Kevin S H Ng, Sean D Graham, Mingyang Guo, Tim Langen, and Tilman Pfau. New states of matter with fine-tuned interactions: quantum droplets and dipolar supersolids. *Reports on Progress in Physics*, 84(1):012403, Jan 2021.

[35] Hans-Werner Hammer, Andreas Nogga, and Achim Schwenk. Colloquium : Three-body forces: From cold atoms to nuclei. *Reviews of Modern Physics*, 85, 10 2012.

[36] Dalibard J. Les interactions entre particules dans les gaz quantiques. *Cours du Collège de France Chaire Atomes et rayonnement*, (2021).

[37] H. B. G. Casimir and D. Polder. The influence of retardation on the london-van der waals forces. *Phys. Rev.*, 73:360–372, Feb 1948.

[38] D. Petrov, Dimitri M. Gangardt, and Gora V. Shlyapnikov. Low-dimensional trapped gases. *Journal de Physique IV Proceedings*, 116:5–44, 2004. 42 pages, 12 figures, lectures given at the Les Houches School "Quantum Gases in Low Dimensions" (April 2003).

[39] B. DeMarco and D. S. Jin. Onset of fermi degeneracy in a trapped atomic gas. *Science*, 285(5434):1703–1706, 1999.

[40] Noam Gross, Zav Shotan, Servaas Kokkelmans, and Lev Khaykovich. Nuclear-spin-independent short-range three-body physics in ultracold atoms. *Physical Review Letters*, 105(10), Sep 2010.

[41] P. Dyke, S. E. Pollack, and R. G. Hulet. Finite-range corrections near a feshbach resonance and their role in the efimov effect. *Phys. Rev. A*, 88:023625, Aug 2013.

[42] Greiner Markus, Regal Cindy A., and Jin Deborah S. Emergence of a molecular Bose–Einstein condensate from a Fermi gas. *Nature*, 426(6966):537–540, 2003.

[43] T. Bourdel, L. Khaykovich, J. Cubizolles, J. Zhang, F. Chevy, M. Teichmann, L. Tarruell, S. J. J. M. F. Kokkelmans, and C. Salomon. Experimental study of the bec-bcs crossover region in lithium 6. *Phys. Rev. Lett.*, 93:050401, Jul 2004.

[44] M. Olshanii. Atomic scattering in the presence of an external confinement and a gas of impenetrable bosons. *Phys. Rev. Lett.*, 81:938–941, Aug 1998.

[45] R. Jackiw. Delta function potentials in two-dimensional and three-dimensional quantum mechanics. *M. A. B. Bég Memorial Volume*, ed. by A. Ali and P. Hoodbhoy (World Scientific, Singapore,1991).

[46] Steven Weinberg. The quantum theory of fields. 1, 1995.

[47] Ludovic Pricoupenko. Isotropic contact forces in arbitrary representation: Heterogeneous few-body problems and low dimensions. *Physical Review A*, 83(6), Jun 2011.

[48] H. Bethe and R. Peierls. Quantum Theory of the Diplon. *Proceedings of the Royal Society of London Series A*, 148(863):146–156, January 1935.

[49] G V Skorniakov and K A Ter-Martirosian. Three body problem for short range forces. i. scattering of low energy neutrons by deuterons. *Soviet Phys. JETP*, 6 1957.

[50] J. Boronat and J. Casulleras. Monte carlo analysis of an interatomic potential for he. *Phys. Rev. B*, 49:8920–8930, Apr 1994.

[51] D. S. Petrov and G. E. Astrakharchik. Ultradilute low-dimensional liquids. *Phys. Rev. Lett.*, 117:100401, Sep 2016.

[52] Kean Loon Lee, Nils B. Jørgensen, I-Kang Liu, Lars Wacker, Jan J. Arlt, and Nick P. Proukakis. Phase separation and dynamics of two-component bose-einstein condensates. *Phys. Rev. A*, 94:013602, Jul 2016.

[53] David M Larsen. Binary mixtures of dilute bose gases with repulsive interactions at low temperature. *Annals of Physics*, 24:89–101, 1963.

[54] Miki Ota and Gregory Astrakharchik. Beyond lee-huang-yang description of self-bound bose mixtures. *SciPost Physics*, 9(2), Aug 2020.

[55] Michael Bender, Paul-Henri Heenen, and Paul-Gerhard Reinhard. Self-consistent mean-field models for nuclear structure. *Rev. Mod. Phys.*, 75:121–180, Jan 2003.

[56] Franco Dalfovo and Sandro Stringari. Helium nanodroplets and trapped bose–einstein condensates as prototypes of finite quantum fluids. *The Journal of Chemical Physics*, 115(22):10078–10089, 2001.

[57] V. N. Popov. On the theory of the superfluidity of two- and one-dimensional bose systems. *Theoretical and Mathematical Physics*, 1972.

[58] M. A. Baranov, M. Dalmonte, G. Pupillo, and P. Zoller. Condensed matter theory of dipolar quantum gases. *Chemical Reviews*, 112(9):5012–5061, Aug 2012.

[59] Franco Dalfovo, Stefano Giorgini, Lev P. Pitaevskii, and Sandro Stringari. Theory of bose-einstein condensation in trapped gases. *Rev. Mod. Phys.*, 71:463–512, Apr 1999.

[60] Uwe R. Fischer. Stability of quasi-two-dimensional bose-einstein condensates with dominant dipole-dipole interactions. *Phys. Rev. A*, 73:031602, Mar 2006.

[61] R. N. Bisset, R. M. Wilson, D. Baillie, and P. B. Blakie. Ground-state phase diagram of a dipolar condensate with quantum fluctuations. *Phys. Rev. A*, 94:033619, Sep 2016.

[62] T. Koch, T. Lahaye, J. Metz, B. Fröhlich, A. Griesmaier, and T. Pfau. Stabilization of a purely dipolar quantum gas against collapse. *Nature Physics*, 4(3):218–222, Feb 2008.

[63] J Metz, T Lahaye, B Fröhlich, A Griesmaier, T Pfau, H Saito, Y Kawaguchi, and M Ueda. Coherent collapses of dipolar bose–einstein condensates for different trap geometries. *New Journal of Physics*, 11(5):055032, may 2009.

[64] A. R. P. Lima and A. Pelster. Beyond mean-field low-lying excitations of dipolar bose gases. *Phys. Rev. A*, 86:063609, Dec 2012.

[65] F. Wächtler and L. Santos. Quantum filaments in dipolar bose-einstein condensates. *Phys. Rev. A*, 93:061603, Jun 2016.

[66] G. Bismut, B. Laburthe-Tolra, E. Maréchal, P. Pedri, O. Gorceix, and L. Vernac. Anisotropic excitation spectrum of a dipolar quantum bose gas. *Phys. Rev. Lett.*, 109:155302, Oct 2012.

[67] F. Wächtler and L. Santos. Ground-state properties and elementary excitations of quantum droplets in dipolar bose-einstein condensates. *Phys. Rev. A*, 94:043618, Oct 2016.

[68] Matthias Wenzel, Fabian Böttcher, Tim Langen, Igor Ferrier-Barbut, and Tilman Pfau. Striped states in a many-body system of tilted dipoles. *Physical Review A*, 96(5), Nov 2017.

[69] M. Girardeau. Relationship between systems of impenetrable bosons and fermions in one dimension. *Journal of Mathematical Physics*, 1(6):516–523, 1960.

[70] M. D. Girardeau. Permutation symmetry of many-particle wave functions. *Phys. Rev.*, 139:B500–B508, Jul 1965.

[71] M. Gaudin. Un systeme a une dimension de fermions en interaction. *Physics Letters A*, 24(1):55–56, 1967.

[72] C. N. Yang. Some exact results for the many-body problem in one dimension with repulsive delta-function interaction. *Phys. Rev. Lett.*, 19:1312–1315, Dec 1967.

[73] Xi-Wen Guan, Murray T. Batchelor, and Chaohong Lee. Fermi gases in one dimension: From bethe ansatz to experiments. *Rev. Mod. Phys.*, 85:1633–1691, Nov 2013.

[74] J. B. McGuire. Interacting fermions in one dimension. i. repulsive potential. *Journal of Mathematical Physics*, 6(3):432–439, 1965.

[75] J. B. McGuire. Interacting fermions in one dimension. ii. attractive potential. *Journal of Mathematical Physics*, 7(1):123–132, 1966.

[76] B. Sutherland. Beautiful models. *World Scientific*, 2004.

[77] J. B. McGuire. Study of exactly soluble one-dimensional n-body problems. *Journal of Mathematical Physics*, 5(5):622–636, 1964.

[78] Yuta Sekino and Yusuke Nishida. Quantum droplet of one-dimensional bosons with a three-body attraction. *Phys. Rev. A*, 97:011602, Jan 2018.

[79] C. J. Pethick and H. Smith. Bose-einstein condensation in dilute gases. *Cambride University Press*, 2008.

[80] M. Schick. Two-dimensional system of hard-core bosons. *Phys. Rev. A*, 3:1067–1073, Mar 1971.

[81] Christophe Mora and Yvan Castin. Extension of bogoliubov theory to quasicondensates. *Phys. Rev. A*, 67:053615, May 2003.

[82] F Sgarlata, G Mazzarella, and L Salasnich. Effective-range signatures in quasi-1d matter waves: sound velocity and solitons. *Journal of Physics B: Atomic, Molecular and Optical Physics*, 48(11):115301, apr 2015.

[83] A. Cappellaro and L. Salasnich. Finite-range corrections to the thermodynamics of the one-dimensional bose gas. *Phys. Rev. A*, 96:063610, Dec 2017.

[84] H.-W. Hammer and D. T. Son. Universal properties of two-dimensional boson droplets. *Phys. Rev. Lett.*, 93:250408, Dec 2004.

[85] P. Cheiney, C. R. Cabrera, J. Sanz, B. Naylor, L. Tanzi, and L. Tarruell. Bright soliton to quantum droplet transition in a mixture of bose-einstein condensates. *Phys. Rev. Lett.*, 120:135301, Mar 2018.

[86] Cheng-Hsun Wu, Ibon Santiago, Jee Woo Park, Peyman Ahmadi, and Martin W. Zwierlein. Strongly interacting isotopic bose-fermi mixture immersed in a fermi sea. *Phys. Rev. A*, 84:011601, Jul 2011.

[87] Lei Pan, Shu Chen, and Xiaoling Cui. Many-body stabilization of a resonant p-wave fermi gas in one dimension. *Phys. Rev. A*, 98:011603, Jul 2018.

[88] Elliott H. Lieb and Werner Liniger. Exact analysis of an interacting bose gas. i. the general solution and the ground state. *Phys. Rev.*, 130:1605–1616, May 1963.

[89] A. Muryshev, G. V. Shlyapnikov, W. Ertmer, K. Sengstock, and M. Lewenstein. Dynamics of dark solitons in elongated bose-einstein condensates. *Phys. Rev. Lett.*, 89:110401, Aug 2002.

[90] Subhasis Sinha, Alexander Yu. Cherny, Dmitry Kovrizhin, and Joachim Brand. Friction and diffusion of matter-wave bright solitons. *Phys. Rev. Lett.*, 96:030406, Jan 2006.

[91] I. E. Mazets, T. Schumm, and J. Schmiedmayer. Breakdown of integrability in a quasi-1d ultracold bosonic gas. *Phys. Rev. Lett.*, 100:210403, May 2008.

[92] Ludovic Pricoupenko. Pure confinement-induced trimer in one-dimensional atomic waveguides. *Phys. Rev. A*, 97:061604, Jun 2018.

[93] Stephan Falke, Horst Knöckel, Jan Friebe, Matthias Riedmann, Eberhard Tiemann, and Christian Lisdat. Potassium ground-state scattering parameters

and born-oppenheimer potentials from molecular spectroscopy. *Phys. Rev. A*, 78:012503, Jul 2008.

[94] Yusuke Nishida. Universal bound states of one-dimensional bosons with two- and three-body attractions. *Phys. Rev. A*, 97:061603, Jun 2018.

[95] P R Johnson, D Blume, X Y Yin, W F Flynn, and E Tiesinga. Effective renormalized multi-body interactions of harmonically confined ultracold neutral bosons. *New Journal of Physics*, 14(5):053037, May 2012.

[96] M. Valiente. Three-body repulsive forces among identical bosons in one dimension. *Phys. Rev. A*, 100:013614, Jul 2019.

[97] M. J. Bijlsma, B. A. Heringa, and H. T. C. Stoof. Phonon exchange in dilute fermi-bose mixtures: Tailoring the fermi-fermi interaction. *Phys. Rev. A*, 61:053601, Apr 2000.

[98] L. Viverit, C. J. Pethick, and H. Smith. Zero-temperature phase diagram of binary boson-fermion mixtures. *Phys. Rev. A*, 61:053605, Apr 2000.

[99] S. Yi and L. You. Trapped atomic condensates with anisotropic interactions. *Phys. Rev. A*, 61:041604, Mar 2000.

[100] A. K. Fedorov, I. L. Kurbakov, Y. E. Shchadilova, and Yu. E. Lozovik. Two-dimensional bose gas of tilted dipoles: Roton instability and condensate depletion. *Phys. Rev. A*, 90:043616, Oct 2014.

[101] D Baillie and P B Blakie. A general theory of flattened dipolar condensates. *New Journal of Physics*, 17(3):033028, Mar 2015.

[102] Meghana Raghunandan, Chinmayee Mishra, Kazimierz Łakomy, Paolo Pedri, Luis Santos, and Rejish Nath. Two-dimensional bright solitons in dipolar bose-einstein condensates with tilted dipoles. *Phys. Rev. A*, 92:013637, Jul 2015.

[103] D. Edler, C. Mishra, F. Wächtler, R. Nath, S. Sinha, and L. Santos. Quantum fluctuations in quasi-one-dimensional dipolar bose-einstein condensates. *Phys. Rev. Lett.*, 119:050403, Aug 2017.

[104] R. Nath, P. Pedri, and L. Santos. Phonon instability with respect to soliton formation in two-dimensional dipolar bose-einstein condensates. *Phys. Rev. Lett.*, 102:050401, Feb 2009.

[105] Yongyong Cai, Matthias Rosenkranz, Zhen Lei, and Weizhu Bao. Mean-field regime of trapped dipolar bose-einstein condensates in one and two dimensions. *Phys. Rev. A*, 82:043623, Oct 2010.

[106] Christopher Ticknor, Ryan M. Wilson, and John L. Bohn. Anisotropic superfluidity in a dipolar bose gas. *Phys. Rev. Lett.*, 106:065301, Feb 2011.

[107] Christopher Ticknor. Finite-temperature analysis of a quasi-two-dimensional dipolar gas. *Phys. Rev. A*, 85:033629, Mar 2012.

[108] Stefan S. Natu and S. Das Sarma. Absence of damping of low-energy excitations in a quasi-two-dimensional dipolar bose gas. *Phys. Rev. A*, 88:031604, Sep 2013.

[109] B. C. Mulkerin, R. M. W. van Bijnen, D. H. J. O'Dell, A. M. Martin, and N. G. Parker. Anisotropic and long-range vortex interactions in two-dimensional dipolar bose gases. *Phys. Rev. Lett.*, 111:170402, Oct 2013.

[110] Pawel Zin, Maciej Pylak, Tomasz Wasak, Krzysztof Jachymski, and Zbigniew Idziaszek. Quantum droplets in a dipolar bose gas at a dimensional crossover, 2019.

[111] Yijun Tang, Wil Kao, Kuan-Yu Li, Sangwon Seo, Krishnanand Mallayya, Marcos Rigol, Sarang Gopalakrishnan, and Benjamin L. Lev. Thermalization near integrability in a dipolar quantum newton's cradle. *Phys. Rev. X*, 8:021030, May 2018.

[112] A. Macia, D. Hufnagl, F. Mazzanti, J. Boronat, and R. E. Zillich. Excitations and stripe phase formation in a two-dimensional dipolar bose gas with tilted polarization. *Phys. Rev. Lett.*, 109:235307, Dec 2012.

[113] A. Macia, J. Boronat, and F. Mazzanti. Phase diagram of dipolar bosons in two dimensions with tilted polarization. *Phys. Rev. A*, 90:061601, Dec 2014.

[114] Zhen-Kai Lu, Yun Li, D. S. Petrov, and G. V. Shlyapnikov. Stable dilute supersolid of two-dimensional dipolar bosons. *Phys. Rev. Lett.*, 115:075303, Aug 2015.

[115] Leo Radzihovsky, Peter B. Weichman, and Jae I. Park. Superfluidity and phase transitions in a resonant bose gas. *Annals of Physics*, 323(10):2376–2451, 2008.

[116] Zav Shotan, Olga Machtey, Servaas Kokkelmans, and Lev Khaykovich. Three-body recombination at vanishing scattering lengths in an ultracold bose gas. *Phys. Rev. Lett.*, 113:053202, Jul 2014.

[117] M. A. Baranov, A. Micheli, S. Ronen, and P. Zoller. Bilayer superfluidity of fermionic polar molecules: Many-body effects. *Phys. Rev. A*, 83:043602, Apr 2011.

[118] Goulven Quéméner and John L. Bohn. Electric field suppression of ultracold confined chemical reactions. *Phys. Rev. A*, 81:060701, Jun 2010.

[119] Andrea Micheli, Zbigniew Idziaszek, Guido Pupillo, Mikhail A. Baranov, Peter Zoller, and Paul S. Julienne. Universal rates for reactive ultracold polar molecules in reduced dimensions. *Phys. Rev. Lett.*, 105:073202, Aug 2010.

[120] A. Frisch, M. Mark, K. Aikawa, S. Baier, R. Grimm, A. Petrov, S. Kotochigova, G. Quéméner, M. Lepers, O. Dulieu, and F. Ferlaino. Ultracold dipolar molecules composed of strongly magnetic atoms. *Phys. Rev. Lett.*, 115:203201, Nov 2015.

[121] René Stock, Andrew Silberfarb, Eric L. Bolda, and Ivan H. Deutsch. Generalized pseudopotentials for higher partial wave scattering. *Phys. Rev. Lett.*, 94:023202, Jan 2005.

[122] K. Kanjilal and D. Blume. Coupled-channel pseudopotential description of the feshbach resonance in two dimensions. *Phys. Rev. A*, 73:060701, Jun 2006.

[123] D. S. Petrov. Proceedings of the les houches summer schools, session 94, edited by c. salomon, l. f. cugliandolo and g. v. shlyapnikov. *Oxford University Press*, 2013.

[124] Volodymyr Pastukhov. Ground-state properties of dilute one-dimensional bose gas with three-body repulsion. *Physics Letters A*, 383(9):894–897, 2019.

[125] Eric Braaten and H.-W. Hammer. Universality in few-body systems with large scattering length (example in p.359). *Physics Reports*, 428(5):259–390, 2006.

[126] G. Guijarro, A. Pricoupenko, G. E. Astrakharchik, J. Boronat, and D. S. Petrov. One-dimensional three-boson problem with two- and three-body interactions. *Phys. Rev. A*, 97:061605, Jun 2018.

[127] M. Valiente and V. Pastukhov. Anomalous frequency shifts in a one-dimensional trapped bose gas. *Phys. Rev. A*, 99:053607, May 2019.

[128] Chetan Nayak, Steven H. Simon, Ady Stern, Michael Freedman, and Sankar Das Sarma. Non-abelian anyons and topological quantum computation. *Rev. Mod. Phys.*, 80:1083–1159, Sep 2008.

[129] Ivan Morera, Bruno Juliá-Díaz, and Manuel Valiente. Quantum liquids and droplets with low-energy interactions in one dimension, 2021.

[130] Qi Gu and Lan Yin. Phonon stability and sound velocity of quantum droplets in a boson mixture. *Phys. Rev. B*, 102:220503, Dec 2020.

[131] Tobias Ilg, Jan Kumlin, Luis Santos, Dmitry S. Petrov, and Hans Peter Büchler. Dimensional crossover for the beyond-mean-field correction in bose gases. *Phys. Rev. A*, 98:051604, Nov 2018.

université PARIS-SACLAY

ÉCOLE DOCTORALE
Physique en l'Île-de-France (PIF)

Title: Beyond-mean-field effects in ultracold gases

Keywords: Bose-Bose Mixture, Quantum Droplets, Effective Three-Body Interactions

Abstract: Ultracold gases are well controllable quantum systems that are described by a set of few parameters. The idea to look at systems with partially attractive and repulsive forces, fine-tuned to an approximate overall cancellation of the mean-field term, provide an interesting platform for studying various beyond-mean-field phenomena, remarkable recent examples being quantum droplets and dipolar supersolids. In this manuscript, we take a step towards understanding the phase diagram of the 1D Bose-Bose mixture with attractive interspecies and repulsive intraspecies contact interactions. We address the one-dimensional three-body problem with two- and three-body interactions that we solve analytically. Then, we develop the perturbation theory for systems with a weak two-body potential interaction, where the attractive and repulsive parts compensate each other. We calculate in every dimension the leading nonpairwise contribution, which represents an effective three-body interaction. We apply this result particularly to tilted dipoles in quasi-low-dimensional geometries. Interestingly, we show the consistency of this few-body perturbative approach with the Bogoliubov one. Finally, we present a way to engineer an effective three-body force to stabilize some bosonic systems near a narrow Feshbach resonance.

Titre: Effets au-delà du champ moyen dans les gaz ultra-froids

Mots clés: Mixture Bosonique, Goutelettes quantiques, Interactions effectives à trois corps

Résumé: Les gaz ultrafroids sont des systèmes quantiques bien contrôlables qui sont décrits par un petit ensemble de paramètres. L'idée d'étudier des systèmes avec des forces partiellement attractives et répulsives, ajustées de manière à obtenir une faible valeur de champ moyen, fournit une plateforme intéressante pour étudier divers phénomènes allant au-delà de cette approximation classique : des exemples récents remarquables étant les gouttelettes quantiques et les supersolides dipolaires. Dans ce manuscrit, nous progressons dans la compréhension du diagramme de phase d'un mélange Bose-Bose 1D avec des interactions de contact interespèces attractives et intra-espèces répulsives. Ceci nous amène à aborder le problème unidimensionnel de trois bosons avec des interactions à deux et trois corps que nous résolvons analytiquement. Nous développons ensuite la théorie des perturbations pour des systèmes où la valeur de champ moyen est très faible (ou disparait). Nous calculons dans toutes les dimensions la contribution principale au-delà du champ moyen qui représente une interaction effective à trois corps. Nous appliquons particulièrement ce résultat aux dipôles inclinés dans des géométries à quasi-basse dimension. De manière intéressante, nous montrons la cohérence de cette approche perturbative à quelques corps avec celle de Bogoliubov. Enfin, nous présentons un moyen de concevoir une force effective à trois corps utile pour stabiliser certains systèmes bosoniques proche d'une résonance de Feshbach étroite.

Université Paris-Saclay
Espace Technologique / Immeuble Discovery
Route de l'Orme aux Merisiers RD 128 / 91190 Saint-Aubin, France